5-2-2007

The Extent of Perturbation of Skin Models by Transdermal Penetration Enhancers Investigated by 31P NMR and Fluorescence Spectroscopy

Charmita Patricia Burch

THE EXTENT OF PERTURBATION OF SKIN MODELS BY TRANSDERMAL PENETRATION ENHANCERS INVESTIGATED BY ^{31}P NMR AND FLUORESCENCE SPECTROSCOPY

by

Charmita P. Burch

Under the Direction of Jerry C. Smith, Ph.D.

ABSTRACT

The molecular basis of the potent transdermal enhancement activity of a series of iminosulfuranes, structure provided where X = H, Cl, Br, and I, is being investigated skin models.

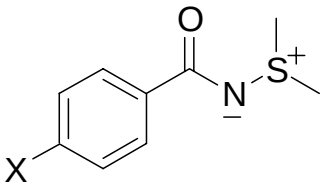

X = H, Cl, I, Br

It has been shown (*J. Lipid Res. 46(2005), 2192-2201.*) that correlations exist between the activity of the aforementioned transdermal penetration enhancers (TPE) and the extent to which these agents bind to DMPC vesicles and perturb the gel to liquid crystal phase transition measured by calorimetry. The degree to which the perturbation of these compounds extends into the bilayer interior in contrast to surface activity is unclear. To gain insight into this issue, the ^{31}P NMR resonance from DMPC and DMPC-cholesterol unilamellar vesicles have been split by the slowly penetrating paramagnetic metal ion Pr^{+3}. The extent to which this perturbation is attenuated by transdermal penetration enhancers has been investigated as a function of Pr^{+3} exposure time and iminosulfurane concentration. The effect of these iminosulfuranes on bilayer integrity is also being

explored by monitoring the induced release of carboxyfluorescein from DMPC and DMPC- cholesterol unilamellar vesicles.

INDEX WORDS: transdermal penetration enhancers, iminosulfurane, NMR, DMPC, fluorescence, carboxyfluorescein, shift reagents.

THE EXTENT OF PERTURBATION OF SKIN MODELS BY TRANSDERMAL PENETRATION ENHANCERS INVESTIGATED BY ^{31}P NMR AND FLUORESCENCE SPECTROSCOPY

by

CHARMITA P. BURCH

A Dissertation Submitted in Partial Fulfillment of the Requirements for the Degree of

Doctor of Philosophy

in the College of Arts and Sciences

Georgia State University

2007

THE EXTENT OF PERTURBATION OF SKIN MODELS BY TRANSDERMAL PENETRATION ENHANCERS INVESTIGATED BY ^{31}P NMR AND FLUORESCENCE SPECTROSCOPY

by

CHARMITA P. BURCH

Major Professor: Jerry C. Smith
Committee: Stuart Allison
Kathryn Grant

Electronic Version Approved:

Office of Graduate Studies
College of Arts and Sciences
Georgia State University
May 2007

Acknowledgements

To my Lord and Savior, Jesus Christ, I give thanks. When I had given up on my dreams, the Lord opened a door and gave me the grace to walk through and complete this journey. Through the years of challenge and difficulty, His grace has been sufficient.

To my parents, Patricia and David Burch, I want to thank you for your love and support. When I wanted to give up and come home you encouraged me, supported me and gave me sound advice. I could not have done this without you.

To my sister, Dionne, and my brother-in-law, Kendall, I thank you for your love and prayers.

To Dr. Jerry Smith, I thank you for being a wonderful advisor. It has been an honor and a privilege to work with you. I have learned so much from you. You allowed me to work independently and caused me to stretch beyond my comfort zone. Thank for our daily discussions about the progress of the projects and debating with me about my ideas. They taught me to articulate my research.

I would also like to acknowledge and extend my heartfelt gratitude to the following persons in the chemistry department who have made the completion of this dissertation possible. To Dr. A.L. Baumstark Chair, Department of Chemistry, I thank you for the support and encouragement through the years. To Dr. Lucjan Strekowski and Dr. Maged Henary, I thank you for providing the iminosulfuranes for me to study. To Dr. Kathyrn Grant, I thank you for challenging me and taking time to review my dissertation in painstaking detail. I appreciate all your work and time. Dr. Stuart Allison, I would also like to thank for taking time to review my dissertation and asking challenging questions.

Dr. Sekar, I thank you for your help using the 500 MHz NMR. Dr. Robert Simmons, I thank you for always making yourself available to look at my samples under the electron microscope.

This research was supported by National Science Foundation grant, BIR-9214443, the GAAAN fellowship, and the Ambrose H. Pendergrast Fellowship.

Table of Contents

List of Tables

List of Equations

List of Figures

List of Abbreviations

CF	carboxyfluorescein
CSA	chemical shift anisotropy
DMPC	L-α-1,2-dimyristol-sn-glycero-3-phosphocholine
DMSO	dimethylsulfoxide
DSC	differential scanning calorimetry
EDTA	ethylene diamine tetraacetic acid
FFA	free fatty acids
HEPES	N-[2-hydroxyethyl]piperazine-N′-[2-ethanesulfonic acid]
IR	infrared
NOESY	nuclear overhauser effect spectroscopy
SC	stratum corneum
SUV	small unilamellar vesicles
T_m	melting temperature
TPE	transdermal penetration enhancer
TX-100	Triton X-100

1. Introduction

Within the past decade, there has been an increase in the desire to administer drugs transdermally. The advantage of transdermal administration includes elimination of the first-pass effect by the liver, avoidance of the degradation of drugs by the gastrointestinal tract, sustained and controlled release of drugs, and greater compliance from patients. The skin provides an effective barrier to water loss, protects the body from unwanted influences, and prevents the permeation of environmental substances and the entrance of foreign material into the body. This barrier function of the skin is an obstacle to be overcome by transdermal drug delivery. In order to effectively utilize the possibilities created by the use of topically applied drugs, it becomes necessary to understand the nature of skin and mechanisms or other substances that could control the extent of its barrier function. Controlling the barrier function of skin topically would allow medicines to permeate the skin and access the blood supply allowing for systemic delivery of drugs. The advantages of this type of drug delivery include targeting specific areas of the body and decreasing the amount of drug necessary for effect as compared to drugs taken orally.

1.1. Structure of Skin and Its Barrier Function

Skin, the largest organ of the body is composed of several layers including the epidermis and dermis (Figure 1-1). Its thickness is typically 0.1- 1.0 mm, depending on location in the body. The dermis is the largest part of the skin and serves as a means of protection for the underlying organs and provides nutrient necessary for the growth and differentiation of the cells in the epidermis. The epidermis is separated from the dermis by a basale membrane. In the first two layers of epidermis skin cells are synthesized and

in the remaining layers the cells undergo transitions to finally become the characteristically flat corneocytes embedded in a lipid bilayer found in the stratum corneum (SC). The one cell thick layer just above the basale membrane is the stratum basale. In this layer, epidermal stem cells undergo cell division and begin the slow 2 -3 week journey through the higher epidermal layers until reaching the surface layer. The stratum spinosum, the next layer of the epidermis, is typically 2-7 cells thick with polyhedral shaped cells.[1] These preformed stratum corneum cells are present with enzymes.[2] The phospholipids in the cell membranes are degraded into glycerol and free fatty acids, whereas the glycosylceramides are degraded into ceramides.[3] In the transition from stratum spinosum to the stratum granulosum, the organelles are formed in the endoplasmic reticulum and are expelled into the extracellular space surrounding the cells.[2] The stratum granulosum consists of 2-3 layers of diamond-shaped cells. The cytoplasm of these cells looks like thick granules corresponding to the name of this layer. These thick granules are the precursors for the corneocytes located in the SC.[2] In this layer, the majority of the keratin, a structural protein, is produced. In the next thin single layer of cells known as stratum lucidum, the cells lose their nuclei and cell organelles. As the epidermal cells transition to the final layer, the volume of the intercellular space increases from 2 cell layers to 15 layers. The outer layer of the epidermis is the stratum corneum (SC), also known as the horny layer, and contains 10-30 layers of flattened hexagonal dead skin cells where the number of layers depends on the skin location. For example, the skin on the abdomen has a thinner SC with fewer layers of dead skin cells than those found on the bottom of feet. This layer provides the main barrier function of the skin and is typically 0.01 mm, at most 10 percent of the total thickness of skin. The

stratum corneum is a composed of keratinized cells in a lipid bilayer. The bilayer is composed of a milieu of at least six different ceramides with differing head groups and fatty acid chain lengths, free fatty acids (FFA) with greater than 20 carbons, cholesterol, and cholesterol sulfates.[3] The structure is most commonly compared to a brick wall, hence the structure is described by a "brick and mortar model" as shown in Figure 1-2. The bricks in the wall represent the corneocytes or dead skin cells. The mortar in between the bricks is a lipid bilayer composed of a mixture of ceramides, free fatty acids, cholesterol, and cholesterol sulfate. Perturbation of the stratum corneum usually results in a metabolic response that restores the barrier function and limits the bioavailability of drugs administered transdermally.[4]

There are three primary routes of entry into the stratum corneum which include the movement of molecules via the sebaceous glands of hair follicles, across the stratum corneum or by way of the sweat glands.[5] Movement of molecules through an intact SC can be subdivided into two possible routes of entry, transcellular and intercellular.[5] As illustrated in Figure 1-3, the transcellular route involves the movement of drugs across alternating layers of corneocytes and lipid bilayer in order to reach viable tissue. The intercellular and most likely route of permeation into the SC and eventually to the blood supply is through the lipid matrix that surrounds the corneocytes. This disruption could occur through mechanisms such as compounds intercalating into the lipid bilayer or modifying the inherent solubility of skin lipids thereby allowing drugs to penetrate the SC that would normally be unable to overcome the barrier function.[6] A significant effort has been applied to understanding the mechanism through which topically applied drugs can interact with the intercellular bilayer and ultimately overcome the barrier function of

the skin. Realistically, there are very few drugs available that have a high enough permeability coefficient to permeate an intact SC via passive strategies. These drugs are effective at low doses, have relatively small molar masses (< 400 Da) and are lipophilic.[7] There are few drugs that meet these qualifications. As a result, passive transdermal drug delivery is limited to cardiovascular, hormone replacement, contraception, smoking, pain, and motion sickness treatment. [8] Therefore, there is a need for a method of enhancing drug delivery to the viable cells located beneath the SC. From this need arose a method known as transdermal penetration enhancement.

1.2. Transdermal Penetration Enhancers

Several techniques have been developed to facilitate the movement of drugs across the SC and enhance transdermal drug delivery. There are five classifications of methods for improving delivery: drug or vehicle interactions, vesicles and particles, removal or bypass of the SC, electrically assisted methods and modification of the SC.[5] Drug or vehicle interactions involve changing the flux of the drug (Equation 1-1) where flux is dm/dt. If the vehicle of the drug is volatile, upon its evaporation it leaves a supersaturated solution of the drug in a thermodynamic state such that it has a flux greater than one milligram per hour and can overcome the barrier function of the SC.[5]

$$\frac{dm}{dt} = \frac{DC_oK}{h}$$

Equation 1-1 Steady-State flux.[5]
dm/dt is the cumulative mass of pass a unit area of membrane per unit of time.
D is the diffusion coefficient.
C_o is the donor drug concentration.
K represents the partition coefficient of the solute that exists between membrane and bathing solution.
h is the thickness of the membrane.

Another drug vehicle interaction is one in which a vehicle permeates the skin first and "drags" the drug through the skin.[5] The use of prodrugs involves molecules that only become biologically active after enzymes generate the active forms. [8] Finally, the vehicle can increase the solubility of the drug.[5]

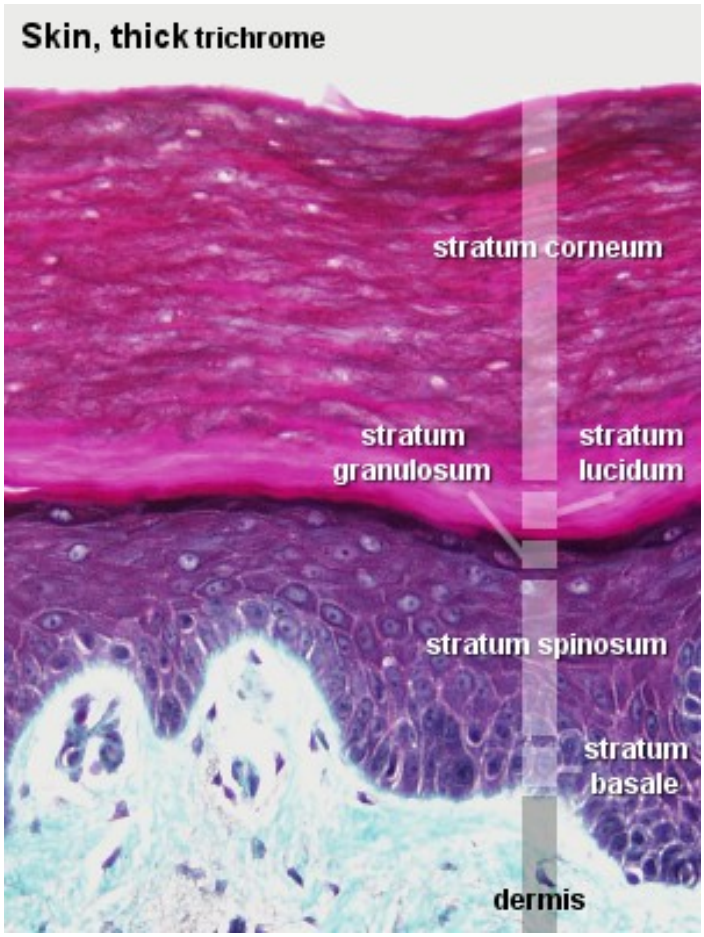

Figure 1-1 Structure of the Skin.[9]

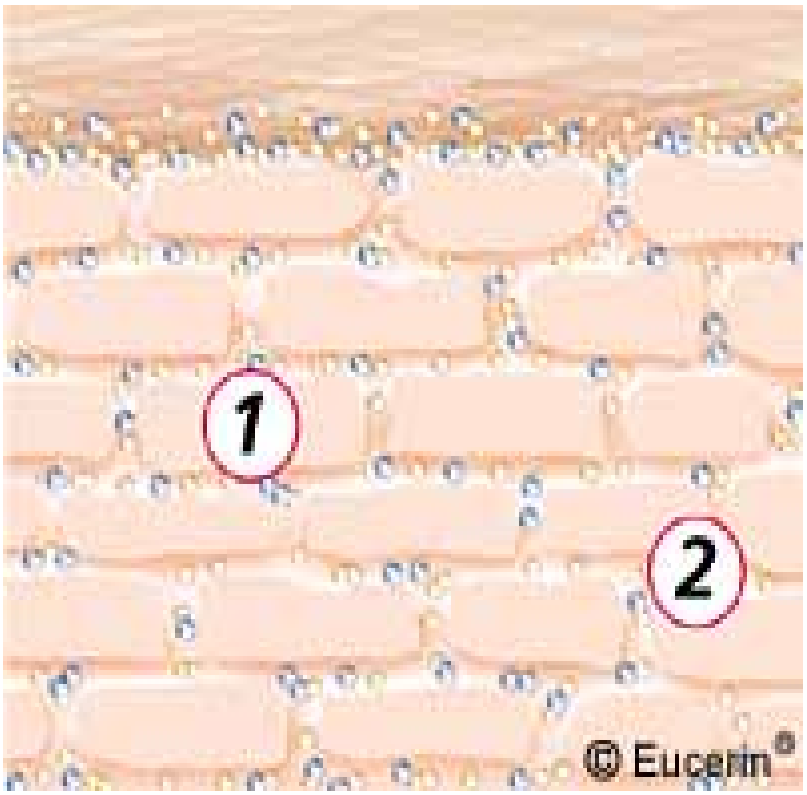

Figure 1-2 "Brick and Mortar" model of the stratum corneum.[10]

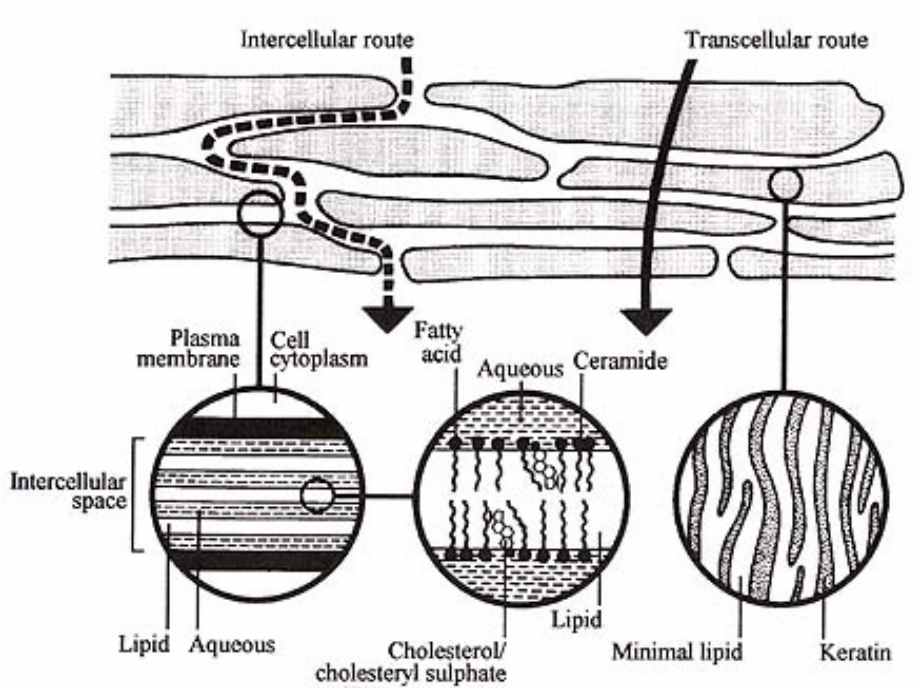

Figure1-3 Stratum corneum and two routes of drug penetration.[5]

Another classification of transdermal penetration involves bypassing or removing the SC. The SC can be bypassed using injections below the horny layer or via the hair follicles in the SC. Recent developments have created the resurgence of this technique that had been abandoned after the realization that the use of tiny needles caused skin damage. Adaptations of this concept include the use of hundreds of microneedles that are coated with the drug or contain the drug to be injected.[5] This method enhances transdermal drug delivery five times. Follicular delivery involves the use of colloidal particles to introduce drugs into the epidermis via the hair follicles. [5]The SC can be removed by chemical peels, dermabrasions, microdermabrasions, and adhesive tape stripping.[11]

Electrically assisted methods of transdermal penetration enhancement include iontophoresis, ultrasound, electroporation, magentophoresis, radio waves and photomechanical waves. Iontophoresis uses a low electric field to create a potential gradient across the membrane in order to transfer charged drugs and most recently neutral and zwitterionic drugs across the SC.[12] The success of iontophoresis is limited by the size of the drug. Some drugs are also able to overcome the barrier of the SC by ultrasound techniques known as sonophoresis or phonophoresis. Ultrasound is vibration at frequencies beyond the human audible range. The force of these sonic waves can increase the fluidity of the SC lipids or the drugs, apply pressure and force molecules through the skin, or perturb the SC lipids to facilitate the movement of drugs across the skin barrier 1000 times greater than normal flux in absence of the sound waves.[13] In a similar manner short high voltage electric pulses produce aqueous pathways across the lipid bilayer in an

application known as electroporation.[7] Electroporation produces transient pores and enables larger molecules than the aforementioned iontophoresis.

The final method of transdermal penetration and focus of this dissertation is the alteration of the SC via hydration or chemical penetration enhancers. A class of enabling compounds has been targeted to the stratum corneum to allow substances to cross the skin barrier. These compounds are known as transdermal penetration enhancers (TPEs) and enhance the skin penetration of drugs via solvation, interaction with the polar head groups of bilayers, disruption of lateral bilayer packing, inducing transitions in the lamellar phases, or protein-lipid interactions.[4] These compounds must be able to reversibly disrupt skin barrier function, be active at low concentrations, be nontoxic, and non-irritating. Finally, they must be soluble in nontoxic, non-irritating media. A variety of different compounds meet these qualifications including water, hydrocarbons, pyrrolidones, fatty acids, esters, alcohols, surfactants, amides, polyols, terpenes, oxazolidines, enzymes, polymers, inhibitors of lipid synthesis, azone and its derivatives, sulfoxides and their analogs, and synergistic mixtures of any of the aforementioned compounds (Figure 1-4).[5]

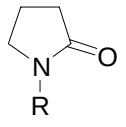

pyrrolidone

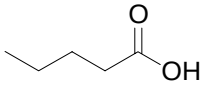

fatty acid

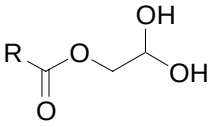

ester

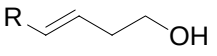

alcohol

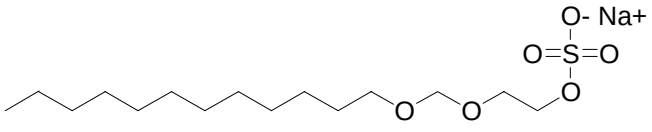

surfactant, sodium laureth

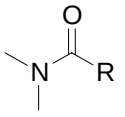

amide

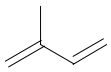

isoprene

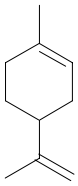

terpene

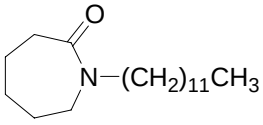

azone®

sulfoxide analog, DMSO

Figure 1-4 Representative structures of transdermal penetration enhancers.
R is any alkyl group.

The action of these compounds can be subdivided into three main avenues, lipid action, protein alteration and promotion of partitioning of drugs (Figure 1-5). Lipid action is a result of fluidization, phase separation, polarity alteration and lipid extraction.[8] Fluidization occurs when hydrophobic lipid enhancers insert in between the hydrophobic tails of the lipids or polar enhancers interact with the polar head groups of the lipids and alter the highly organized structure of the lipid matrix in the SC making the bilayer more fluid. In phase separation TPEs, either create a water pool or form an inverted micelle in the multilayer lipid matrix. Polarity alteration, another lipid interaction of TPEs, occurs when the presence of the enhancers induces repulsion between neighboring lipid molecules. This repulsion disrupts the packing of the lipids and allows drugs to overcome the barrier function of the SC. Finally, lipids can be extracted from the bilayer to create a less dense lipid matrix. Protein alteration can be a function of an enhancer interacting with protein structures and splitting the SC, thus removing the densely packed nature of the SC or denaturing the keratin found in the corneocytes and creating vacuoles introducing a less restrictive entry point for drugs.[8] Promotion of drug partitioning involves the use of enhancers to increase the flux of a drug across the SC. The mechanism of action for many effective transdermal penetration enhancers involves more than one mechanism.

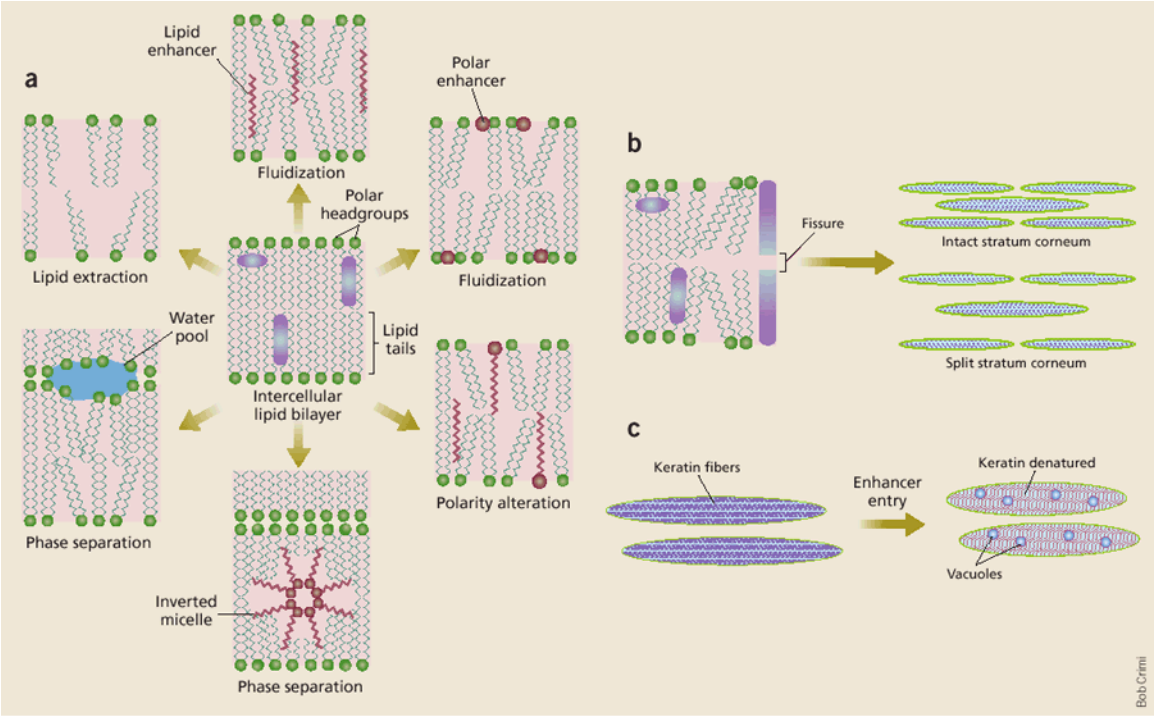

Figure 1-5 Possible mechamisms of action for chemical penetration enhancers. [8]

Water is continuously present in the skin and maintained at constant levels. The SC can hold three-five times its mass in water.[14] The action of skin hydration is two-fold. The presence of water alters the homeostatic gradient and allows for the increase in flux of polar molecules. Secondly, hydrating the skin raises the temperature of the site and swells the corneocytes; as a result the SC is less compact and drugs cross the SC more easily.[14] Pyrrolidines and their derivatives are heterocyclic amides. At low concentrations, pyrrolidones denature the keratin in the corneocytes; where as at higher concentrations, they increase water content and increase fluidity of the lipid matrix.[15] Alkyl pyrrolidines are known to intercalate in the SC lipid bilayer, thus creating greater fluidity in the bilayer.[16] Fatty acids disrupt the packing of the lipid bilayer and increase the permeability of SC. Additionally, some fatty acids act as solvent in the SC: as the fatty acid enters the SC, drugs with a high affinity for the fatty acids are dragged into the SC.[17] Alcohols have been observed to be most effective in enhancing penetration of the SC when the chain length is between 10-12 carbons.[18] Based on these observations and the fact that the carbon chain on the most effective alcohols is similar to the length of the carbon chain on steroid nucleus of cholesterol, it is thought that the penetration enhancement is from the interaction of alcohols with the ceramide–cholesterol or cholesterol-cholesterol interactions in the SC.[18] Both fatty acids and alcohols enhance transdermal penetration by disordering packing arrangement of SC lipid matrix and creating aqueous pores, and by forming complexes with drugs and making them more lipophilic.

There are four types of surfactants: cationic, anionic, nonionic, and zwitterionic. The use of surfactants is limited because most irritate the skin causing tightness, inflammation and erythema.[19] Cationic surfactants are the most damaging to the skin followed by anionic surfactants which are intermediate and nonionic surfactants which are the least irritating. There are two mechanisms of action attributed to charged surfactants, interaction with SC proteins, and extraction of SC lipids by micelle solubilization. [19] Nonionic surfactants result in the least amount of damage to the SC. Consequently, their ability to serve as penetration enhancers is limited. However, nonionics can be used in conjunction with charged surfactants by forming mixed micelles and limiting the deleterious effect of cationic and anionic surfactants.[19] Urea is an amide that is an effective transdermal penetration enhancer. Its mechanisms of action include serving as a moisturizer by increasing water content and lowering the phase transition of the lipid bilayers, thus allowing drugs to permeate the SC more easily.[20] Long exposure time to urea breaks down the keratin.[20] Terpenes are naturally occurring compounds made of varying arrangements and numbers of isoprene units. The differing structures of terpenes work well with different drugs. However, terpenes disrupt the lipid matrix in the SC, interact with the SC proteins and improve partitioning of drugs.[21] Azone® (1-dodecylazacycloheptan-2-one), a TPE currently in clinical trials, distributes homogeneously through the SC lipid matrix and as suggested by molecular modeling, the polar lactam group may force apart the polar head groups in the SC lipid matrix to increase membrane fluidity.[22, 23] Some silicone polymers act as penetration enhancers by increasing the hydrophobicity of the skin surface and in doing so influence the partitioning of hydrophobic drugs into the SC.[24] Dimethyl sulfoxide is has been widely

used in the medical field since the 1960's. [25] It has a high dielectric constant because the polarity of the sulfur and oxygen bond. At low concentrations, DMSO denatures the proteins in the corneocytes and promotes swelling by displacing the water in the interior of the corneocytes. DMSO is most effective at concentrations greater than 60 percent.[25] At these concentrations, DMSO interacts with the polar head groups of the lipid matrix by displacing surrounding water molecules. As a result, channels form in the multilayer lipids of the SC.[25] A series of iminosulfuranes isoelectronic with the sulfoxide group in DMSO (Figure 1-5), where X = H, Cl, Br, and I has been shown to function as potent TPEs in human cadaver and hairless mouse skin. However the mechanism of action is not understood. [26, 27]

1.3. Biological Data of Iminosulfuranes

Since iminosulfuranes are isoelectronic with the sulfoxide group of DMSO, these iminosulfuranes were screened to determine whether their biological activity is similar to that of DMSO.[26] These compounds were initially screened using hairless mouse skin, a highly permeable skin model.[28] If the iminosulfuranes proved active in the mouse skin, it could be an indication that these compounds would be active in human skin. Several parameters were measured in the mouse skin. Two of those parameters to be discussed are ER_J and Q_{24}. ER_J is the ratio of hydrocortisone flux across skin samples in the presence of selected iminosulfuranes to the flux value observed in control experiments. Q_{24} is the amount of hydrocortisone that passes through the skin in 24 hours. The results are summarized in Table 1.

Table 1-1 Permeation parameters of hydrocortisone on hairless mouse skin.[23, 28]

Substituents	ER_J	Q_{24} (μg/cm^2)
Control	1.00	43.1 ± 5.2
DMSO	1.37	45.5 ± 12.1
H	0.88	32.1 ± 10
Cl	1.51	61.9 ± 12.1
I	1.6	121 ± 24
Br	21	996 ± 192

Based on the results DMSO does not appear to have significant activity in comparison to the control. The iodo and chloro derivatives exhibit similar activity to DMSO. The bromo derivative shows activity similar to Azone®, a transdermal penetration enhancer, that is currently used in clinical trials.[28]

Since the bromo and iodo derivatives were the most active compounds in the series of iminosulfuranes tested, further studies were conducted to determine whether the activity would be extended to human cadaver skin.[23] Permeation measurements of hydrocortisone, in the presence of iminosulfurane derivatives, flux and Q_{24}, are shown in Table 2 and support the permeation studies conducted using hairless mouse skin.

Table 1-2 Permeation parameters of hydrocortisone on cadaver skin. [23]

Substituents	ER_J	Q_{24} (μg/cm^2)
Control	1	22.1 ± 5.1
Br	17.0	319.7 ± 24.6
I	0.8	26.0 ± 3.9

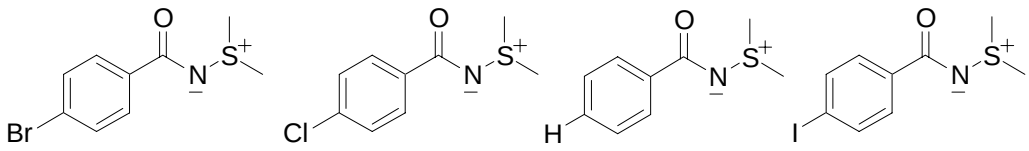

Figure 1-6 Structure of iminosulfuranes.

The permeation of the hydrocortisone in the presence of 0.4 M bromo derivative is significantly higher than in its absence or in the presence of the iodo derivative. Additionally, as concentration of the bromo derivative increases from 0.0 M to 0.4 M, there is a significant increase of the flux of hydrocortisone and caffeine and the amount of hydrocortisone and caffeine present increases over 24 hours.[23]

Because TPEs are known to cause skin irritation, cytotoxicity studies of the iodo and bromo derivative were performed on epidermal keratinocytes and dermoblasts. Cell viability for both the keratinocytes and the dermoblasts showed a decrease in viability with increasing concentrations of iminosulfuranes; however at concentrations less than 0.2 M, there was no statistically significant effect on cell viability.[23] In contrast at concentrations between 0.7 M and 0.9 M, there was a 50 percent decrease in cell viability; therefore ideal concentrations for the use of these TPEs would be less than 0.2 M.

1.4. Phospholipids as Models for Skin

The barrier function of skin resides in the SC which consists of keratin filled dead cells surrounded by a crystalline lamellar lipid. Because the corneocytes are so dense, it is unlikely that TP's applied to the surface of the skin will be able to diffuse through the dense protein structures. Consequently, the most likely route of entry is through the lipid regions surrounding the corneocytes. In order to develop a model system for lipid matrix for the purpose of observing the effect of TPEs on such models, it is necessary to understand the nature of the lipids in the SC and make comparisons to the particular models of choice (DMPC and DMPC-cholesterol liposomes).

The lipid matrix is composed of at least nine different ceramides with lengths varying from 16-33 carbons, cholesterol, and free fatty acids most commonly containing 22 and 24 carbons.[3, 29] Ceramides are amphipathic molecules and are capable of forming stable bilayers in the presence of cholesterol and either a free fatty acid or cholesteryl sulfate.[30] The lipids in the SC form the traditional multilamellar bilayers. Freeze fracture electron microscope studies of human SC show that the lamellar phase has two components, one with a periodicity of 13 nm and the other with a periodicity of 6 nm.[31] Diffraction patterns show that the lateral packing in absence of FFA is hexagonal. However,when FFA is added, the lateral packing changes to orthorhombic. Since orthorhombic packing is more densely packed than hexagonal, the barrier function of SC is supported by the presence of FFA.[31] The chain lengths of ceramides are longer than those of phospholipids typically used in liposomes. Additionally, the head groups of ceramides are small in comparison to those of phospholipids and contain different functional groups such as amides and hydroxyls. Consequently, they are capable of forming intermolecular and intramolecular hydrogen bonds which lends to the difference in the structure of the lipid matrix found in SC and that of phospholipids.[31] Additionally, it has been shown that mixtures of SC lipids can be used to prepare small unilamellar vesicles in a similar way to phospholipid SUV's.[30]

While they are little to no phospholipids present in the SC lipid matrix, phospholipid bilayers provide a useful means of investigating the molecular mechanisms responsible for the activity of transdermal penetration enhancers. Phospholipids are the simplest models that approximate some of the properties of a biological membrane. They structurally resemble bilayers, have a similar thickness and water permeability, as well as

exhibiting similar bending rigidity, surface tension, and viscosity. DMPC, a synthetic lipid, is often used because it undergoes phase transition at a convenient temperature (23.6°C). In a model skin system consisting of DMPC unilamellar vesicles, it has been shown that correlations exist between the biological activity of the aforementioned transdermal penetration enhancers (TPE) and the extent to which these agents bind to DMPC vesicles and perturb the gel to liquid crystal phase transition measured by calorimetry.[27]

1.5. Role of Cholesterol

Cholesterol is an amphiphilic lipid whose structure differs greatly from that of phospholipids and ceramides. The hydrophobic portion of cholesterol is the steroid nucleus which consists of three cyclohexane rings and one cyclopentane ring. The hydroxyl group on the ring serves as the polar head of molecule. Therefore, cholesterol is classified as a lipid with a bulky, stiff hydrophobic tail and a small hydrophilic head.[32] Cholesterol is present in all mammalian cell membranes and is known to order bilayers. The presence of cholesterol in phospholipids induces a change in the morphology of the bilayer that is different from liquid-crystalline state or gel state and produces a new phase described as a liquid–ordered state.[33] In a liquid-crystalline lamellar state, the phospholipids form a bilayer. However their motion has liquid-like properties. In contrast, the lipid hydrocarbon chains in the gel state are extended and tilted slightly to allow for tight packing. Because of the tight packing, there is limited rotation of the hydrocarbons and there is a limited number of water molecules bound to the polar headgroups. The liquid ordered phase is characterized when the rigid steroid nucleus of cholesterol is located in the top portion of the hydrocarbon tail of the phospholipid and

the hydrocarbon tail of cholesterol is in the more disordered part of the bilayer. The cholesterol orders the hydrocarbon tail deep within the bilayer and limits their isomerizations. As a result, there a fewer kinks in the phospholipid bilayer (< 18 carbons) and the width of the bilayer increases.[33] The ordering of the lipids also limits the permeability of molecules through the bilayer. In systems without cholesterol, the disordered kinks produce regions of packing defects. It is through the local regions of defects that small molecules are able to permeate the bilayer. Finally cholesterol in the bilayer decreases the surface area of phospholipids at the interface of water and interferes with the hydrogen bonding or weak electrostatic interactions that occur between phosphate groups of individual phospholipids.[33]

Johnson et al. have shown that there is a correlation between the flux of small (< 500 Da) lipophilic compounds across SC lipids and DMPC and DMPC/cholesterol bilayers where the concentration of cholesterol is 40 mole percent. [34] Based on the compounds evaluated, it was shown that the DMPC and DMPC/cholesterol models exhibited the same qualitative effects. However, there was a departure in the quantitative analysis of the lateral diffusion coefficients in the models. In the DMPC model, the observed diffusion coefficients for the small molecules differed 15-fold from the SC lipid model.[34] There was less of a departure in diffusion coefficients of DMPC/ 40 mole percent cholesterol model compared to SC lipids in that there was only a 3-fold difference.[34] Consequently, DMPC and DMPC/cholesterol preparations can provide useful qualitative information about the effect of iminosulfurane derivatives on the membrane integrity. For quantitative results more information can be obtained from DMPC/cholesterol bilayers than from DMPC alone.

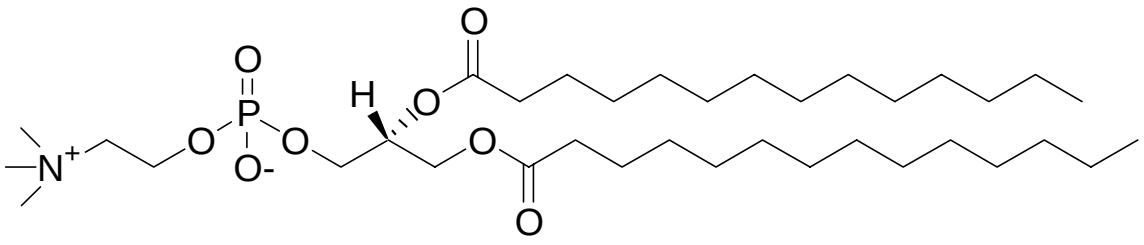

a)

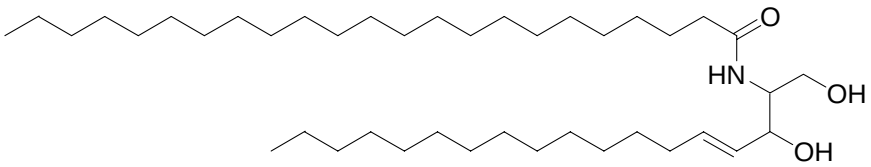

b)

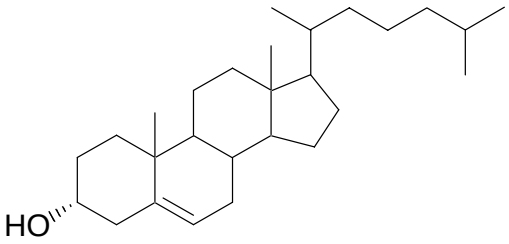

c)

Figure 1-7 Structure of lipids.
a) DMPC b) Ceramide c) Cholesterol

1.6. Effect of Iminosulfuranes on Bilayer Integrity

In order to understand the structure and phase behavior of lipid bilayers in the presence of transdermal penetration enhancers, more specifically the derivatives of iminosulfuranes, there are commonly used physicochemical principles such as those employed by differential scanning calorimetry (DSC), isothermal titration calorimetry (ITC), nuclear magnetic resonance (NMR), fluorescence, x-ray diffraction, and infrared (IR). Because lipids form highly organized structures when they are hydrated, their structures are dependent on various conditions such as temperature, pH, pressure, and the presence of perturbing compounds. DSC is a useful technique for determining the lipid phase transitions of membrane lipids. The principle upon which it operates is the comparison between a sample and an inert reference heated linearly with time. Typically, the sample is a suspension of vesicles in solvent and the inert reference is water or buffer. As long as the lipid does not undergo a phase transition, there in no temperature change and the temperature differential is zero. Once the lipid undergoes a physical conformational change such as a phase transition, there is a temperature differential between the two samples; consequently the instrument changes either the power input or the rate of heat flow to eliminate the differential.[35] After the phase transition is complete, the baseline reestablishes.

It has been shown that correlations exist between the activity of the aforementioned transdermal penetration enhancers (TPE) and the extent to which these agents bind to DMPC vesicles and perturb the gel to liquid crystal phase transition measured by calorimetry. DMPC liposomes undergo two phase transitions, pretransition and main phase transition. Pretransition is characterized by transition of the lipid bilayer

from gel to ripple layer organization, where chain packing changes from a distorted orthorhombic to a hexagonal lattice.[35] The main phase transition occurs when the lipid organization changes from ripple to fluid. Barrow et al. report the effect of 10 mole percent of iminosulfuranes on the pretransition and main phase transitions. [27] The pretransition peak broadens in the presence of 10 mole percent TPEs, which could indicate that they interact with the polar head groups supporting a surface interaction.[27] The bromo derivative of the iminosulfurane caused a shoulder to appear before the main phase transition of DMPC, which could support the destabilization of the DMPC bilayer.[27] The introduction of the bromo derivative into a solution flowing over a DMPC bilayer deposited on a gold support in measurements based on the evanescent wave technique lead to the loss of bilayer mass, suggesting this TPE induced surface degradation of the bilayer had occurred (personal communication). These findings indicate that the iminosulfuranes act through surface dependent interactions. However other results to be discussed support more than surface interaction involvement.

Strong nuclear overhauser effect (NOE) cross peaks between the DMPC surface-located choline $N(CH_3)_3$ moiety protons and the phenyl group protons of the TPEs are also observed.[27] These data suggest that bilayer surface effects may contribute significantly to the mode of action of the compounds. However, previously reported data demonstrate that a NOESY cross peak appears between the terminal methyl of the lipid fatty acid and the phenyl protons of the bromo iminosulfurane. This cross peak suggests that the bromo derivative of the iminosulfurane deeply penetrates into the lipid bilayer causing the phenyl protons to be near the termini of the alkyl chains of DMPC bilayer. However, an alternative interpretation of this NOESY cross peak is that the alkyl chains

of lipids undergo a low-probability bending in vesicles causing the terminal methyl groups to be near the vesicle surface.[36] In view of these observations, ^{31}P NMR has been employed to evaluate whether the activity of the iminosulfuranes described in Figure 1-1 is dependant on their deep penetration into the DMPC and the DMPC-cholesterol bilayers and by extension into the skin. The degree to which the perturbation of these compounds extends into the bilayer interior in contrast to surface activity is unclear. [27]

Carboxyfluorescein is a fluorophore that undergoes self-quenching at high concentrations (100 mM) via the formation of dimers. Once the interior of the vesicle contained the fluorophore in excess of the threshold quenching concentration, vesicles exhibited minimal fluorescence. If the addition of a TPE to the vesicle suspension disturbs the integrity of the bilayer, the carboxyfluorescein is released in a monomer fluorescent form. The release CF is expected to correlate with the perturbation of the bilayer. Therefore, the effects of these iminosulfuranes on bilayer integrity of DMPC and DMPC-cholesterol liposomes have been characterized using fluorescence spectroscopy.

2. Materials and Methods

2.1. Materials and Methods for DMPC Preparations

2.1.1. Materials

Synthetic L-α-1,2-dimyristol-sn-glycero-3-phosphocholine (DMPC) was obtained from Avanti Polar Lipids, Alabaster, Alabama. Potassium chloride, reagent grade was purchased from Baker & Adamson Company, and N-[2-hydroxyethyl]piperazine-N′-[2-ethanesulfonic acid] (HEPES) and cholesterol, 99 percent purity, were obtained from the Sigma Chemical, St Louis, Missouri. Ethylene diamine tetraacetic acid (EDTA) and Methanol, Optima purity, were obtained from Fisher Scientific, Fair Lawn, New Jersey. Chloroform, OmniSolv grade, was obtained from EM Science, Gibbstown, New Jersey. Deuterium oxide was obtained from the Aldrich Chemical Company. Halogenated iminosulfuranes were synthesized by the research group of Professor L. Strekowski.[28]

2.1.2. Vesicle Preparation

Small unilamellar vesicles were prepared by rehydrating DMPC with 10 mM HEPES buffer with 160 mM potassium chloride and 0.8 mM EDTA at pH = 7.5 and used to prepare vesicles by the technique of Bammel et al.[37] The 9 mM suspension was premixed for 5 minutes and sonicated for 40 minutes (40 percent duty cycle) at 35 ºC under a stream of nitrogen. The resulting solution was centrifuged at 130,000 at 35 ºC to remove particulate matter. The supernatant was retained and stored in the oven at 35 ºC. This method produces nominally 300 Å – diameter unilamellar vesicles.

2.1.3. Preparation of ^{31}P NMR Samples

The ^{31}P NMR spectra were obtained at 202 MHz at 35ºC using proton decoupling and a pulse width of 16.5 μs and acquisition time of 0.800 s. The free induction decays were obtained with 6000 transients and a relaxation delay time of 2.0 s and 150 Hz line broadening factor. The spectra were recorded using a Varian Inova 500 MHz Fourier Transform spectrometer. The magnetic field strength was locked to an internal deuterium standard, consisting of 10 percent by volume deuterium oxide that was added to the supernatant retained after vesicle preparation. Probe temperature was 35 °C. All peak shifts were referenced to an external standard of 10 percent by volume of trimethylphosphate and 10 percent by volume of deuterium oxide in 10 mM HEPES buffer with 160 mM potassium chloride and 0.8 mM EDTA at a pH = 7.5. An initial ^{31}P NMR spectrum was acquired without the addition of the Pr^{3+} shift reagent. After obtaining the spectrum of the unilamellar vesicle solution without the shift reagent, 4.5 mM Pr^{3+} was added to the sample. The spectrum was again recorded after maximum resonance separation was achieved, nominally after 18 h, and 10 mole percent iminosulfurane was then added to the sample, after which the spectrum was monitored over an additional 66 h. All spectra were recorded in triplicate unless otherwise noted.

2.1.4. Preparation of Iminosulfurane Solutions

Three millimolar solutions of iminosulfuranes were prepared in HEPES buffer (160 mM KCl and 10 mM HEPES) by adding no more than 4 percent ethanol to aid in dissolution of the iminosulfuranes.

2.2. Materials and Methods for ^{31}P NMR: Iminosulfuranes and DMPC and Cholesterol Preparations

2.2.1. Materials

Cholesterol, 99 percent purity, was obtained from Sigma Chemical, St Louis, Missouri. The remaining materials utilized are described in section 2.1.1.

2.2.2. Vesicle Preparation

DMPC and cholesterol present at 16 mole percent and 30 mole percent were dissolved in chloroform/methanol 2:1 by volume mixing. The phospholipids mixture was dried by rotary evaporation to a thin film. The resulting thin film was placed under high vacuum overnight to further evaporate any additional solvent. Dried films were stored at 0 ºC under vacuum. The dried films were rehydrated with 10 mM HEPES buffer in 160 mM potassium chloride at pH = 7.5 and used to prepare vesicles by the technique described in section 2.1.2.

2.2.3. Preparation of ^{31}P NMR Samples

Samples were prepared as described in section 2.1.3. without EDTA.

2.3. Materials and Methods for Carboxyfluorescein Preparations

2.3.1. Materials

A mixture of isomers of (5)-and(-6)-carboxyfluorescein (CF) was purchased from Molecular Probes and purified before use. Cholesterol, 99 percent purity, Sephadex G-50 and Sephadex LH-20 were obtained from Sigma Chemical, St Louis, Missouri. Triton X-100, electrophoresis grade was obtained from Fisher Scientific, Fair Lawn, New Jersey. Additional materials are referenced in section 2.1.1.

2.3.2. Purification of Carboxyfluorescein

In order to the prepare carboxyfluorescein liposomes, the CF was recrystallized and purified according to a protocol written by Zuidam et al.[38] In order to remove the polar contaminants, CF was dissolved in ethanol and boiled with activated charcoal in a water bath. The charcoal was filtered and the resultant solution was recrystallized with the addition of ice cold water and cooled slowly at -20 ºC overnight. The precipitate was dried with a Büchner funnel and then in a vacuum dessicator.[38]

To remove the hydrophobic contaminants, a 2 M solution was prepared with the previously purified CF by dissolving the CF in NaOH and adjusting the pH to 7.5 by the addition of 6 M HCl while heating the solution to 50 ºC to aid in dissolution. The resultant solution was placed on a Sephadex LH-20 hydrophobic column (2.5 x 40 cm). The sample was eluted using HEPES buffer (10 mM HEPES, 160 mM potassium chloride and 0.8 mM EDTA). Hydrophobic impurities remained on the top of the column as a nonfluorescent residue. The purity of the collected fractions was examined using silica gel thin layer chromatography with a solvent system of chloroform, methanol, and water with a by volume ratio of 65:25:4. The pure fractions were pooled and adjusted to the 100 mM for liposome preparation. The concentration of the pooled fractions was determined by measuring the absorbance at 492 nm, since the molar extinction coefficient of CF is 75,000 M^{-1} cm^{-1} at 492 nm.[38] All absorbance measurements were made using a CARY 3G UV-visible spectrophotometer.

2.3.3. Calibration Curve and Self-Quenching Measurements of Carboxyfluorescein

A set of standard dilutions was prepared from a 0.057 mM stock solution of carboxyfluorescein in HEPES buffer. Sequential tenfold dilutions were made concentrations and the fluorescence of the resulting solutions was measured using a using a Photon Technology Instrumentation QuantaMaster™ Spectrofluorometer. The same stock solution was used to prepare test solutions for assessing the range in which CF self-quenches. Data were recorded using FeliX™ software. The excitation wavelength was 460 nm and emission was scanned from 480- 650 nm at a 2 nm spectral bandwidth and 1 nm step size with a 1 s integration time.

2.3.4. Stern-Volmer Analysis

Solutions of carboxyfluorescein were injected with variable amounts of bromo and iodo derivative using a Hamilton syringe. The fluorescence was recorded using a Photon Technology Instrumentation QuantaMaster™ Spectrofluorometer. Data were processed using FeliX™ software. The fluorescence emission of CF was recorded at 523 nm (λ_{ex} = 492 nm).

2.3.5. Preparation of Vesicles with CF

Vesicles encapsulated with carboxyfluorescein were prepared as described in section 2.1.2 and shown in Figure 2-1. However; the DMPC and DMPC-cholesterol preparations were suspended in a 100 mM CF solution prior to sonication. Unencapsulated CF was removed using a Sephadex G-50 (2.5 x 40 cm) water jacketed column equilibrated with HEPES buffer and pre-saturated with CF-free vesicles made from DMPC and DMPC-cholesterol depending upon the lipid used to encapsulate the CF.

The vesicles were eluted using HEPES buffer (10 mM HEPES, 160 mM potassium chloride and 0.8 mM EDTA).

2.3.6. Electron Microscopy

The electron micrographs were obtained using a JEOL 100CX-II Transmission Electron Microscope. Ten microliters of the vesicle suspension were placed on a nickel formvar coated grid and allowed to sit for one minute. The excess suspension was removed with filter paper. The remaining sample was negatively stained with 1 percent uranyl acetate.

2.3.7. Determination of CF Release from Vesicles

The release of CF was used to measure the integrity of the bilayer. Fluorescence intensities were obtained with a Photon Technology Instrumentation QuantaMaster™ Spectrofluorometer maintained at 35°C. Data were processed using FeliX™ software. The fluorescence emission of CF was recorded at 523 nm (λ_{ex} = 492 nm) at a 2 nm spectral bandwidth and 1 nm step size with a 1 s integration time. Measurements were taken in one second intervals. 100 μL of vesicles encapsulated with CF was combined with varying concentrations and diluted to total volume of 2.2 ml with HEPES buffer (10 mM HEPES and 160 mM potassium chloride). The emission fluorescence intensity was measured before and after the addition of 20 percent v/v Triton X-100 for a final concentration of 1 percent.

$$R(t) = \frac{I(t) - I(0)}{I(\infty) - I(0)} \times 100$$

Equation 2-1 Equation for the percent release of CF.
R(t) is the percentage of CF released. I(t) is fluorescence intensity at time t. I(0) is initial fluorescence intensity and I(∞) is maximum fluorescence intensity.

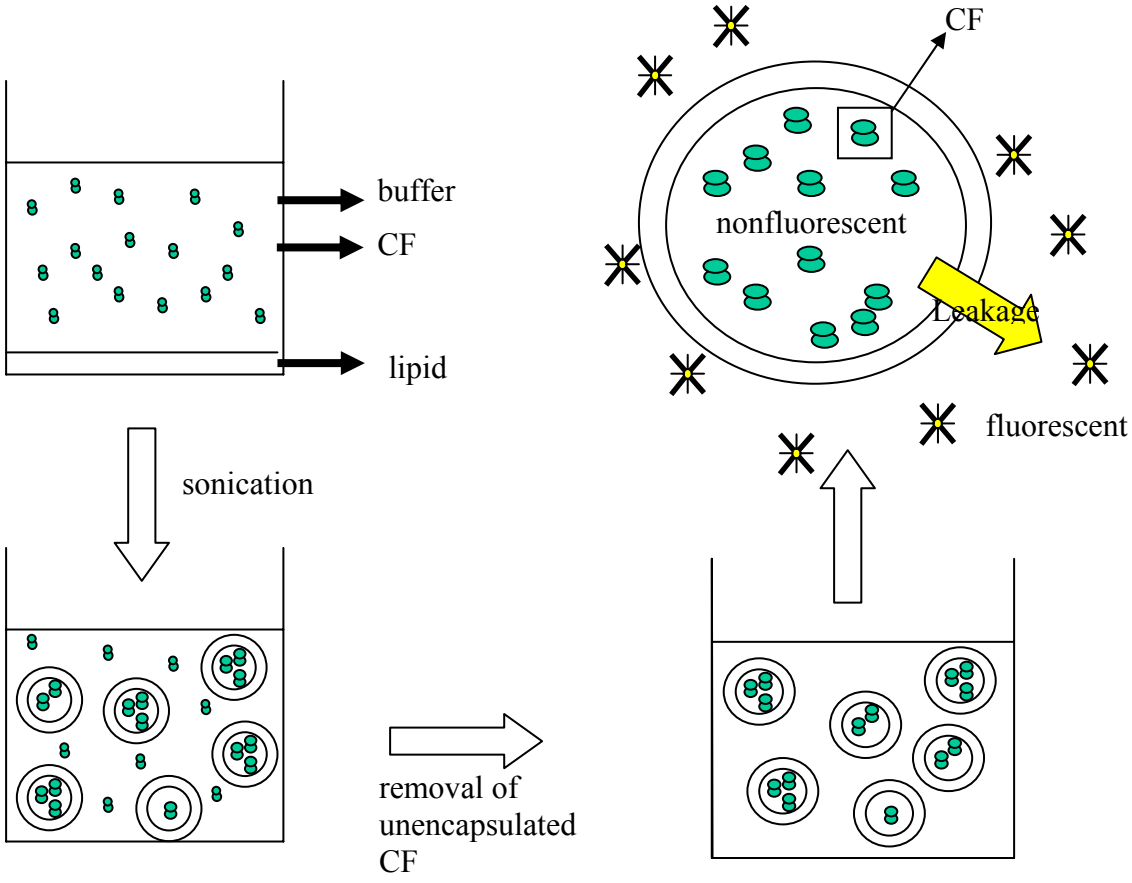

Figure 2-1 Scheme for the preparation of carboxyfluorescein liposomes.

3. Results

3.1. Interaction of Bromo Derivatives with DMPC Liposomes

Figure 3-1 illustrates the effect of bromo iminosulfurane derivative on DMPC liposomes hydrated in HEPES buffer containing EDTA. The data were fit by linear regression. Peaks shifts were referenced to an external trimethylphosphate standard in HEPES buffer with EDTA (see the Materials and Methods section 2.1.3). In DMPC vesicles containing no cholesterol, the bromo derivative decreases the ^{31}P resonance separation at a rate that is only marginally greater than that due to vesicle aging (Figure 3-1). At 0.1 mole percent, the bromo derivative appears to inhibit the reduction due to the normal aging as observed in the control. The vesicles do exhibit an aging effect. However, when the bromo derivative concentration is 0.2 mole percent or greater, the peak separation decay rate is greater than the decay of the vesicles alone. A plot of the slopes from the regression fit is plotted versus mole percent (Figure 3-2). At 5 and 10 mole percent, there is a significant difference in the slopes, indicating an increase in the decay of peak separation in the presence of bromo iminosulfuranes at these concentrations.

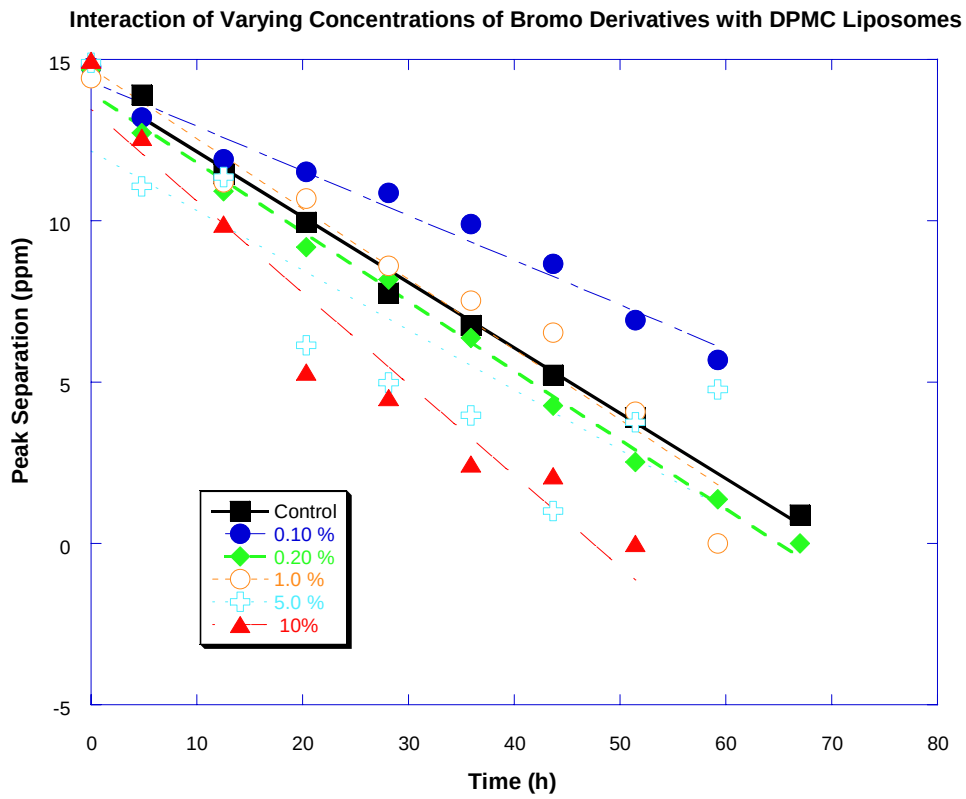

Figure 3-1 Interaction of varying concentrations of bromo iminosulfurane derivative with DMPC liposomes in HEPES buffer with EDTA.
Data were fit by linear regression. Peaks shifts were referenced to an external trimethylphosphate standard in HEPES buffer with EDTA (see the Materials and Methods section 2.1.3).

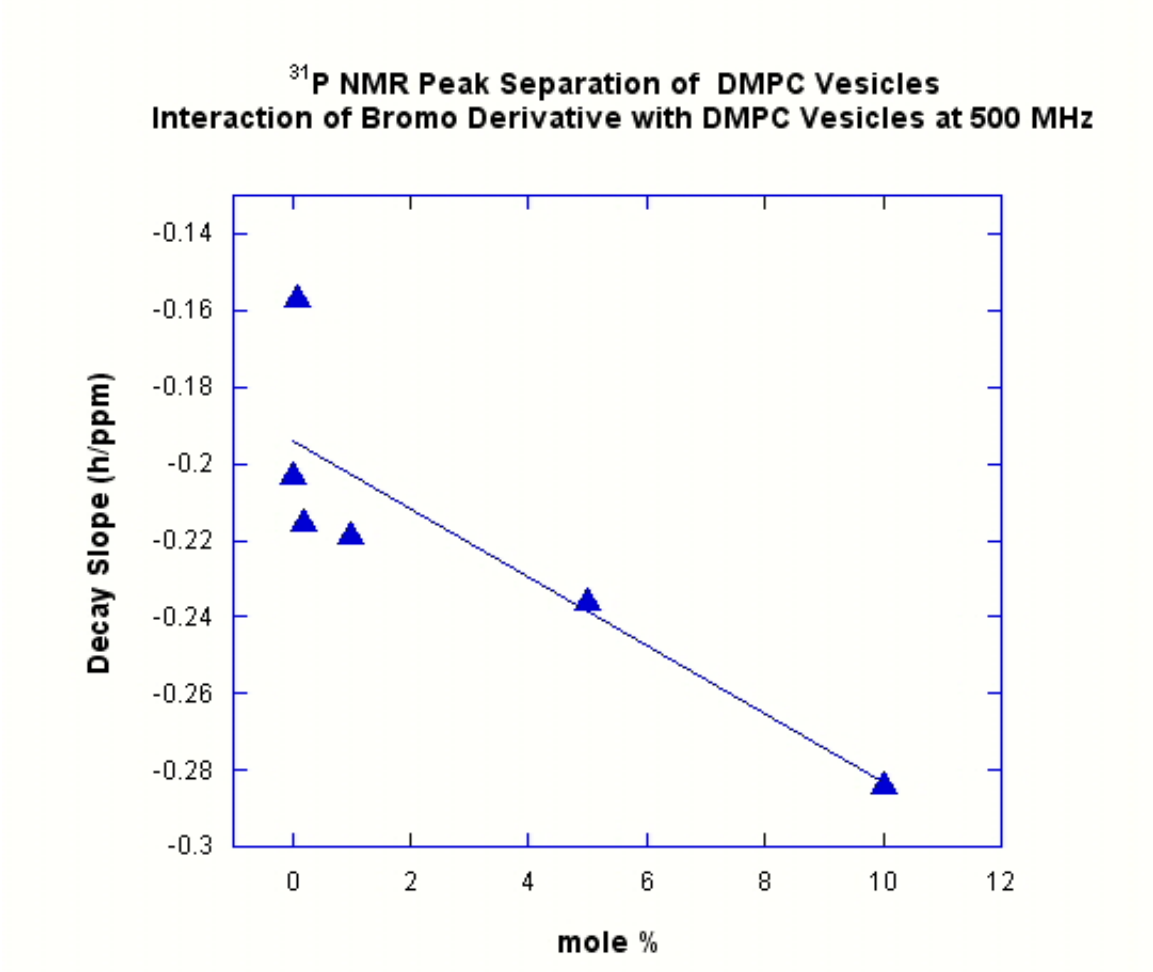

Figure 3-2 Plot of slopes of varying concentrations of bromo iminosulfurane derivative of DMPC liposomes in HEPES buffer with EDTA.
Data were fit by linear regression. Peaks shifts were referenced to an external trimethylphosphate standard in HEPES buffer with EDTA (see the Materials and Methods section 2.1.3).

3.1. Interaction of Varying Concentrations of Iodo Derivatives with DMPC Liposomes

The decay of peak separation of varying concentrations of iodo iminosulfurane derivative of DMPC liposomes in HEPES buffer with EDTA was plotted (Figure 3-3). The data were fit using second order polynomials. At 0.1 mole percent, the iodo derivative appears to inhibit the reduction due to the normal aging as observed in the control. In DMPC vesicles containing no cholesterol, concentrations of at least 1 mole percent iodo derivative also decrease the ^{31}P resonance separation, but at a rate that is only marginally greater than that due to vesicle aging (Figure 3-3). Increasing the concentration of the iodo derivative increases the decay of peak separation. However, in contrast to the control, the peaks do not collapse to zero within 54 h, but reach a plateau.

3.2. Summary of Interactions of Iminosulfurane Derivatives with DMPC Liposomes at 10 mole Percent and 20 mole Percent

After 10 h, the 10 mole percent of the bromo derivative accelerates the decay of peak separation. The peak separation versus time plot exhibits saturation when the chloro or iodo TPE derivatives are present (Figures 3-3 and 3-4). The chloro derivative appears to inhibit the reduction due to the normal aging as observed in the control. The ^{31}P peak separation corrected for the aging effect exhibits saturation 20 h after the bromo derivative has been added**.** The effect of the chloro and iodo derivatives could not be distinguished from the aging effect in the control, TPE–free, DMPC vesicles.

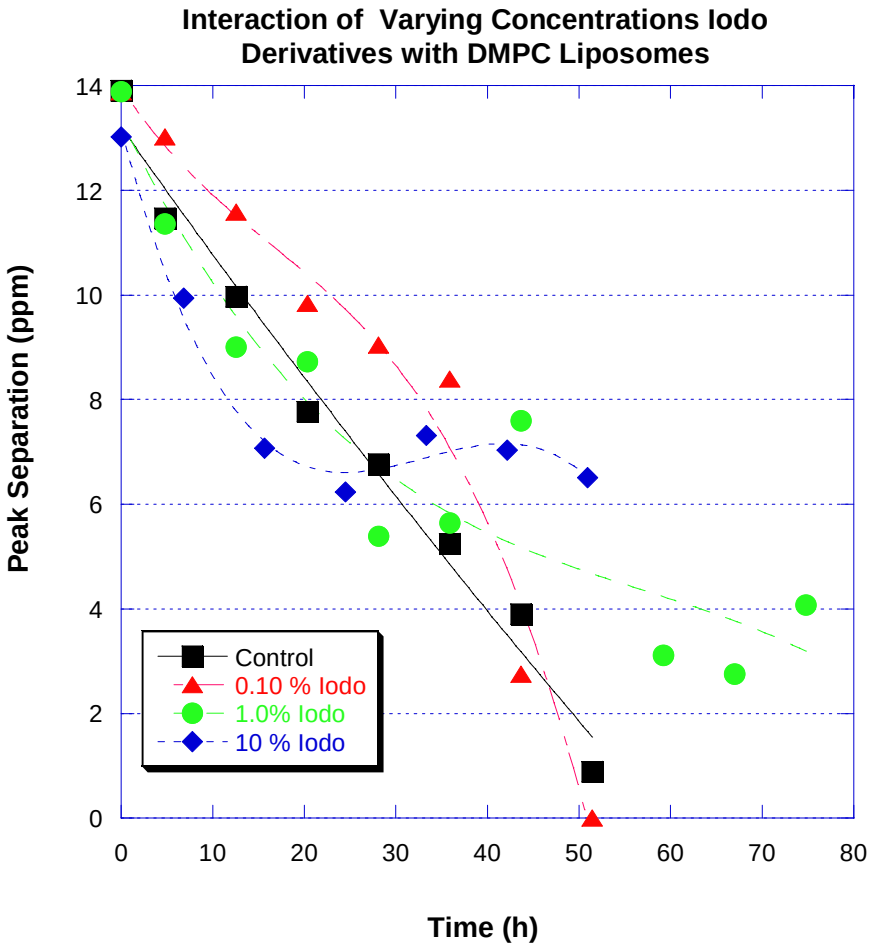

Figure 3-3 Interaction of varying concentrations of iodo iminosulfurane derivatives with DMPC liposomes in HEPES buffer with EDTA.
Data fit using a 2nd order polynomial. Peaks shifts were referenced to an external trimethylphosphate standard in HEPES buffer with EDTA (see the Materials and Methods section).

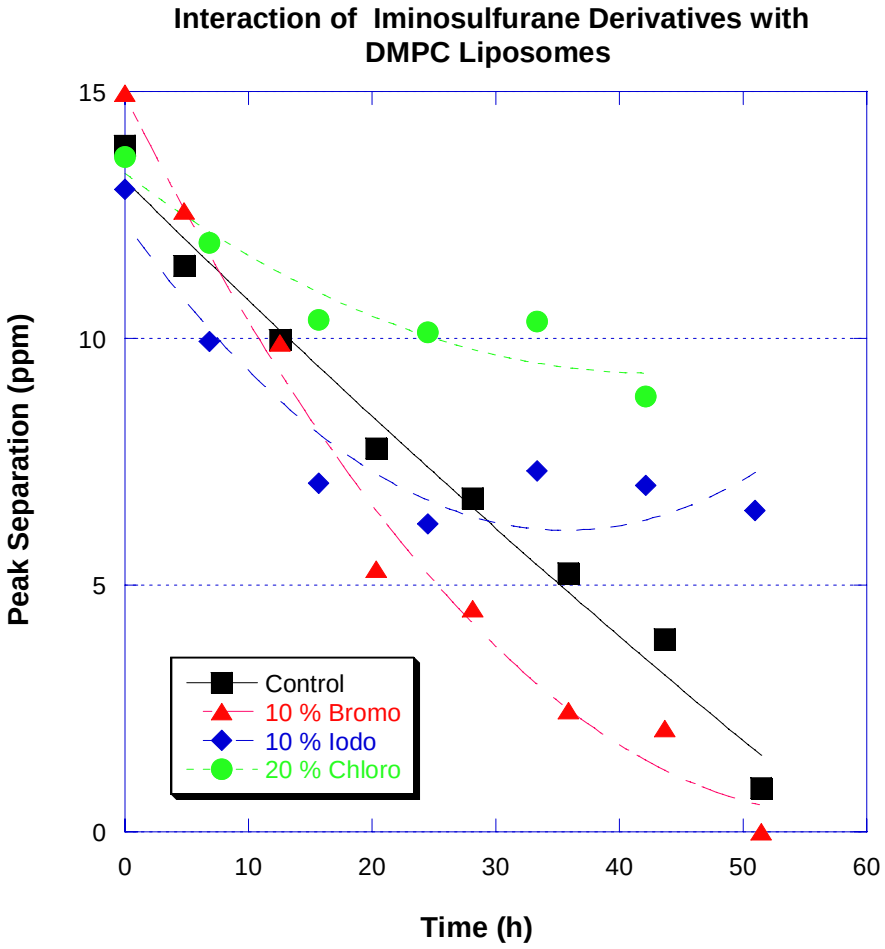

Figure 3-4 Interaction of iminosulfurane derivatives with DMPC liposomes.
Data were fit using 2nd order polynomial. Peaks shifts were referenced to an external trimethylphosphate standard in HEPES buffer (see the Materials and Methods section).

3.3. Effect of Praseodymium Ion on DMPC Liposomes

Since the EDTA present in the HEPES buffer chelates a portion of the Pr^{3+}, removal of the EDTA requires significantly less shift reagent. A plot of shift reagent versus ^{31}P chemical shift separation between the inside and outside phosphate resonances was fit with a 2nd order polynomial (Figure 3-5). Peak separation increases with an increase in concentration of shift reagent, but approaches a maximum with 4.5 mM shift reagent. Results were similar to those observed with the addition of calcium and lanthanum ions to outside of the phospholipid vesicles formed from egg phosphatidylcholine.[39] Hutton et al. also showed the effect praseodymium encapsulated in the interior of the vesicles on peak separation. These titration curves were used to determine inner and outer radii of lipid bilayers and had a similar shape as the curve in Figure 3-5. Figure 3-6 shows the spectra of DMPC without EDTA in the buffer after the addition of 0.90 mM Pr^{3+}. The resonances from the inner and outer leaflet collapse within 25 h. After the addition of 1.35 mM $Pr^{3+}$and 4.5 mM Pr^{3+}, the resonances collapse within 33 h as shown in Figures 3-7 and 3-8, respectively. Decays of peak separation of DPMC liposomes without EDTA in the buffer vary with different concentrations of Pr^{3+}. The data were fit with linear regressions (Figure 3-9). Increasing the shift reagent concentration increased the rate of decay.

3.4. Effect of Bromo and Iodo Derivatives on DMPC Liposomes in Absence of EDTA in the Buffer

Figure 3-8 shows the spectra of DMPC after the addition of 4.5 mM Pr^{3+} over time. Spectrum (a) was obtained before the addition of shift reagent. Spectra (b-f) were obtained in over a period of 42 h. The spectra in Figures 3-10 and 3-11 show the effect

of 10 mole percent bromo iminosulfurane derivative and 10 mole percent iodo iminosulfurane with DMPC liposomes in HEPES buffer, respectively. In spectrum (a) are the phosphorus signals with no shift reagent. Spectra (b-j) illustrate the effect of the appropriate derivative as a function of time. Peaks shifts were referenced to an external trimethylphosphate standard in HEPES buffer (see the Materials and Methods section 2.1.3). The peak separations obtained from these spectra were plotted as a function of time (Figure 3-13). The data were fit by a 2^{nd} order polynomial. In DMPC vesicles containing no cholesterol, the bromo derivative decreases the ^{31}P resonance separation to zero within 51 h, whereas the decrease in the peak separation caused by the presence of the iodo derivative was more than half of its original value. The decay rates attributed to the effect of the bromo and iodo derivatives were greater than in their absence.

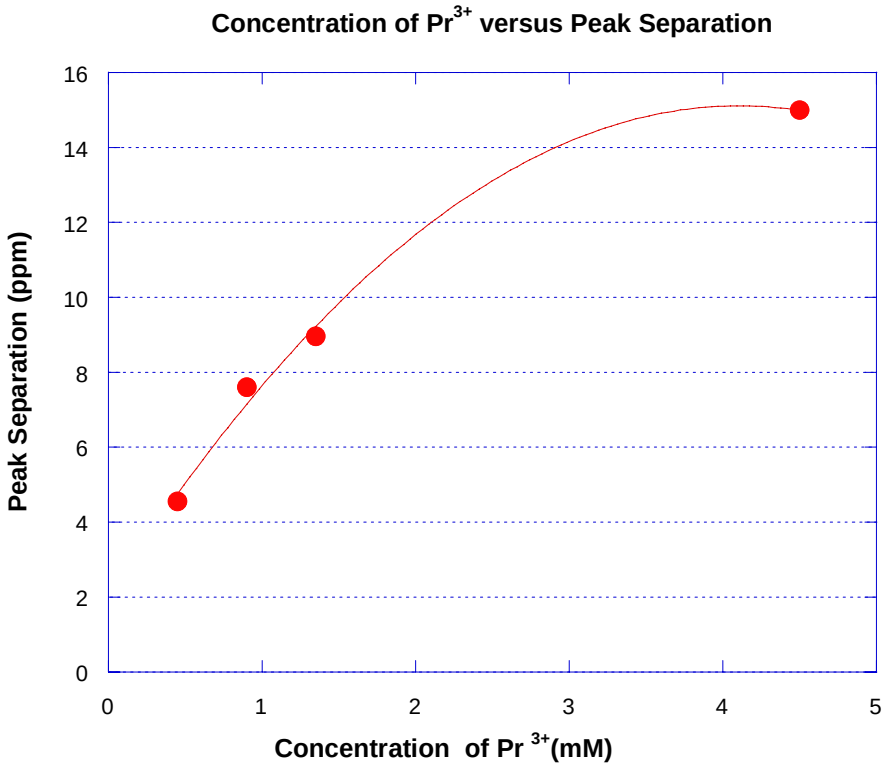

Figure 3-5 ^{31}P chemical shift separation between inside and outside phosphate resonances versus the concentration of Pr^{3+}.
The data was fit with a 2nd order polynomial.

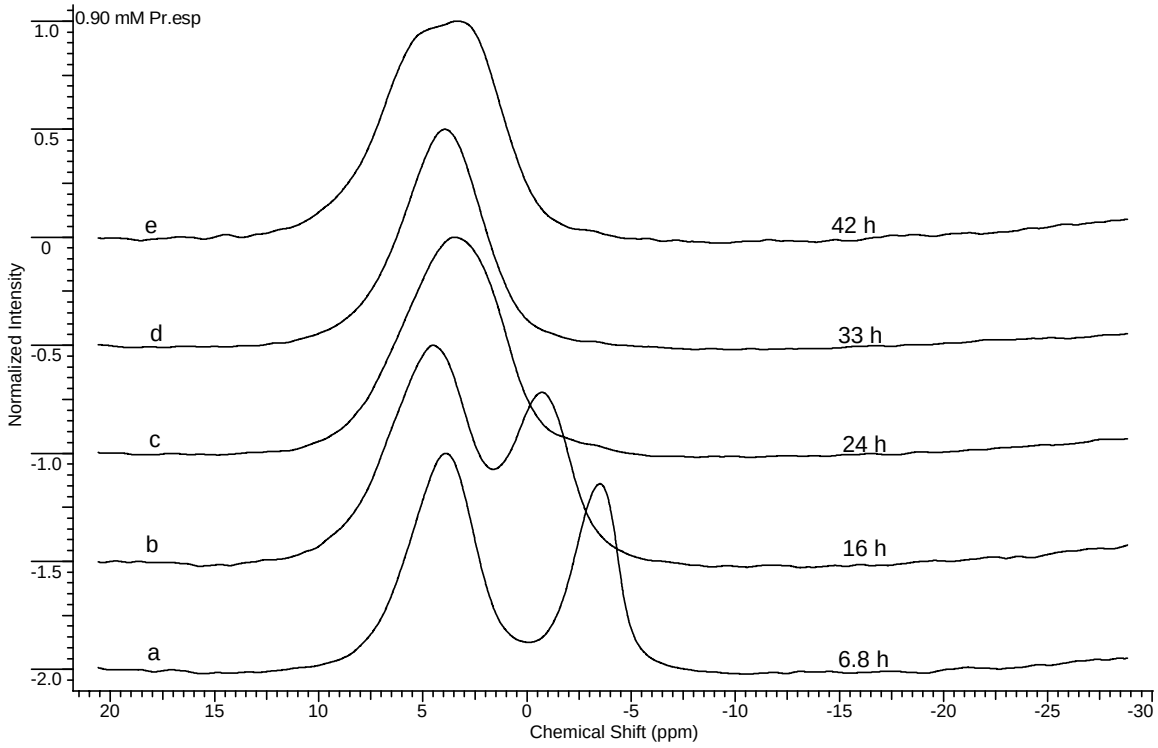

Figure 3-6 Spectra of DMPC liposomes with 0.90 mM Pr^{3+}.
Spectra (a-e) were obtained after the addition of 0.90 mM $PrCl_3$. Peaks shifts were referenced to an external trimethylphosphate standard in HEPES buffer (see the Materials and Methods section 2.1.3).

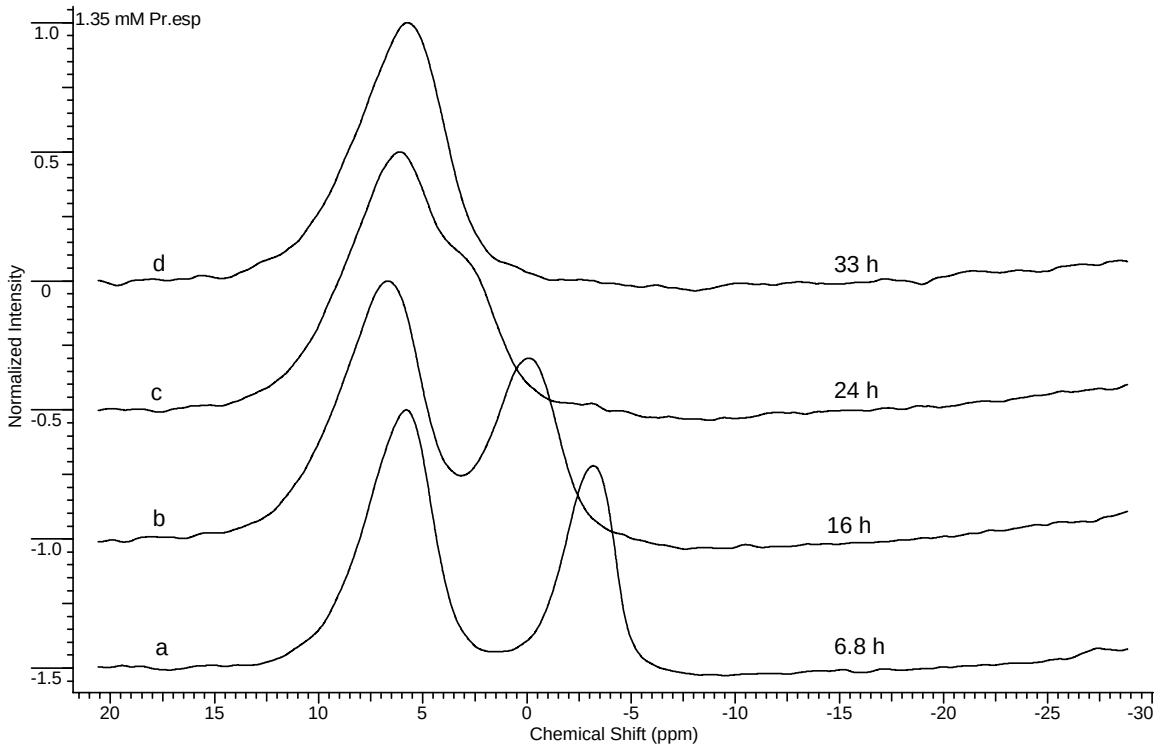

Figure 3-7 Spectra of DMPC liposomes with 1.35 mM Pr^{3+}.
Spectra (a-d) were obtained after the addition of 1.35 mM $PrCl_3$. Peaks shifts were referenced to an external trimethylphosphate standard in HEPES buffer (see the Materials and Methods section 2.1.3).

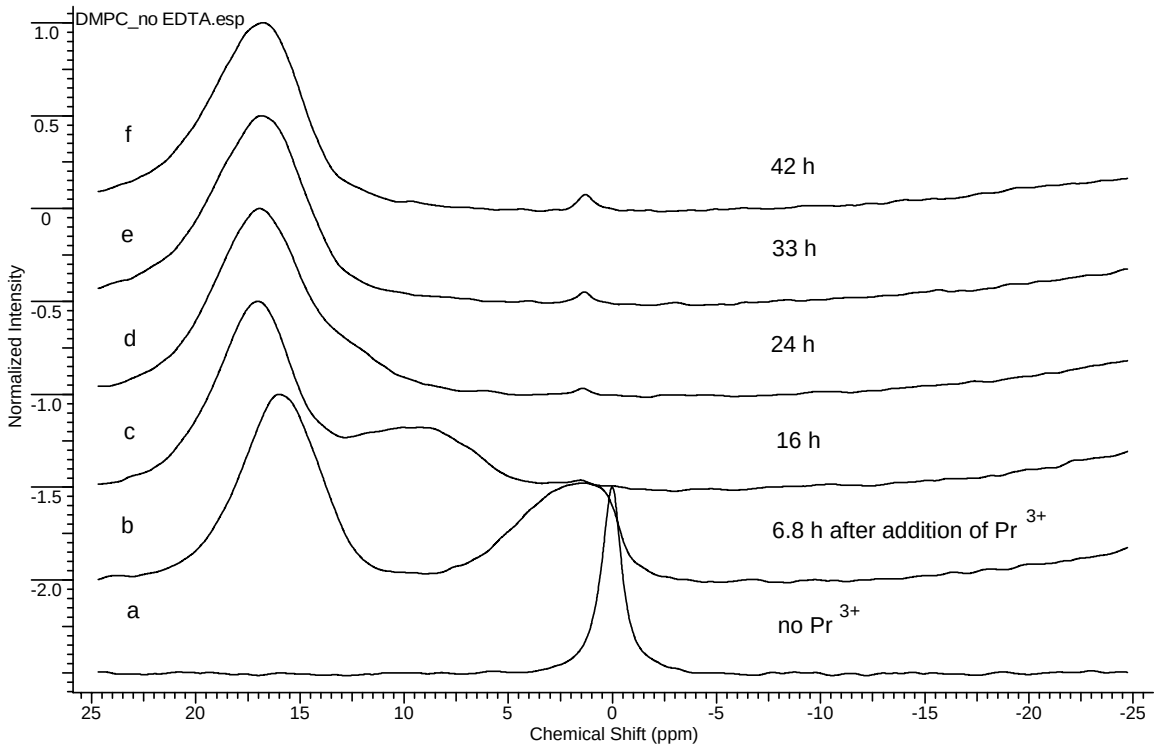

Figure 3-8 Spectra of DMPC liposomes with no EDTA.
(a) is the phosphorus signal with no Pr^{3+}. Spectra (b-f) were obtained after the addition of 4.5 mM $PrCl_3$ Peaks shifts were referenced to an external trimethylphosphate standard in HEPES buffer (see the Materials and Methods section 2.1.3).

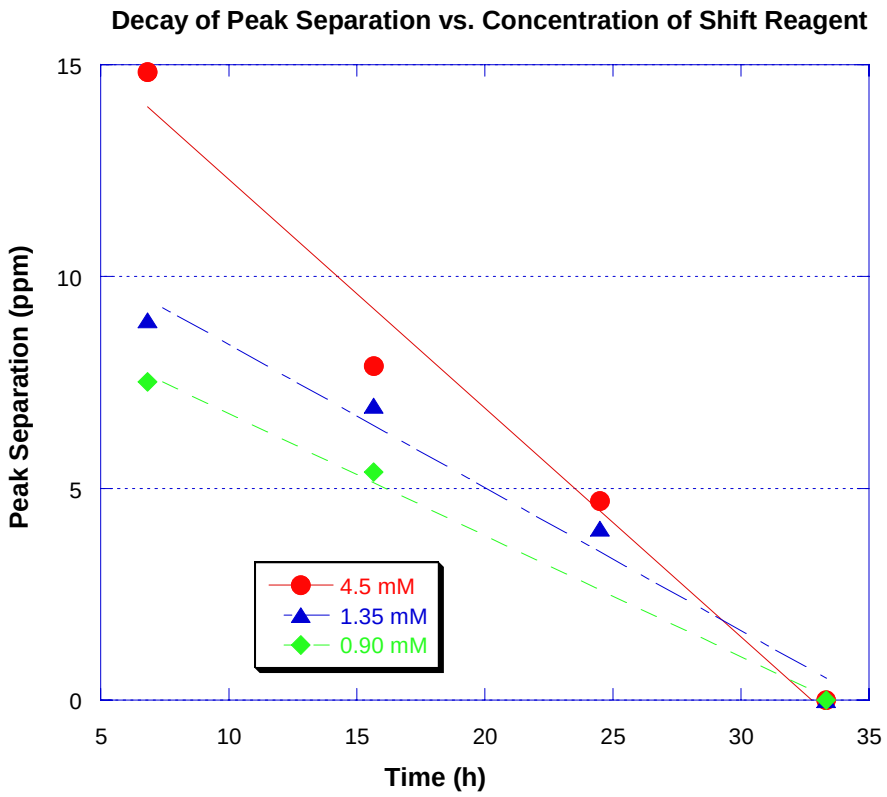

Figure 3-9 The peak separation of DMPC decays in absence of iminosulfurane derivatives at varying concentrations of Pr^{3+}.
The data were fit by a linear regression.

3.5. Comparisons of Decay Rates with DMPC Liposomes Containing Varying Concentrations of Cholesterol

The ^{31}P NMR spectra were acquired for liposomes containing varying mole percent of cholesterol, more specifically 8.8, 16, 27, and 35 as described in Material and Methods section 2.1.3. Figures 3-13, 3-14, 3-15, and 3-16 show the spectra these liposomes containing 8.8, 16, 27, and 35 mole percent of cholesterol, respectively. After the addition of 0.45 mM of Pr^{3+}, the decay of peak separation was monitored over time. The resonances associated with the inner and outer leaflet of liposomes containing 8.8 mole percent collapsed to one peak within 25 h. The peak separation of liposomes containing 16 mole percent and 27 mole percent decreased to 5.5 ppm over 84 h and 8.97 ppm over 66 h respectively. The liposomes containing 35 mole percent cholesterol exhibited the smallest decay of peak separation with resonances separated by 11 ppm after 92 h. The stability of the liposomes varied with concentration of cholesterol as shown by Figure 3-17. The peak separations were plotted as a function of time for the different liposomes preparations. The data from 8.8 and 16 mole percent were fit with a 2^{nd} order polynomial, whereas the data from 27 and 35 mole percent were fit with a 3^{rd} order polynomial. Increasing the concentration of cholesterol stabilizes the liposome, thereby minimizing the decrease in peak separation over time.

3.6. ^{31}P NMR of DMPC and 16 Mole Percent Cholesterol

Figure 3-7 shows the peak separation of DMPC liposomes containing 16 mole percent cholesterol over time. Spectrum (a) is the ^{31}P resonance in absence of shift reagent. Within minutes of the addition of the slowly penetrating shift reagent, the single

phosphorus peak is split into two peaks, allowing for differentiation of the inner and outer leaflet. However, maximum peak separation occurs within 18 h of the addition of Pr^{3+}(Spectra b-c).

Figure 3-8 shows the control which is the peak separation of DMPC liposomes containing 16 mole percent cholesterol over time. Spectrum (a) is the resonance of the phosphorus head group in absences of shift reagent. Within minutes of the addition of the slowly penetrating shift reagent, the single phosphorus peak is split into two peaks allowing for differentiation of the inner and outer leaflet. However, maximum peak separation occurs within 18 h of the addition of Pr^{3+}(Spectra b-d). The peak separation is monitored over the next 66 h (Spectra e-n). After 84 h the peak separation decreases to 5.5 ppm.

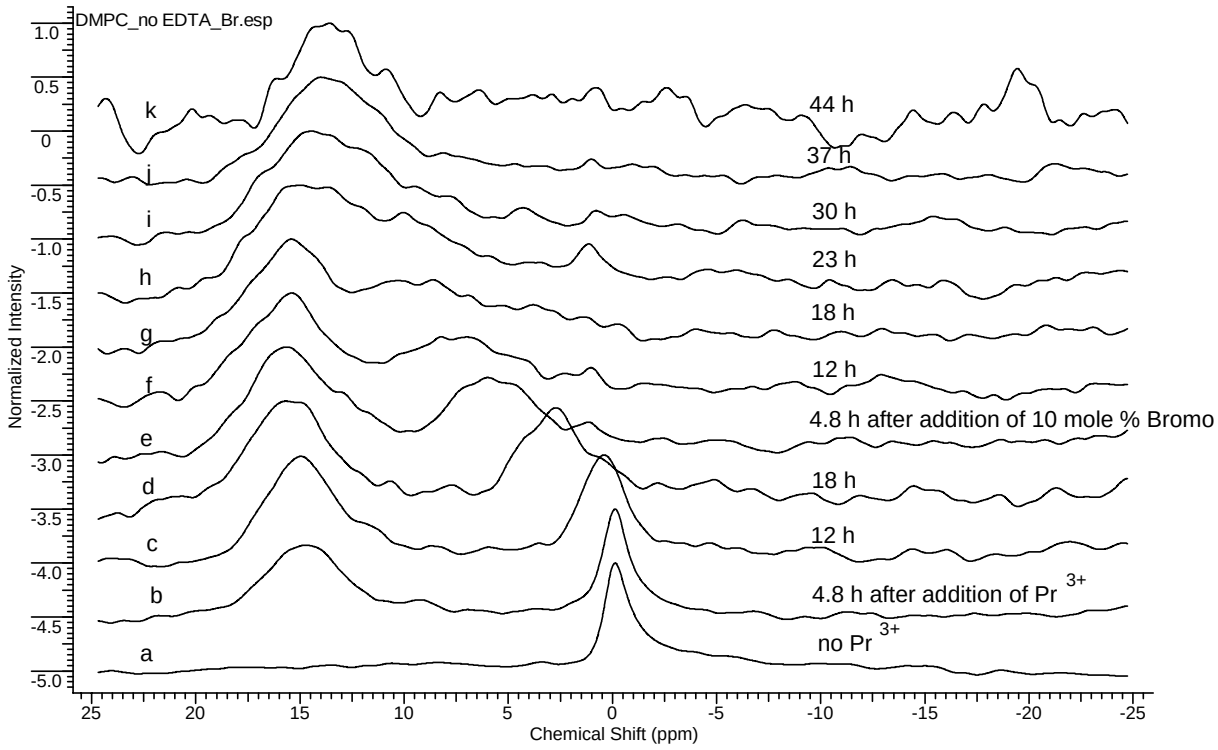

Figure 3-10 Spectra of DMPC liposomes with no EDTA after addition of 10 mole Percent bromo compound.

(a) is phosphorus signal with no Pr^{3+}. Spectra (b-n) were obtained after the addition of 4.5 mM $PrCl_3$ Peaks shifts were referenced to an external trimethylphosphate standard in HEPES buffer (see the Materials and Methods section 2.1.3).

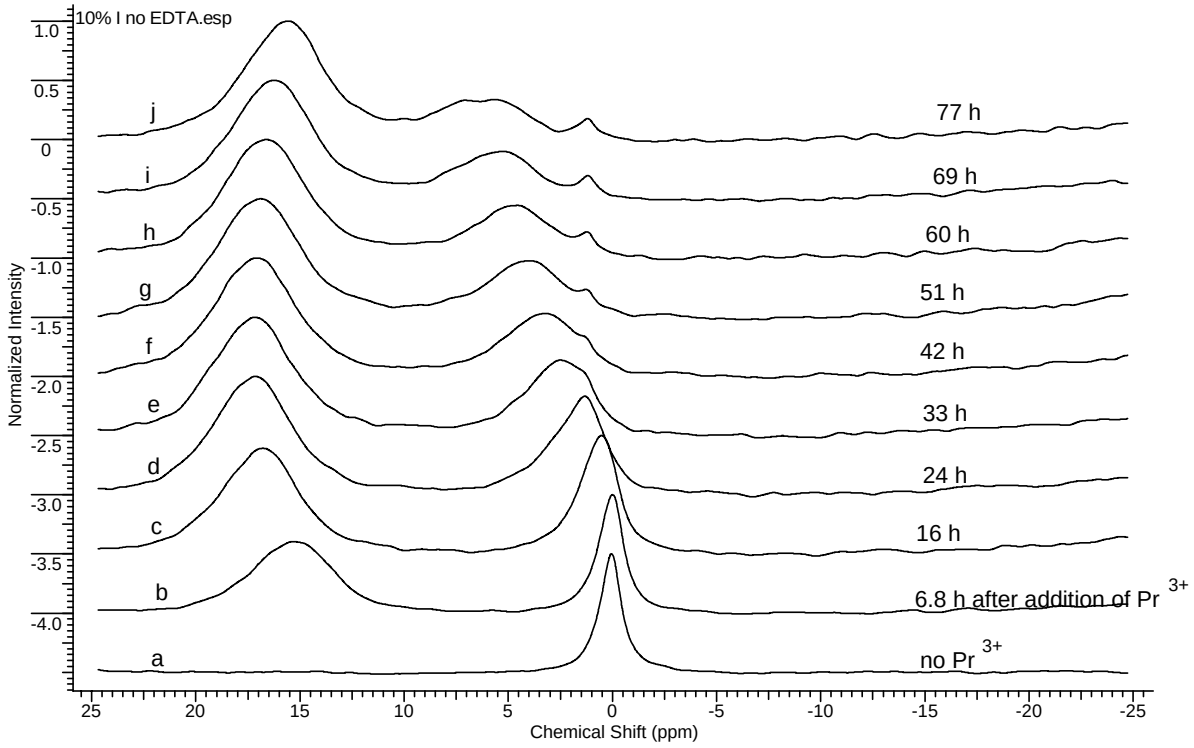

Figure 3-11 Spectra of DMPC Liposomes with no EDTA after addition of 10 mole percent Iodo compound.

(a) is phosphorus signal with no Pr^{3+}. Spectra (b-j) were obtained after the addition of 0.45 mM $PrCl_3$ Peaks shifts were referenced to an external trimethylphosphate standard in HEPES buffer; see the Materials and Methods section 2.1.3.

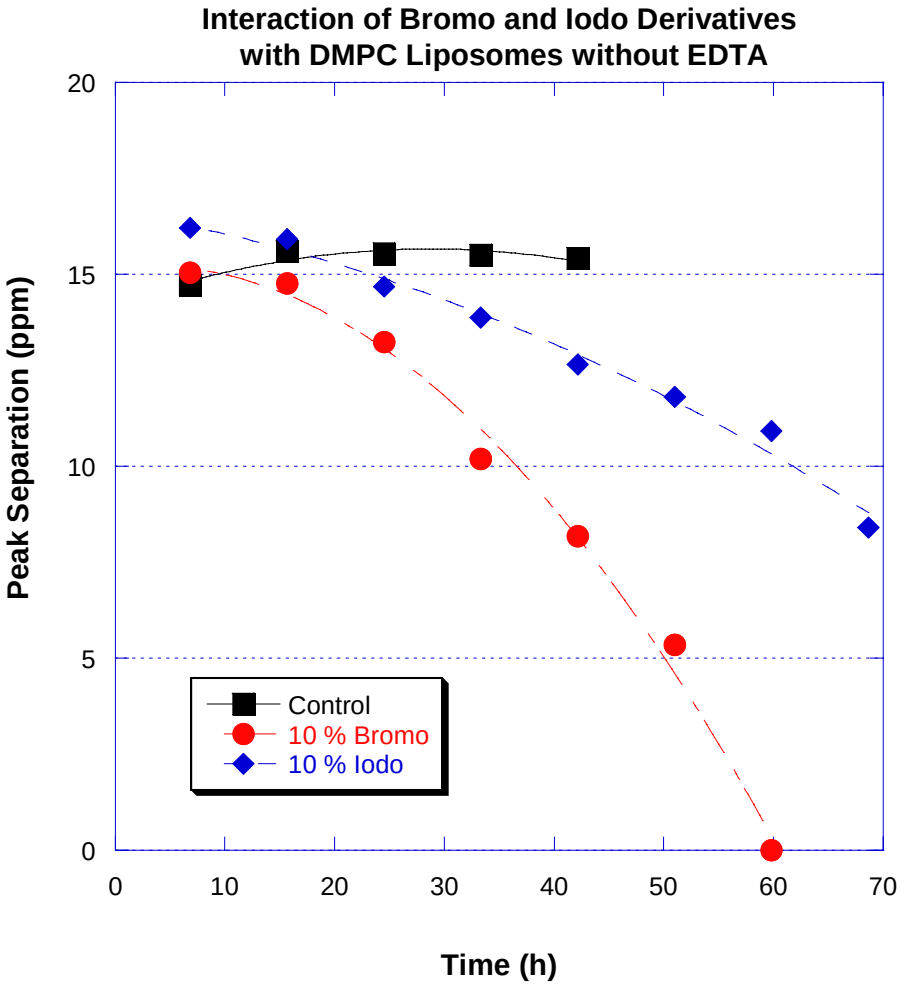

Figure 3-12 The effect of 10 mole percent bromo and iodo derivatives on ^{31}P resonances seen in DMPC liposomes without EDTA.
Data were fit with 2nd order polynomials.

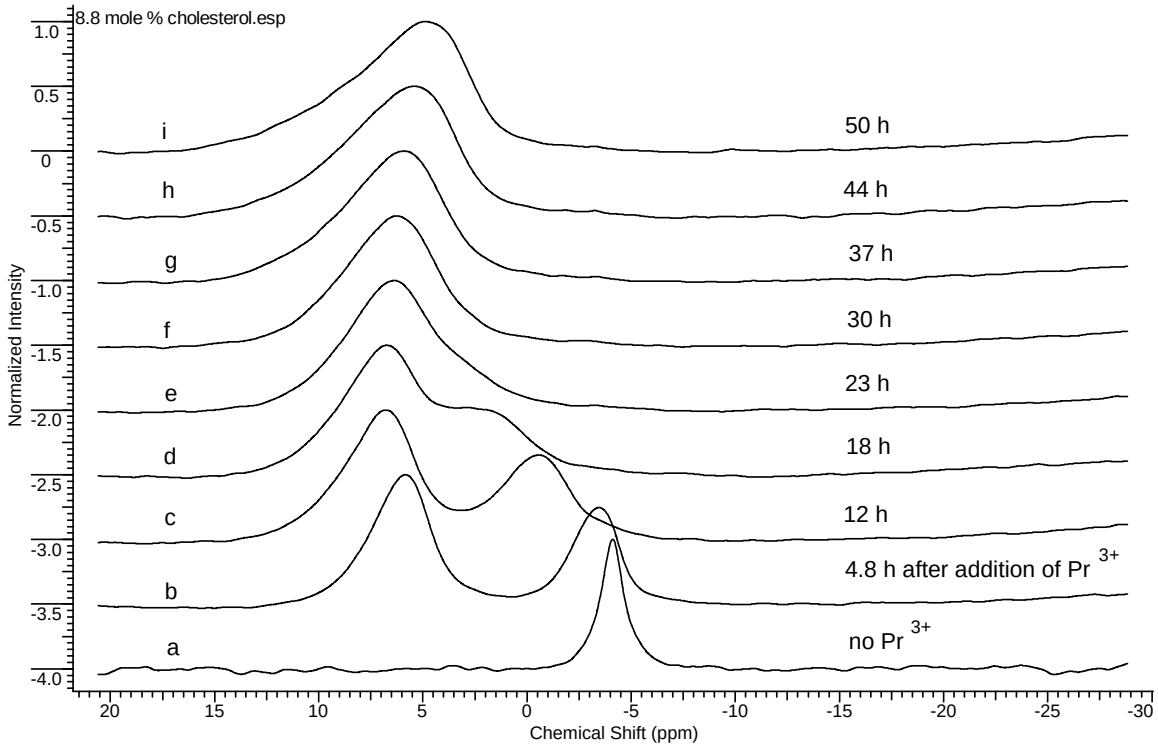

Figure 3-13 Spectra of DMPC liposomes with 8.8 mole percent cholesterol.
(a) is phosphorus signal with no Pr^{3+}. Spectra (b-i) were obtained after the addition of 4.5 mM $PrCl_3$ Peaks shifts were referenced to an external trimethylphosphate standard in HEPES buffer (see the Materials and Methods section 2.1.3).

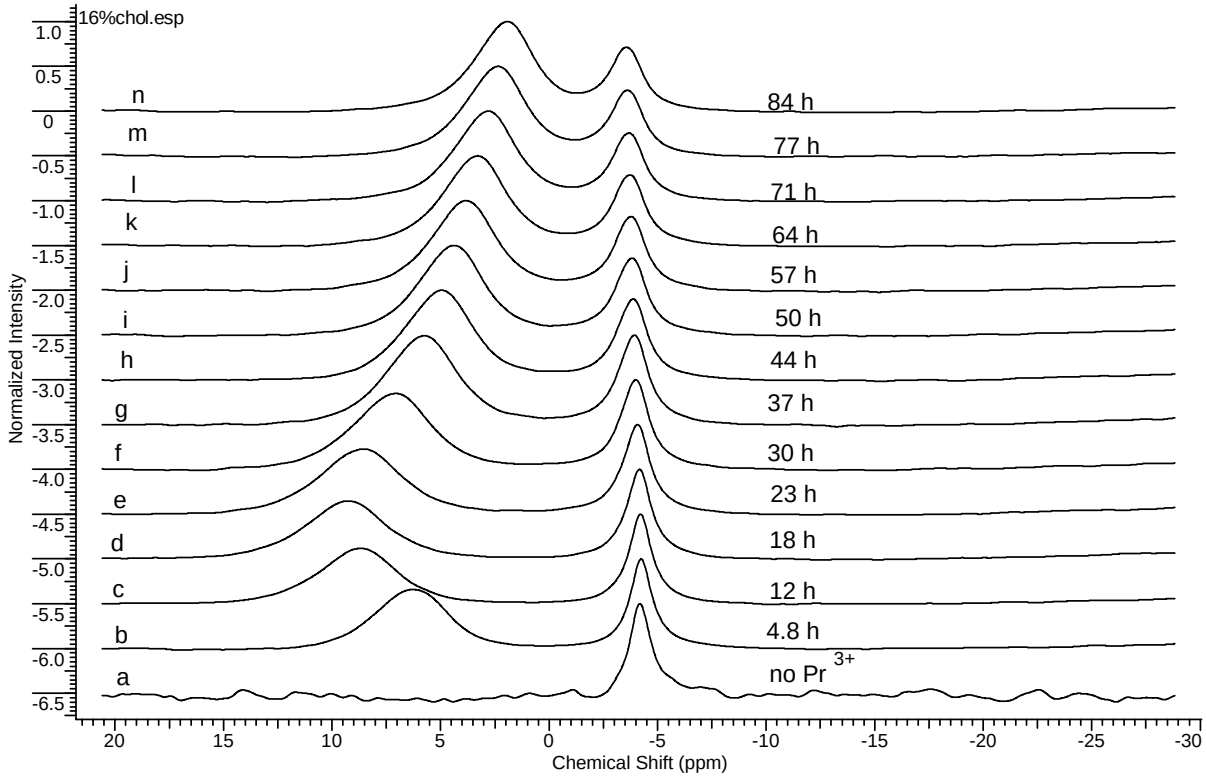

Figure 3-13 DMPC and 16 mole percent cholesterol.
(a) is phosphorus signal with no Pr^{3+}. Spectra (b-n) were obtained after the addition of 0.45 mM $PrCl_3$ Peaks shifts were referenced to an external trimethylphosphate standard in HEPES buffer (see the Materials and Methods section 2.1.3).

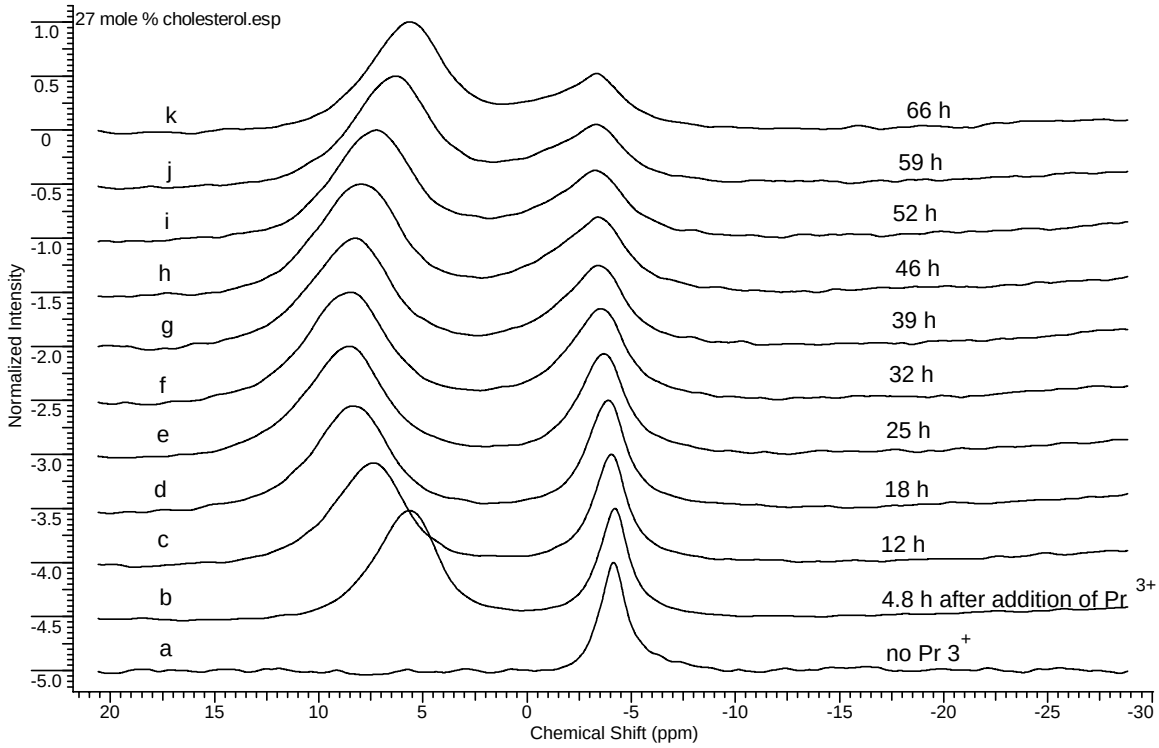

Figure 3-14 Spectra of DMPC iposomes 27 mole percent cholesterol.
(a) is phosphorus signal with no Pr^{3+}. Spectra (b-k) were obtained after the addition of 0.45 mM $PrCl_3$ Peaks shifts were referenced to an external trimethylphosphate standard in HEPES buffer (see the Materials and Methods section 2.1.3).

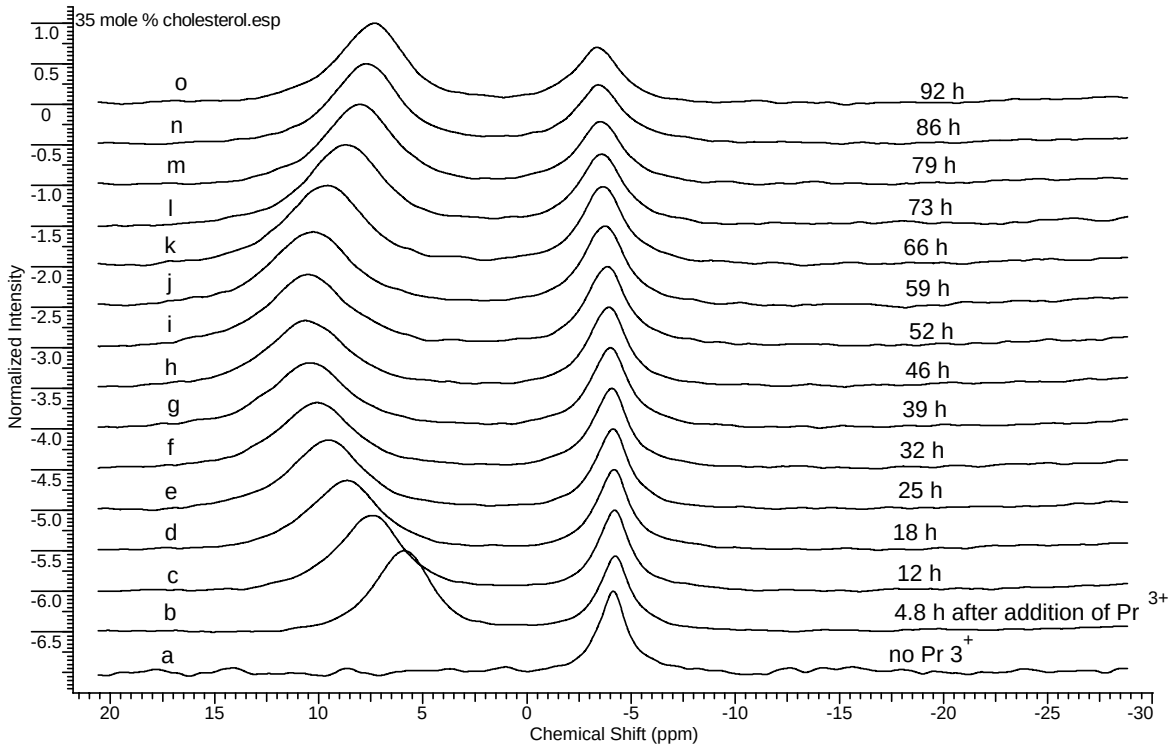

Figure 3-15 Spectra of DMPC liposomes with 35 mole percent cholesterol.
(a) is phosphorus signal with no Pr^{3+}. Spectra (b-n) were obtained after the addition of 0.45 mM $PrCl_3$ Peaks shifts were referenced to an external trimethylphosphate standard in HEPES buffer (see the Materials and Methods section 2.1.3).

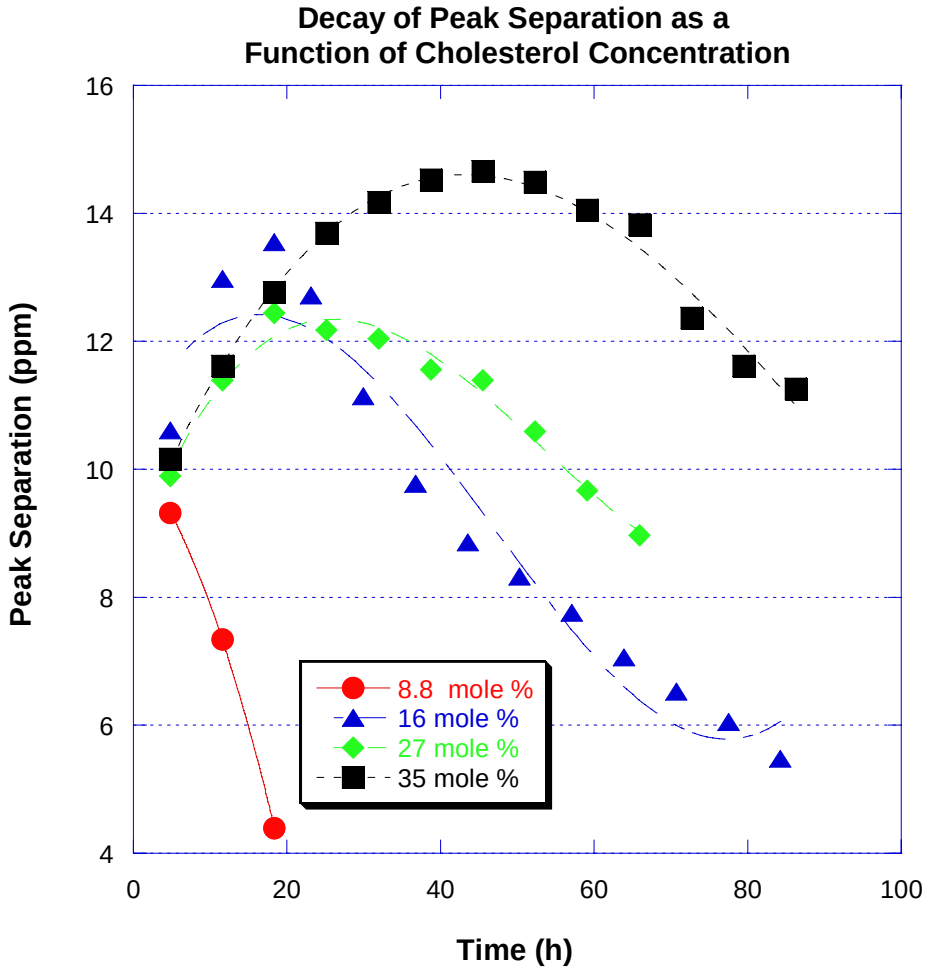

Figure 3-16 Decay of ^{31}P resonance separation as a function of cholesterol concentration.
8.8 mole percent cholesterol was fit with a 2nd order polynomial, whereas 16 mole percent 27 mole percent and 35 mole percent were fit with a 3rd order polynomial.

Figure 3-9 illustrates the spectra obtained from the interaction of 10 mole percent bromo derivative with DMPC containing 16 mole percent cholesterol. After the maximum peak separation between the inner and outer leaflet was achieved, 10 mole percent bromo iminosulfurane was added (Figure 2.3-5). The effect of the bromo derivative on the splitting was monitored as a function of time over a period of 66 h. In DMPC vesicles containing 16 mole percent cholesterol, the addition of the bromo derivative causes a collapse of the splitting to zero within 30 h.

Figure 3-10 illustrates the effect of the iodo derivative after the maximum peak separation between the inner and outer leaflet was achieved (Spectra b-c). The effect of the addition of 10 mole percent iodo iminosulfurane on the splitting was monitored as a function of time over a period of 66 h. The addition of the iodo derivative causes a collapse of the splitting to 2.5 ppm within 66 h.

The change in resonance separation in the presence of 10 mole percent chloro derivative is plotted as a function of time in Figure 3-11. The reduction in the splitting induced by the chloro derivative occurs over a longer period of time.

The change in resonance separation in the presence of 10 mole percent hydrogen derivative is plotted as a function of time in Figure 3-12. The reduction in the splitting of induced by the hydrogen derivative occurs over a longer period of time than that of bromo and iodo derivatives.

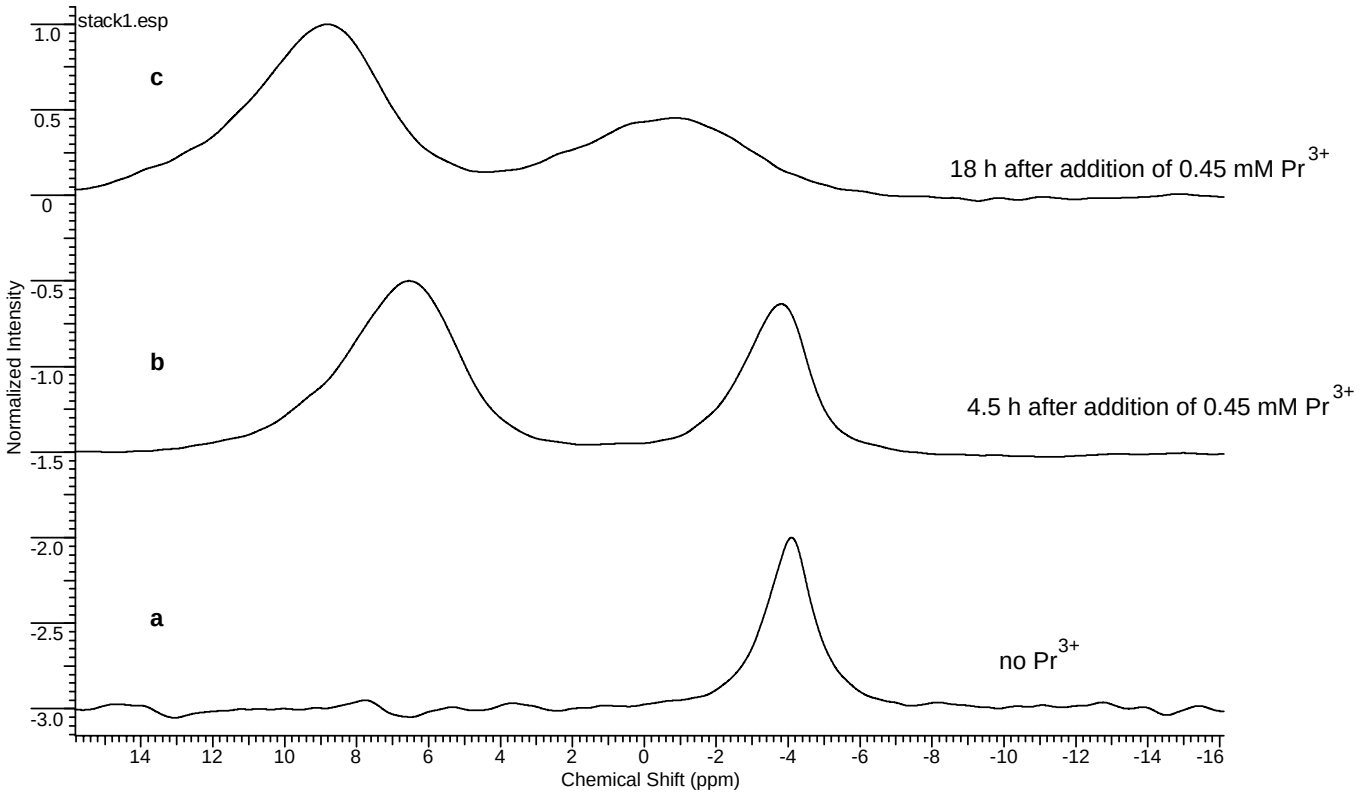

Figure 3-17 The interaction of praseodymium with DMPC and 16 mole percent cholesterol.
(a) is phosphorus signal with no Pr^{3+}. Spectrum (b) is 4.8 h after the addition of 0.45 mM $PrCl_3$. Spectra (c) is 18 h after the addition of 0.45 mM Pr^{3+}.

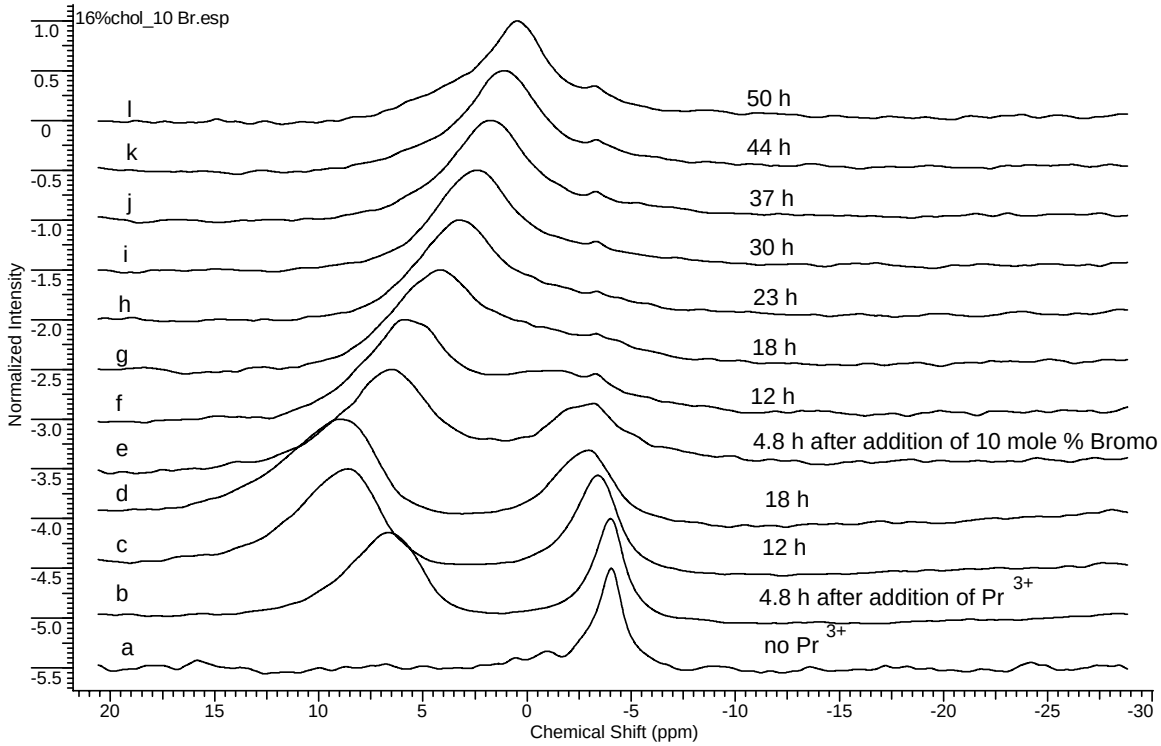

Figure 3-18 DMPC and 16 mole percent cholesterol with 10 mole percent bromo derivative.

(a) is phosphorus signal with no Pr^{3+}. Spectrum (b) is 4.8 h after the addition of 0.45 mM $PrCl_3$. Spectrum (c) is 12 h after the addition of 0.45 mM $PrCl_3$. Spectra (d) is 18 h after the addition of 0.45 mM Pr^{3+}. Spectra (e-l) were obtained after the addition of 10 mole percent bromo derivative after 0.45 mM $PrCl_3$ had been added 18 h earlier. Peaks shifts were referenced to an external trimethylphosphate standard in HEPES buffer (see the Materials and Methods section 2.1.3).

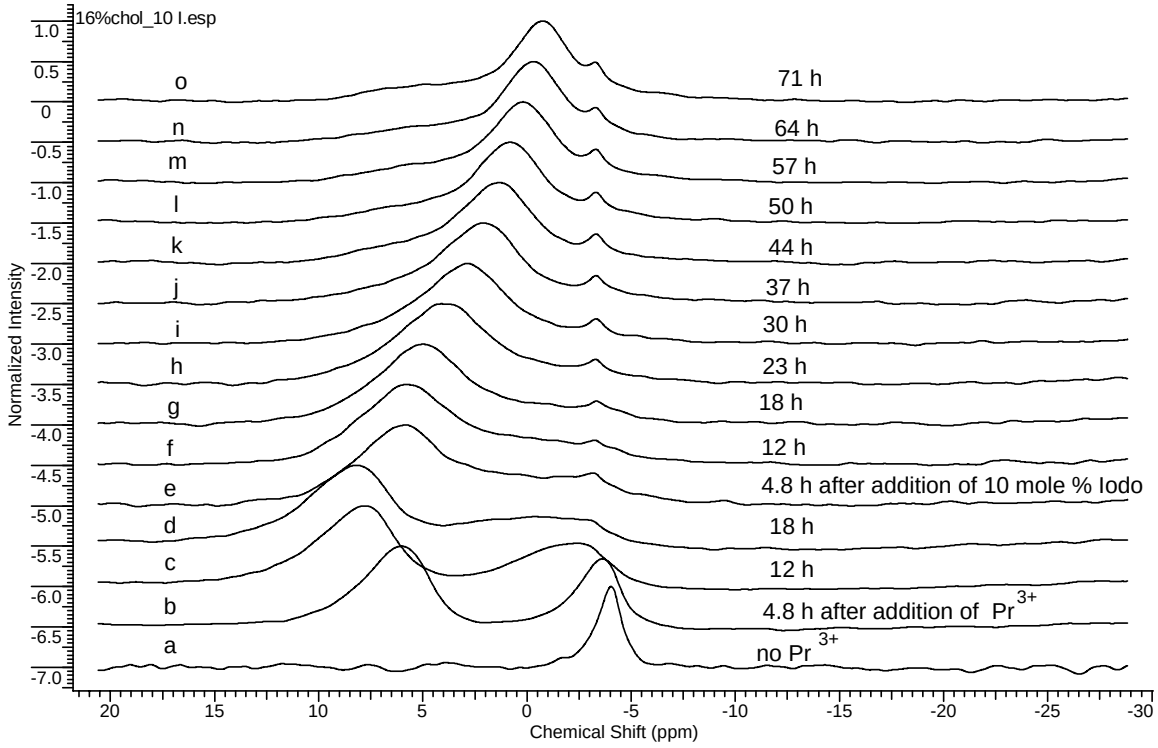

Figure 3-19 DMPC and 16 mole percent cholesterol with 10 mole percent iodo derivative.

(a) is phosphorus signal with no Pr^{3+}. Spectrum (b) is 4.8 h after the addition of 0.45 mM $PrCl_3$. Spectrum (c) is 12 h after the addition of 0.45 mM $PrCl_3$. Spectra (d) is 18 h after the addition of 0.45 mM Pr^{3+}. Spectra (e-o) were obtained after the addition of 10 mole percent iodo derivative after 0.45 mM $PrCl_3$ had been added 18 h earlier. Peaks shifts were referenced to an external trimethylphosphate standard in HEPES buffer (see the Materials and Methods section 2.1.3).

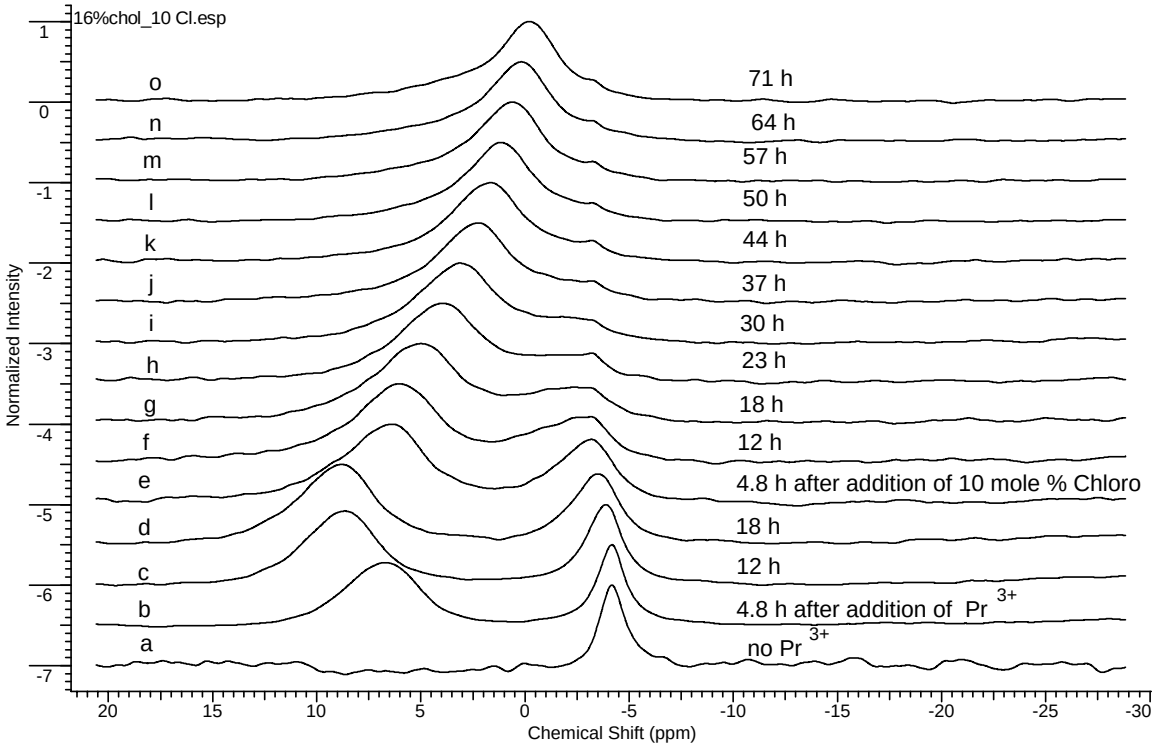

Figure 3-20 DMPC and 16 mole percent cholesterol with 10 mole percent chloro derivative.

(a) is phosphorus signal with no Pr^{3+}. Spectrum (b) is 4.8 h after the addition of 0.45 mM $PrCl_3$. Spectrum (c) is 12 h after the addition of 0.45 mM $PrCl_3$. Spectra (d) is 18 h after the addition of 0.45 mM Pr^{3+}. Spectra (e-o) were obtained after the addition of 10 mole percent chloro derivative after 0.45 mM $PrCl_3$ had been added 18 h earlier. Peaks shifts were referenced to an external trimethylphosphate standard in HEPES buffer (see the Materials and Methods section 2.1.3).

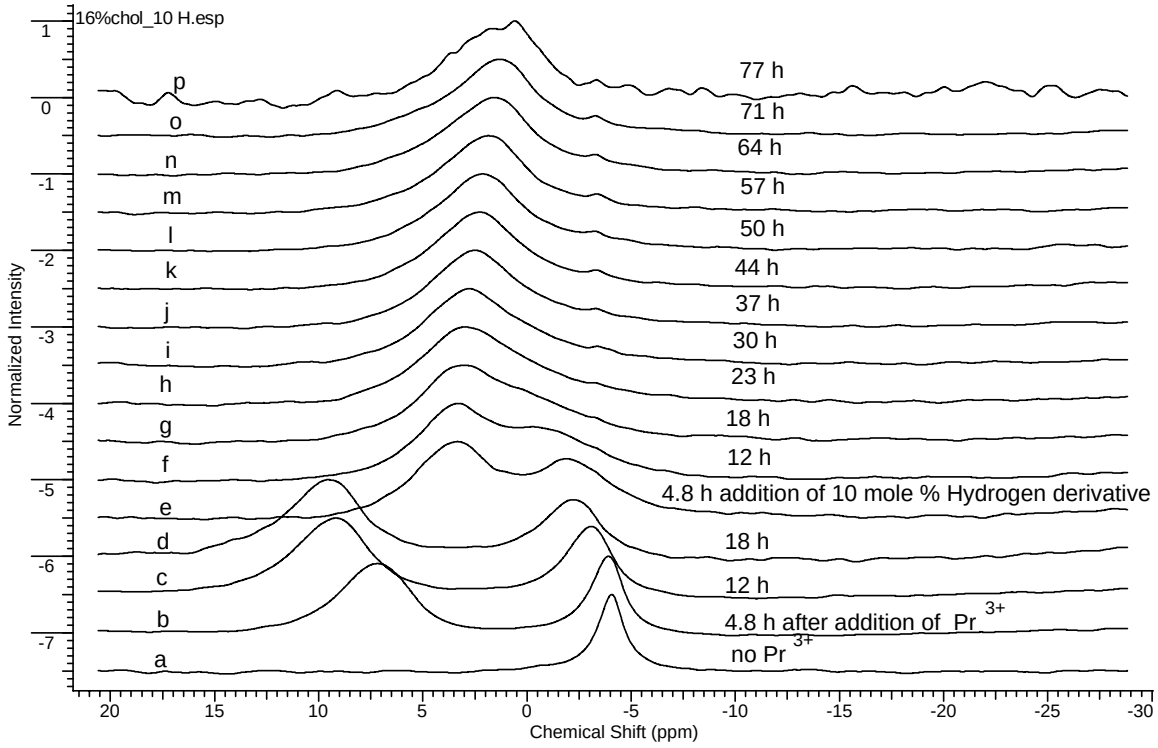

Figure 3-21 DMPC and 16 mole percent cholesterol.
(a) is phosphorus signal with no Pr^{3+}. Spectrum (b) is 4.8 h after the addition of 0.45 mM $PrCl_3$. Spectrum (c) is 12 h after the addition of 0.45 mM $PrCl_3$. Spectra (d) is 18 h after the addition of 0.45 mM Pr^{3+}. Spectra (e-p) were obtained after the addition of 10 mole percent hydrogen derivative after 0.45 mM $PrCl_3$ had been added 18 h earlier. Peaks shifts were referenced to an external trimethylphosphate standard in HEPES buffer (see the Materials and Methods section 2.1.3).

3.7. Summary Analysis of Iminosulfurane Derivatives with DMPC Liposomes Containing 16 Mole Percent Cholesterol

The change in resonance separation in the absence of transdermal penetration enhancers is plotted as a function of time in the control and demonstrates the effect of these enhancers on the splitting of the ^{31}P resonances associated with the inner and outer leaflet of the vesicle bilayer. After 84 h, the resonances remain separated by 5 ppm in the control spectrum. The addition of the bromo derivative causes a collapse of the splitting to zero within 30 h as shown. The reduction in the splitting induced by the iodo, chloro, and hydrogen derivatives occurs over longer periods of time, but at a rate that is only marginally greater than that due to the control as shown in Figure 3-13. Lines drawn through the data points were obtained by polynomial regression analyses.

3.8. Effect of 30 mole percent Cholesterol on DMPC Liposomes

Increasing the cholesterol content of the DMPC vesicles above 16 mole percent further reduces the rate at which the splitting is collapsed by the iminosulfuranes. The change in resonance separation in the absence of transdermal penetration enhancers is plotted as a function of time in Figure 3-14. After 84 h, the resonances remain separated by 5 ppm in the control spectrum.

The effect of the bromo derivative at 10 mole percent could not be distinguished from the aging effect in the control. However, increasing the concentration of the bromo derivative to 20 mole percent decreases the rate of ^{31}P resonance separation greater than that of the control.

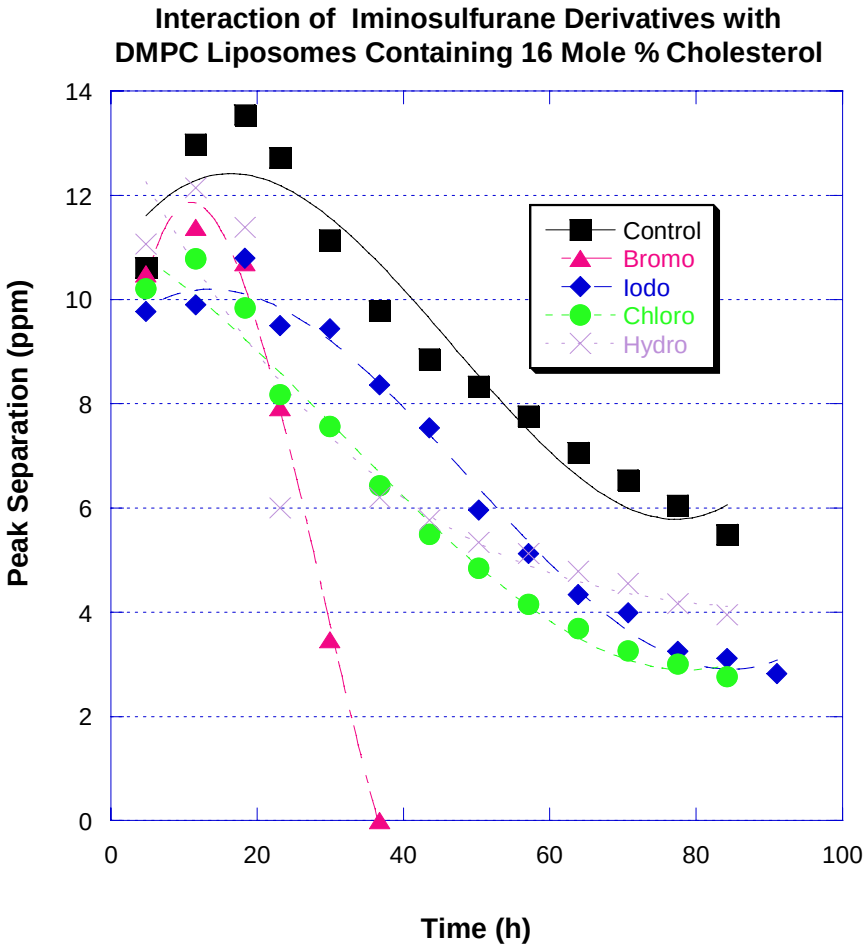

Figure 3-22 Interaction of iminosulfurane derivatives with DMPC and 16 mole percent cholesterol liposomes.
Data fit with polynomial fit. Peaks shifts were referenced to an external trimethylphosphate standard in HEPES buffer (see the Materials and Methods section 2.1.3).

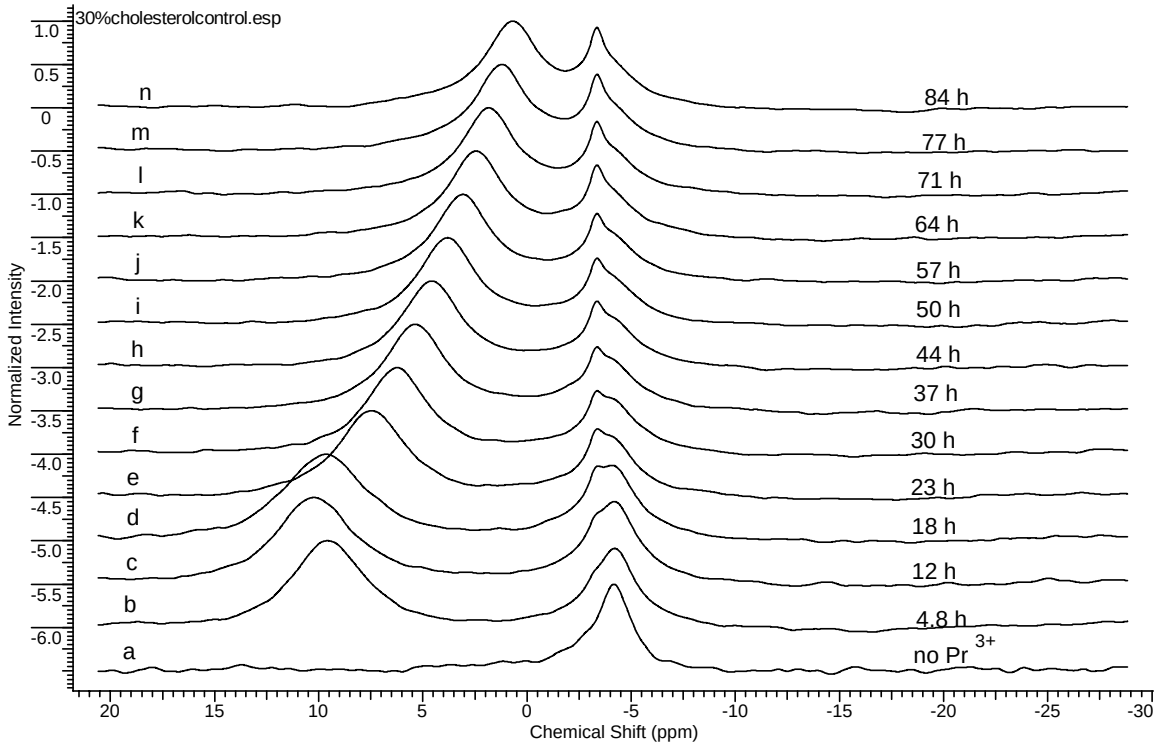

Figure 3-23 DMPC and 30 mole percent cholesterol.
(a) is phosphorus signal with no Pr^{3+}. Spectra (b-n) were obtained after the addition of 0.45 mM $PrCl_3$. Peaks shifts were referenced to an external trimethylphosphate standard in HEPES buffer (see the Materials and Methods section 2.1.3).

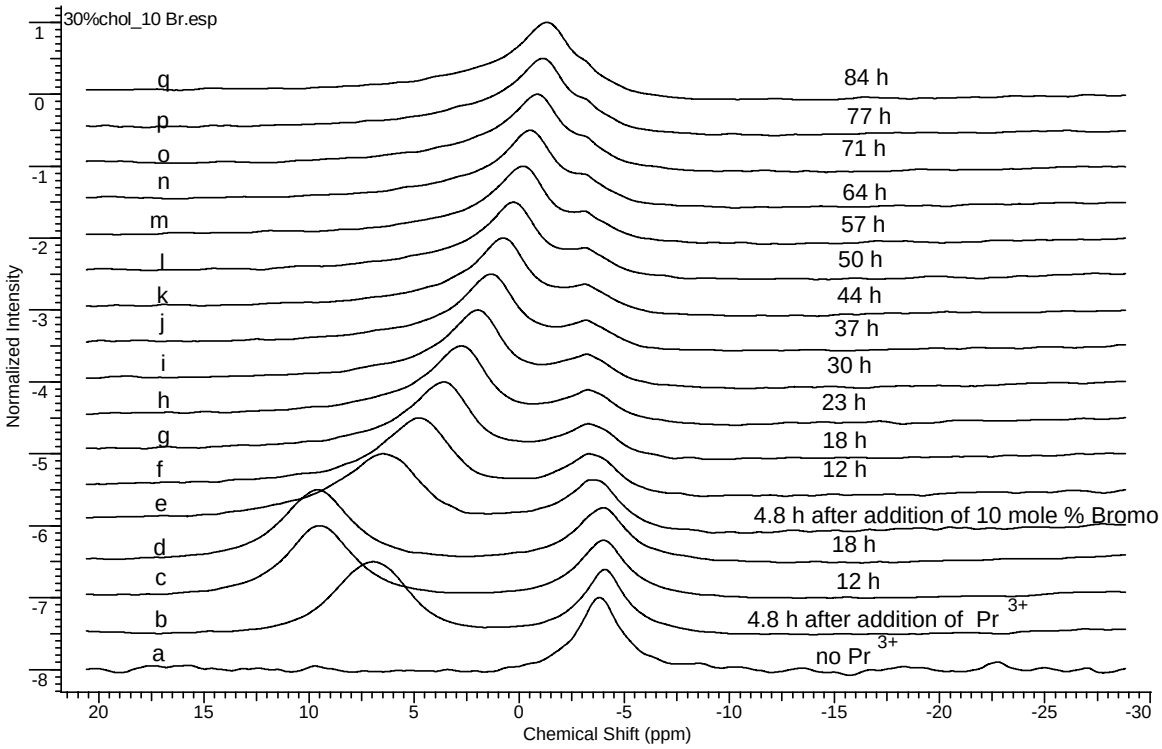

Figure 3-24 DMPC and 30 mole percent cholesterol interaction with bromo derivative.

(a) is phosphorus signal with no Pr^{3+}. Spectrum (b) is 4.8 h after the addition of 0.45 mM $PrCl_3$. Spectrum (c) is 12 h after the addition of 0.45 mM $PrCl_3$. Spectra (d) is 18 h after the addition of 0.45 mM Pr^{3+}. Spectra (e-q) were obtained after the addition of 10 mole percent bromo derivative after 0.45 mM $PrCl_3$ had been added 18 h earlier. Peaks shifts were referenced to an external trimethylphosphate standard in HEPES buffer (see the Materials and Methods section 2.1.3).

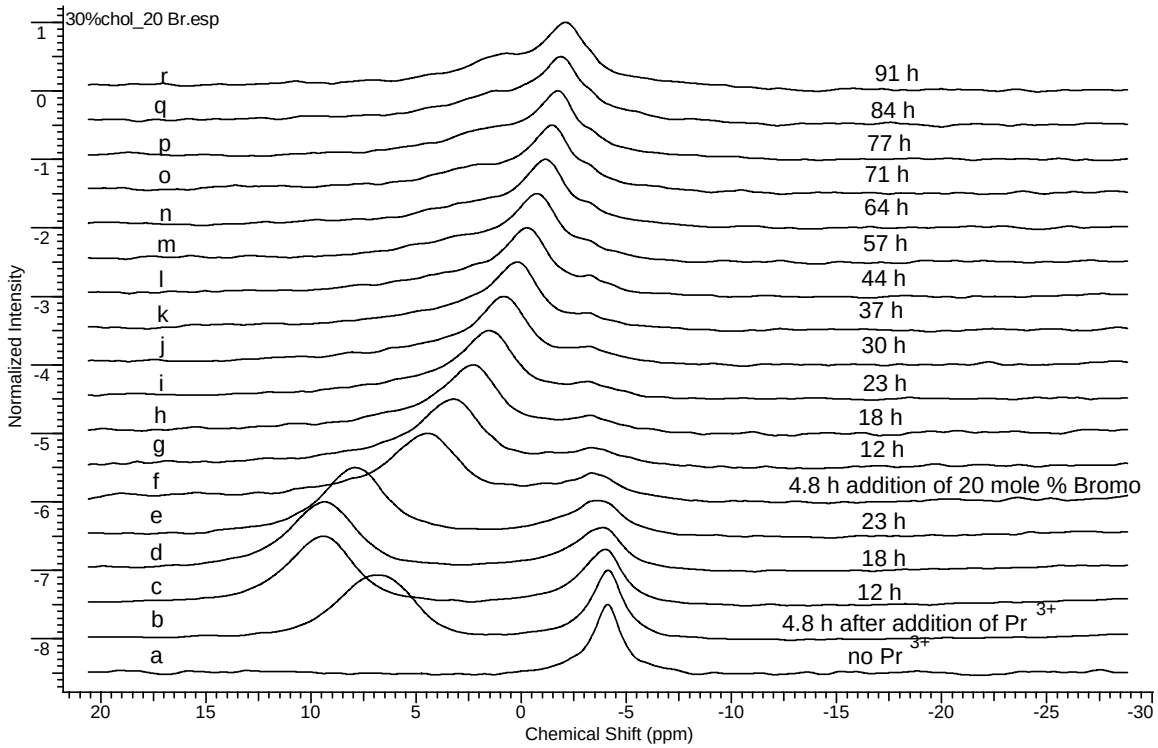

Figure 3-25 DMPC and 30 mole percent cholesterol with 20 Percent bromo derivative.

(a) is phosphorus signal with no Pr^{3+}. Spectrum (b) is 4.8 h after the addition of 0.45 mM $PrCl_3$. Spectrum (c) is 12 h after the addition of 0.45 mM $PrCl_3$. Spectra (d) is 18 h after the addition of 0.45 mM Pr^{3+}. Spectra (f-r) were obtained after the addition of 20 mole percent bromo derivative after 0.45 mM $PrCl_3$ had been added 18 h earlier. Peaks shifts were referenced to an external trimethylphosphate standard in HEPES buffer (see the Materials and Methods section 2.1.3).

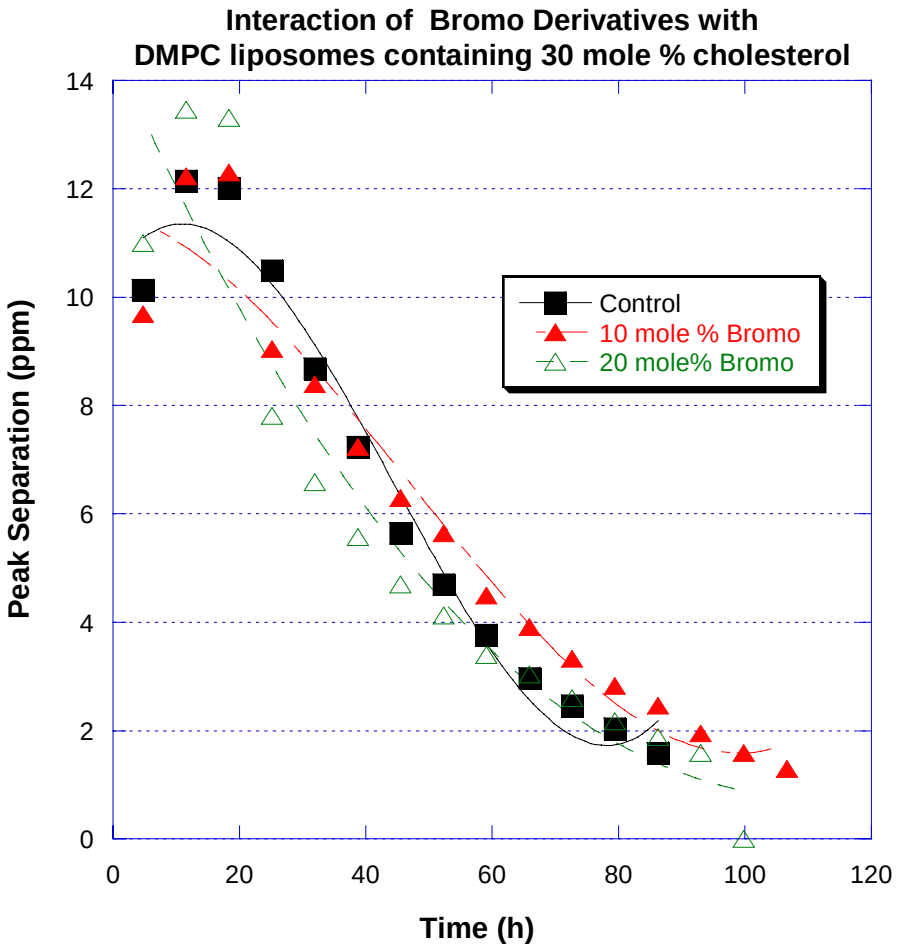

Figure 3-26 Interaction of bromo iminosulfurane derivatives with DMPC and 30 mole percent cholesterol liposomes with varying concentrations.
Data fit with polynomial fit. Peaks shifts were referenced to an external trimethylphosphate standard in HEPES buffer(see the Materials and Methods section 2.1.3).

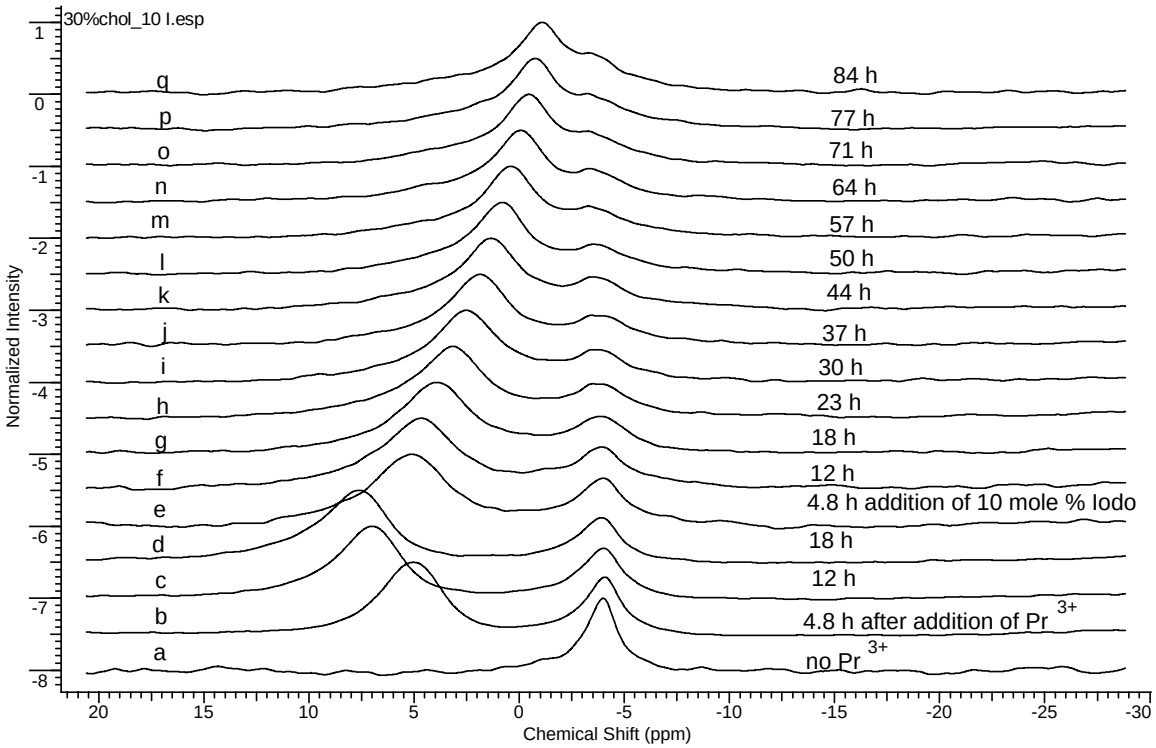

Figure 3-27 DMPC and 30 mole percent cholesterol with addition of 10 percent iodo derivative.

(a) is phosphorus signal with no Pr^{3+}. Spectrum (b) is 4.8 h after the addition of 0.45 mM $PrCl_3$. Spectrum (c) is 12 h after the addition of 0.45 mM $PrCl_3$. Spectra (d) is 18 h after the addition of 0.45 mM Pr^{3+}. Spectra (e-o) were obtained after the addition of 10 mole percent iodo derivative after 0.45 mM $PrCl_3$ had been added 18 h earlier. Peaks shifts were referenced to an external trimethylphosphate standard in HEPES buffer (see the Materials and Methods section 2.1.3).

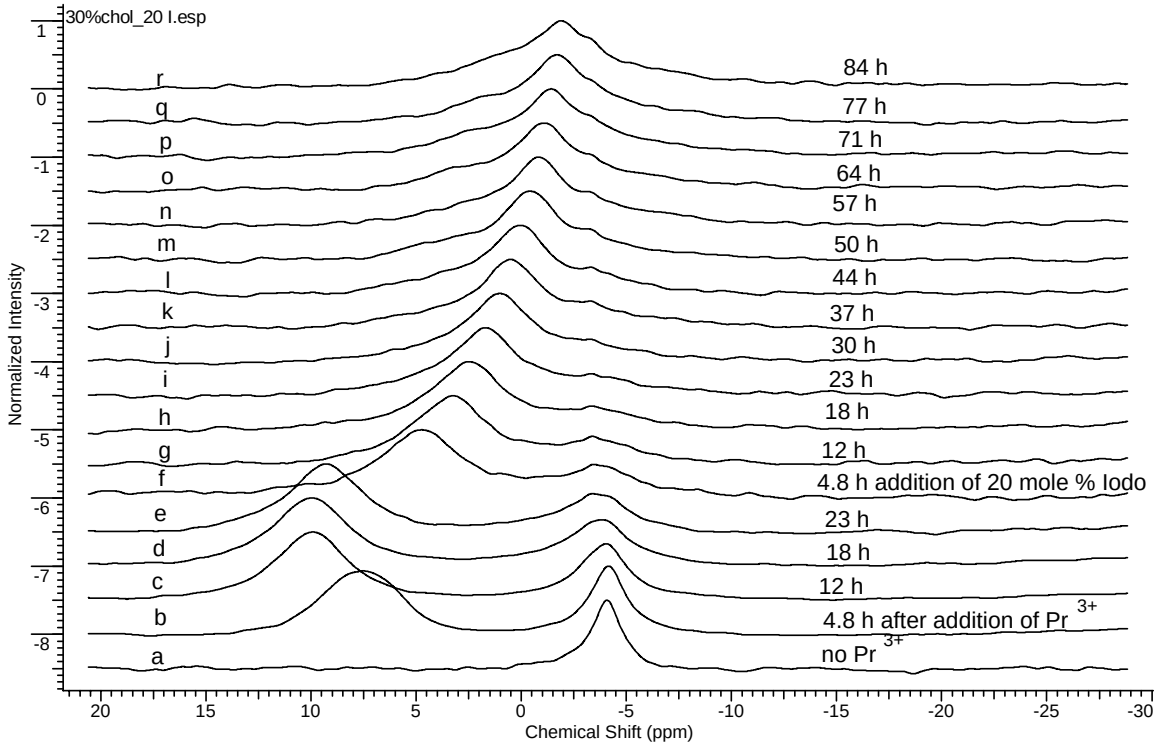

Figure 3-28 DMPC and 30 mole percent cholesterol with 20 percent iodo derivative.

(a) is phosphorus signal with no Pr^{3+}. Spectrum (b) is 4.8 h after the addition of 0.45 mM $PrCl_3$. Spectrum (c) is 12 h after the addition of 0.45 mM $PrCl_3$. Spectra (d) is 18 h after the addition of 0.45 mM Pr^{3+}. Spectra (e-r) were obtained after the addition of 20 mole percent iodo derivative after 0.45 mM $PrCl_3$ had been added 18 h earlier. Peaks shifts were referenced to an external trimethylphosphate standard in HEPES buffer (see the Materials and Methods section 2.1.3).

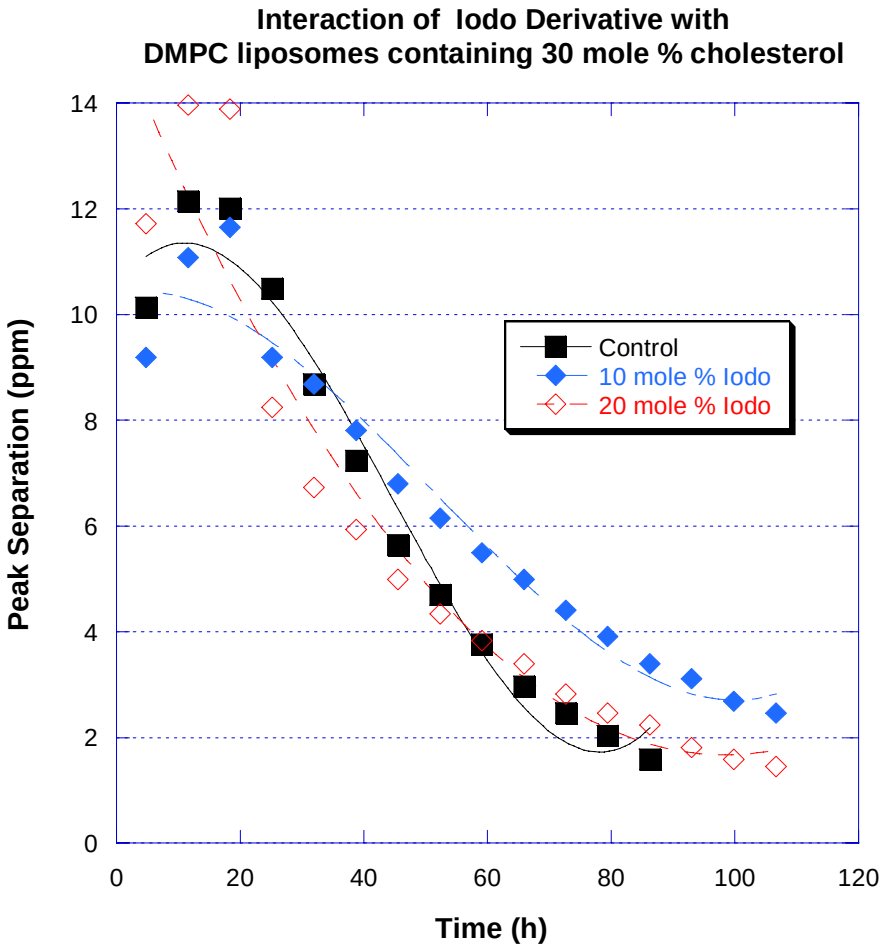

Figure 3-29 Interaction of different concentrations of iodo derivatives with DMPC and 30 mole percent cholesterol liposomes.
Data were fit with 3rd order polynomial fit. Peaks shifts were referenced to an external trimethylphosphate standard in HEPES buffer (see the Materials and Methods section 2.1.3).

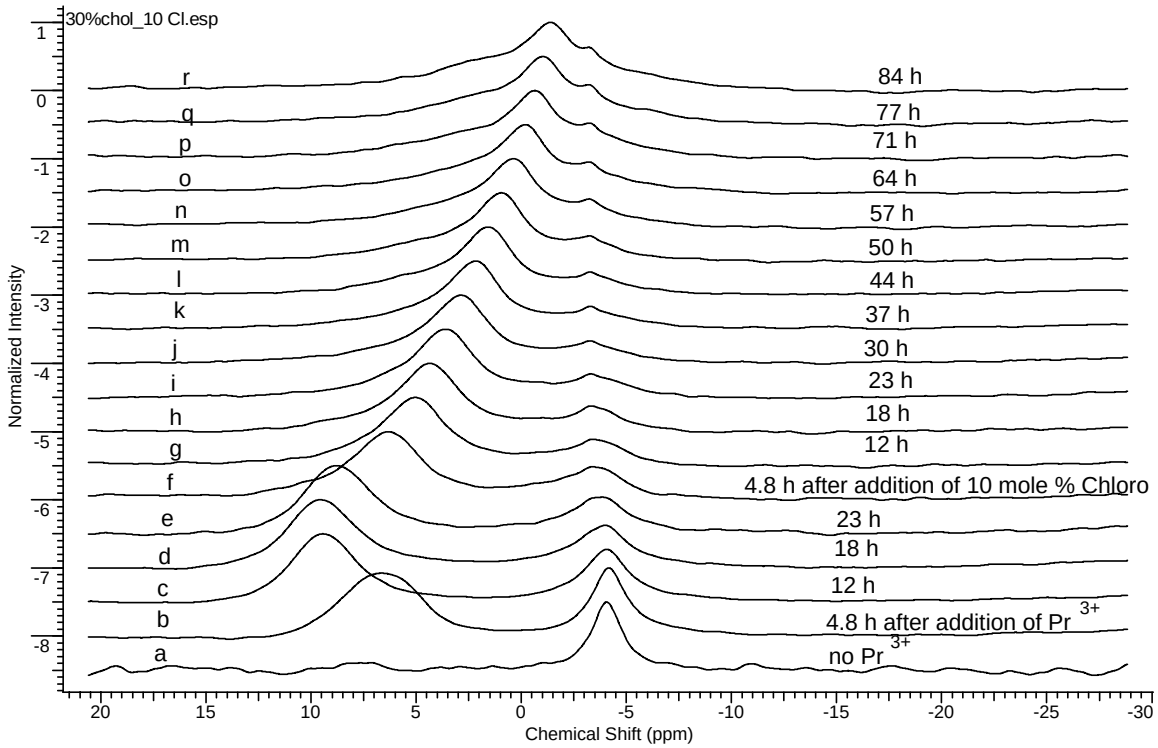

Figure 3-30 DMPC and 30 mole percent cholesterol with 10 mole percent chloro derivative.

(a) is phosphorus signal with no Pr^{3+}. Spectrum (b) is 4.8 h after the addition of 0.45 mM $PrCl_3$. Spectrum (c) is 12 h after the addition of 0.45 mM $PrCl_3$. Spectra (d) is 18 h after the addition of 0.45 mM Pr^{3+}. Spectra (f-r) were obtained after the addition of 10 mole percent chloro derivative after 0.45 mM $PrCl_3$ had been added 18 h earlier. Peaks shifts were referenced to an external trimethylphosphate standard in HEPES buffer (see the Materials and Methods section 2.1.3).

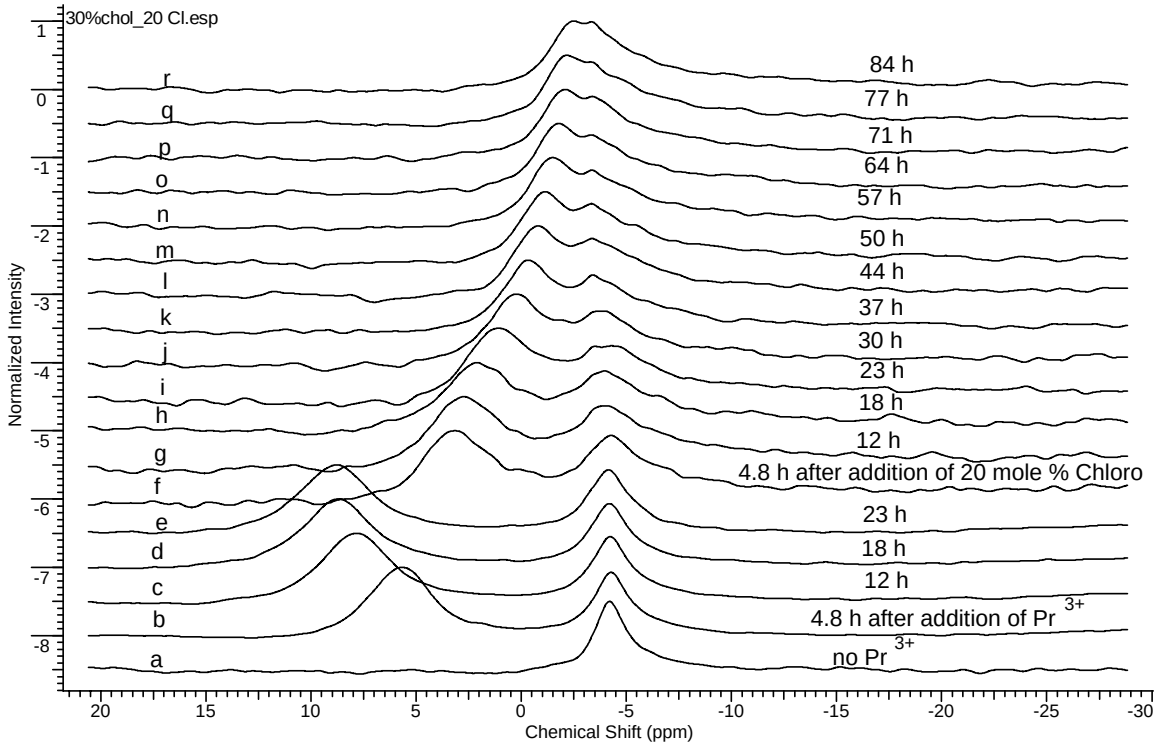

Figure 3-31 DMPC and 30 mole percent cholesterol with 20 mole percent chloro derivative.

(a) is phosphorus signal with no Pr^{3+}. Spectrum (b) is 4.8 h after the addition of 0.45 mM $PrCl_3$. Spectrum (c) is 12 h after the addition of 0.45 mM $PrCl_3$. Spectra (d) is 18 h after the addition of 0.45 mM Pr^{3+}. Spectra (e-r) were obtained after the addition of 20 mole percent chloro derivative after 0.45 mM $PrCl_3$ had been added 18 h earlier. Peaks shifts were referenced to an external trimethylphosphate standard in HEPES buffer (see the Materials and Methods section 2.1.3).

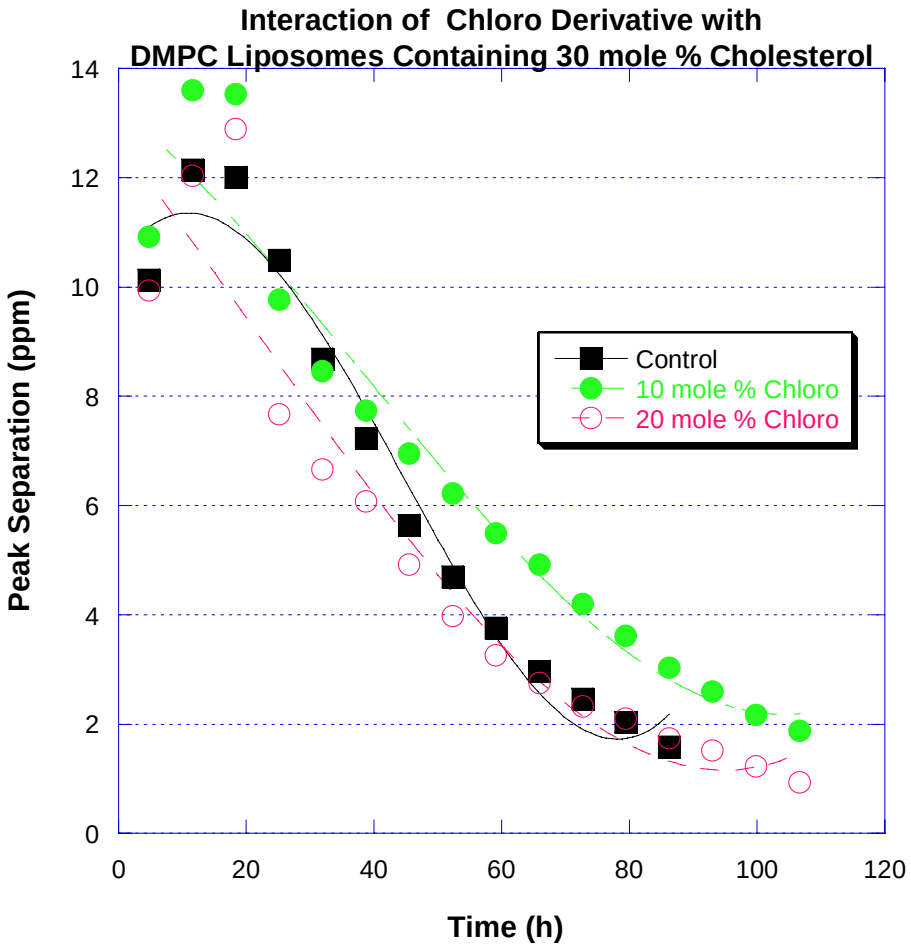

Figure 3-32 Interaction of chloro iminosulfurane derivatives with DMPC and 30 mole percent cholesterol liposomes.
Data were fit with 3rd order polynomial. Peaks shifts were referenced to an external trimethylphosphate standard in HEPES buffer (see the Materials and Methods section 2.1.3).

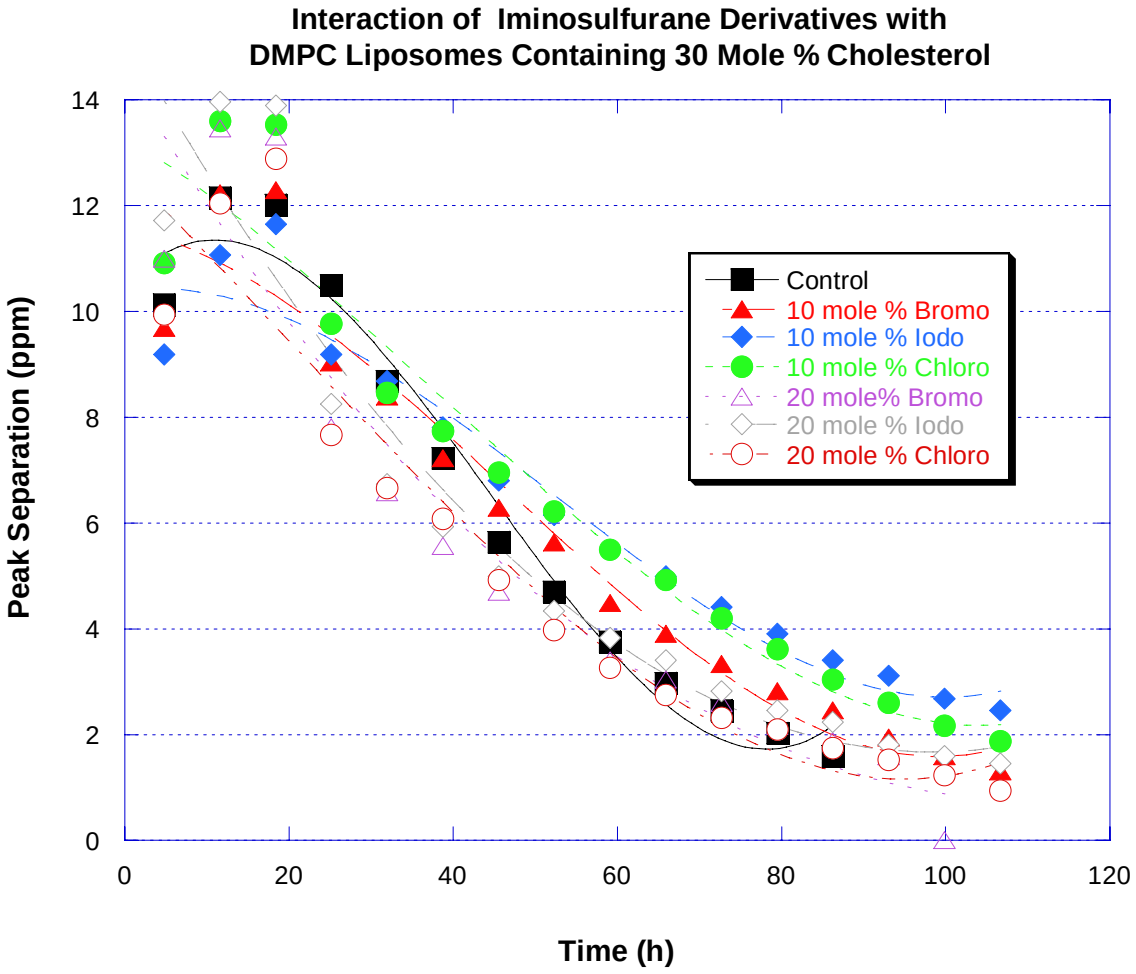

Figure 3-33 Interaction of iminosulfurane derivatives with DMPC and 30 mole percent cholesterol liposomes.
Data were fit with 3rd order polynomial. Peaks shifts were referenced to an external trimethylphosphate standard in HEPES buffer (see the Materials and Methods section 2.1.3).

The effect of the iodo derivative at 10 mole percent could not be distinguished from the aging effect in the control. However, increasing the concentration of the iodo derivative to 20 mole percent decreased the rate of ^{31}P resonance separation collapse greater than that of the control.

3.9. Calibration Curve and Self Quenching of Carboxyfluorescein

Emission spectra of CF were measured at the λ_{max}, 523 nm. Fluorescence of CF is linear over the range 3-30 uM (data not shown). [38] A plot of concentration of CF versus the fluorescence plotted outside of the linear region shows that at concentrations greater than 3 mM, the fluorescence begins to quench. Figure 3-34 shows the decrease in fluorescence as molar concentrations of CF exceed 3 mM. At 100 mM of CF, fluorescence is 95 percent quenched and in excess of 200 mM, fluorescence is 97-98 percent quenched. [40]

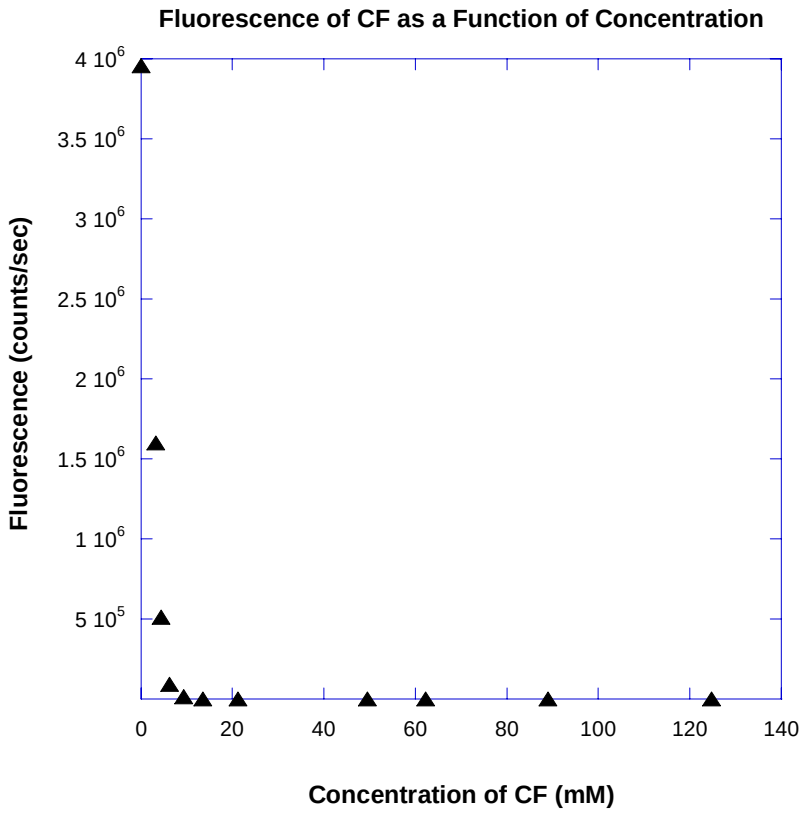

Figure 3-34 Fluorescence of carboxyfluorescein as a function of concentration.

3.10. Stern-Volmer Plots of Bromo and Iodo Derivatives

Halogenated compounds such as iodine and bromine are known to exhibit the heavy atom effect. The heavy atom effect causes the excited state of a fluorophore to be deactivated by collisional quenching. As fluorophores in the excited singlet state collide with halogenated compounds, their energy is transferred to the excited triplet state through intersystem crossing.[41] This process is defined by equation 3-1, which assumes that there is only one class of fluorophores present and that they are equally accessible to quenching.[41] A plot of the ratio fluorescence in the absence of quencher to fluorescence in the presence of quencher versus concentration has a y-intercept of one. The slope of the line is the dynamic quenching constant.

To determine whether the aforementioned iminosulfuranes interfere with the fluorescence of carboxyfluorescein, the change in fluorescence takes into account the dilution effect that occurs upon addition of transdermal agents. Figures 3-25 and 3-26 are the plots of the ratio fluorescence of CF in the absence of quencher to fluorescence of CF in the presence of quencher versus concentration of quencher, where the quenchers are the bromo compound and the iodo compound, respectively. The slope of the Stern-Volmer plot is 0.0028 μM^{-1} for the bromo derivative and -0.00010 μM^{-1} for the iodo derivative; hence K_D, the dynamic quenching constant is zero. The addition of varying concentrations of quencher which is either the bromo compound or the iodo compound in the micromolar quantities has no significant effect on fluorescence of CF.

$$\frac{F_o}{F} = 1 + K_D[Q] = 1 + k_q \tau_o[Q]$$

Equation 3-1 Stern-Volmer equation for collisional quenching.[41]
F_o is the fluorescence in absence of the quencher.
F is the fluorescence in the presence of the quencher.
K_D is the Stern-Volmer quenching constant or dynamic quenching constant.
[Q] is the concentration of the quencher.
K_q is the bimolecular quenching constant.
τ_o is the lifetime of the fluorophore in absence of the quencher.

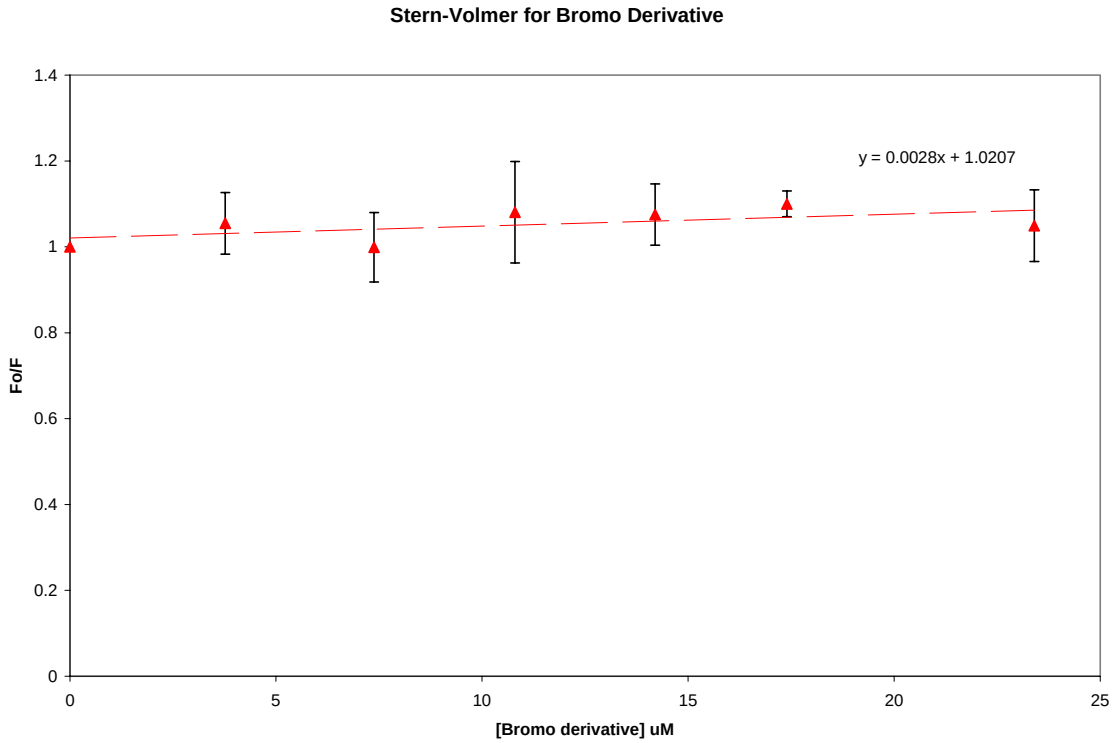

Figure 3-35 Stern-Volmer plot for CF-bromo derivative system quenching of carboxyfluorescein.

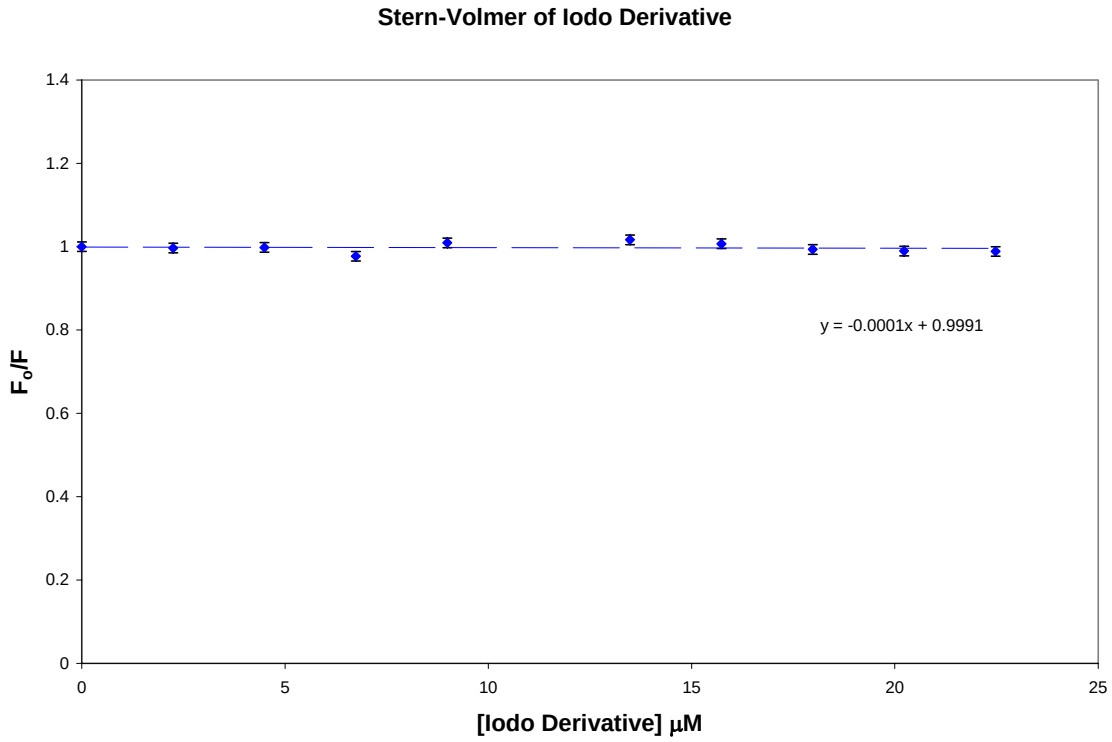

Figure 3-36 Stern-Volmer plot for CF- iodo derivative system quenching of carboxyfluorescein.

3.11. Structural Confirmation of Vesicles Encapsulated with CF

In order to monitor the vesicle preparation, electron micrographs were taken of CF-free vesicles and vesicles encapsulated with CF. The CF-free vesicles have an average diameter of 300 Å (Figure 3-38a), whereas the average diameter of vesicles containing CF increases to 600 Å (Figure 3-38b). The encapsulation of CF doubles the diameter of the vesicles. Similar results were observed with the encapsulation of potential cyanine sensitive dyes into DMPC vesicles; where the vesicle diameter also increased.[37]

3.12. Carboxyfluorescein Release of DMPC Vesicles with Triton X-100

To test the effectiveness of a membrane disruptor, a fluorophore such as CF is encapsulated in the interior of the vesicles at high concentrations. The fluorophore and vesicle will be sonicated to encapsulate the dye. The sonicate will then be passed through a chromatography column to remove the unencapsulated dye. Once the interior of the vesicle contains the fluorophore in the appropriate concentration, the vesicles should exhibit no fluorescence. Next the TPE can be applied to the vesicles. As the lipid bilayer is disrupted, CF will leach out causing a measurable increase in fluorescence. The increase in fluorescence is used to calculate the percent of CF released and provides a measure on the effect of the membrane disruptor on the integrity of the bilayer.

Detergents are known disruptors of bilayers. When 8.5 mM Triton X-100, a nonionic surfactant is added to the DMPC liposomes encapsulated with CF, the CF leaks out over time and eventually all of the CF is released and quenching is relieved, causing the amount fluorescence released to increase to 100 percent within 20 h (Figure3-39).

3.13. The Effect Iminosulfurane Derivatives on Bilayer Integrity Measured by Carboxyfluorescein Release from DMPC Vesicles

The bromo derivative at 3.1, 6.1, and 16.1 mole percent was added to vesicles encapsulated with CF and the resulting fluorescence of CF was monitored for 20 minutes in one second intervals (Figure 3-40). The percentage of CF released was calculated the according to equation 1-1. The maximum percent release was achieved within the time of hand mixing. After the addition of iminosulfurane, the percent release of CF achieved a maximum and decreases and reached a plateau. Addition of 3.1 percent bromo released 23 percent of CF. Doubling the amount of bromo to 6.1 percent caused the percentage of CF released to be 39 percent, almost twice that achieved with 6.1 percent. The addition of 16.1 percent bromo released 61 percent of the encapsulated CF.

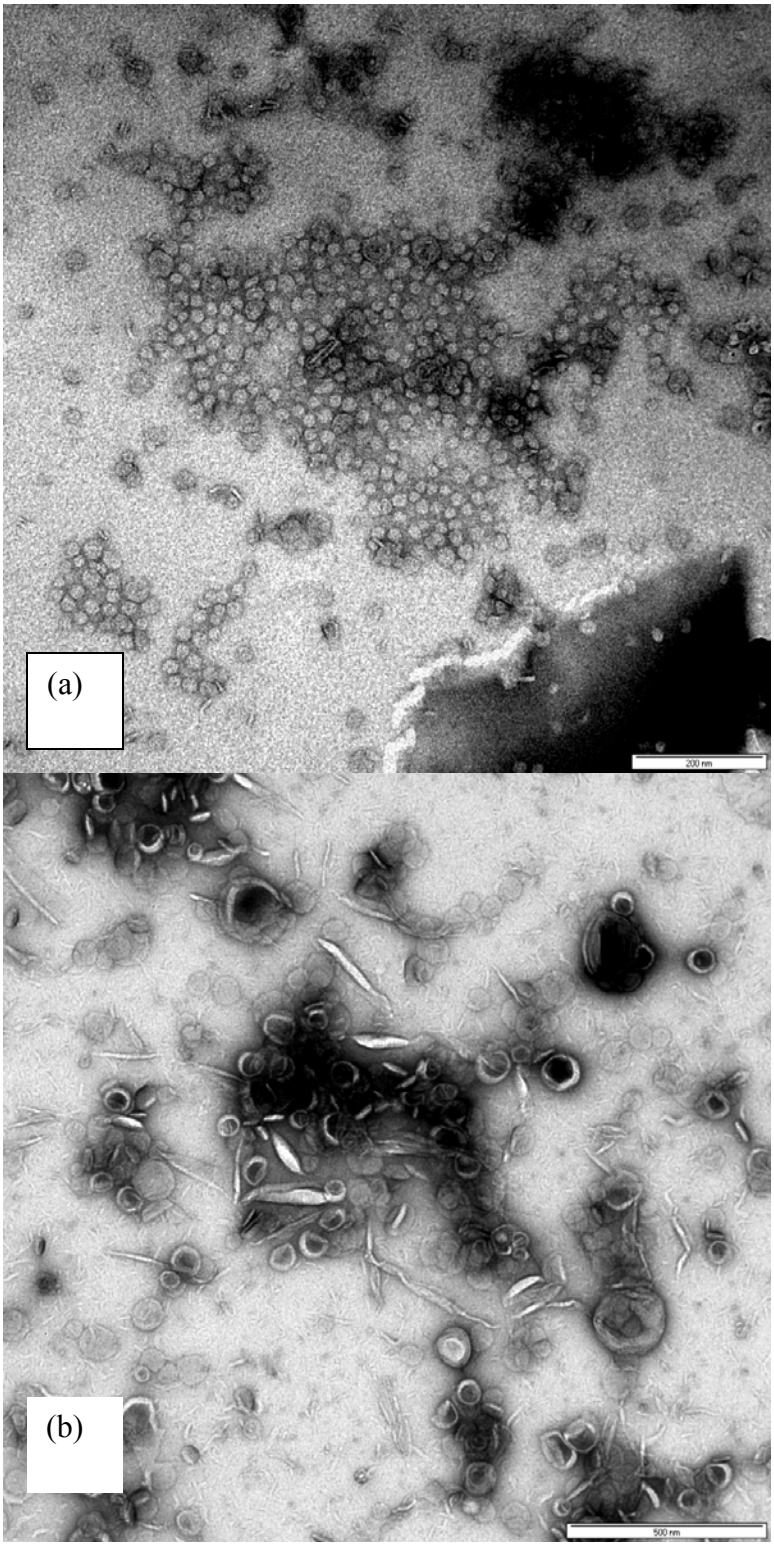

Figure 3-37 Electron micrographs.
(a) is DMPC vesicles. The scale bar is 200 nm. (b) is CF encapsulated in DMPC vesicles. The scale bar is 500 nm. For experimental conditions, see Material and Methods.

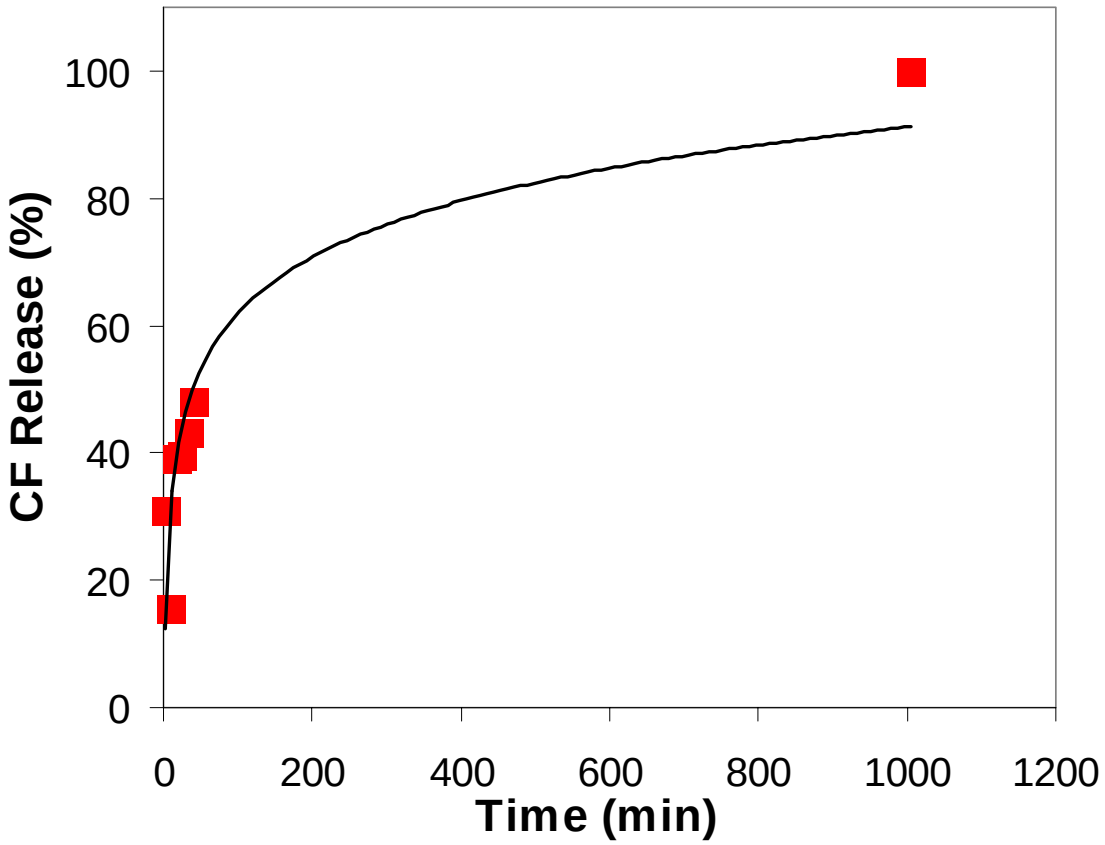

Figure 3-38 Release of carboxyfluorescein in DMPC with addition of 8.5 mM Triton X-100 as a function of time.

3.14. The Effect Bromo and Iodo Iminosulfurane Derivatives on Bilayer Integrity Measured by Carboxyfluorescein Release from DMPC Vesicles Containing 16 Mole Percent Cholesterol

The percent release of CF was monitored as a function of time in one second intervals for 25 minutes (Figures 3-41 and 3-42). The maximum percent release were achieved within the time of mixing. After the maximum release, the percent release of CF decreases and reached a plateau. In the DMPC vesicles containing 16 mole percent cholesterol, there was no CF release with the addition of 3.1 percent bromo derivative. Doubling the amount of bromo derivative to 6.1 percent caused the release of approximately 15 percent of CF. Thirty five percent of CF was released upon the addition of 16 percent bromo derivative. The iodo derivative resulted in an increase of 8.9 percent CF release when 3.5 percent iodo is added. Doubling the amount of iodo added increased the amount of CF released to 25 percent. However, an increase of iodo to 19.1 percent provided only a nominal increase in the percentage of CF released.

3.15. The Effect Bromo and Iodo Iminosulfurane Derivatives on Bilayer Integrity Measured by Carboxyfluorescein Release from DMPC Vesicles Containing 30 Mole Percent Cholesterol

Vesicles containing 30 mole percent cholesterol were treated with varying concentrations of bromo and iodo iminosulfuranes and monitored in one second intervals for 25 minutes (Figures 3-43 and 3-44). The addition of 3.1 and 6.1 mole percent bromo caused 23 percent and 31 percent CF to be released, respectively. The addition of 16.1 mole percent of bromo released 57 percent of the CF. Conversely, the addition of iodo derivative releases less CF than the bromo derivative. The addition of 3.5 percent iodo released 17 percent CF. Increasing the concentration from 7.0 mole percent to 19 mole percent slightly increased the amount of CF released (from 27 percent to 32 percent).

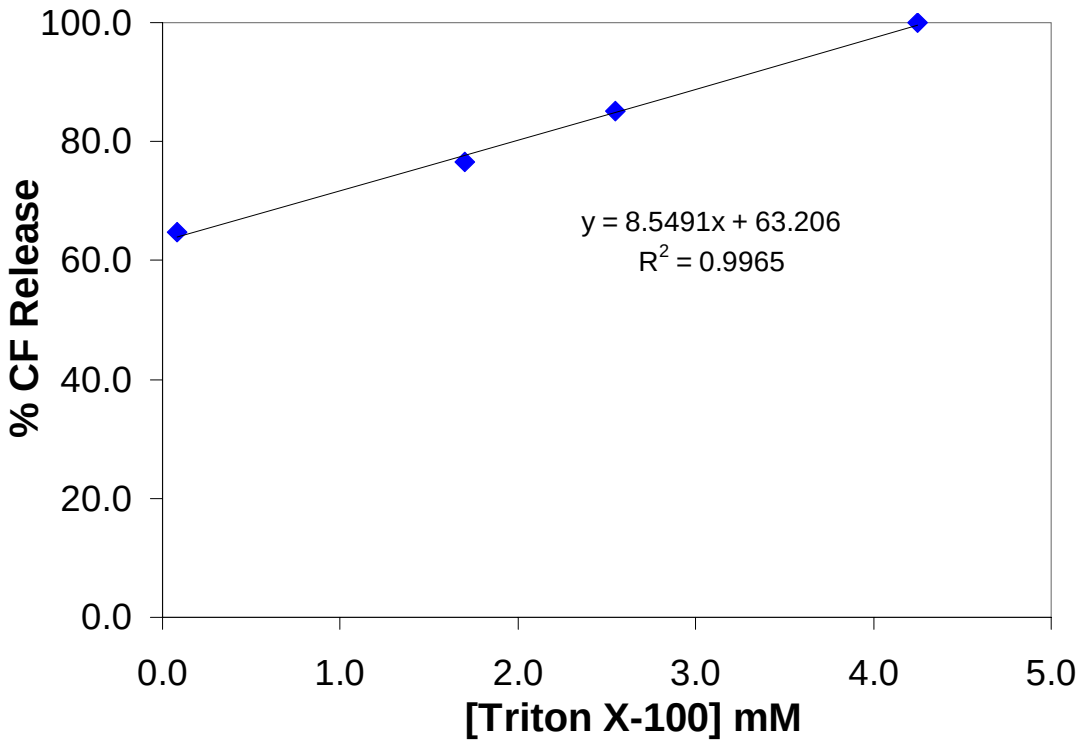

Figure 3-39 The percent of CF released as a function of Triton X-100 concentration.

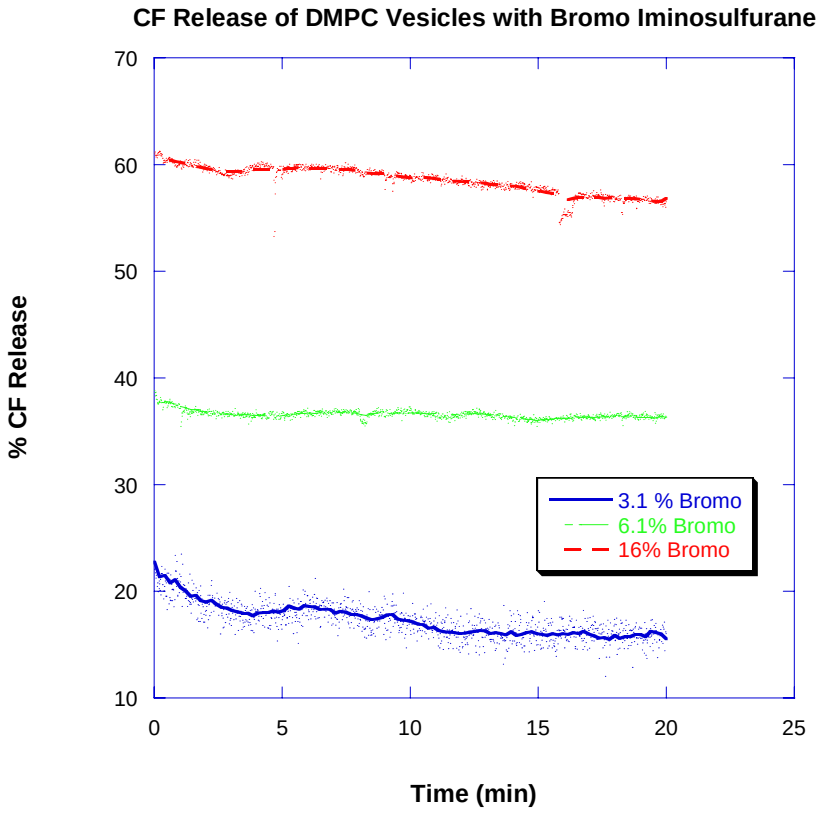

Figure 3-40 Percent changes in release of encapsulated carboxyfluorescein from DMPC vesicles in the presence of increasing concentrations of bromo iminosulfurane derivative.

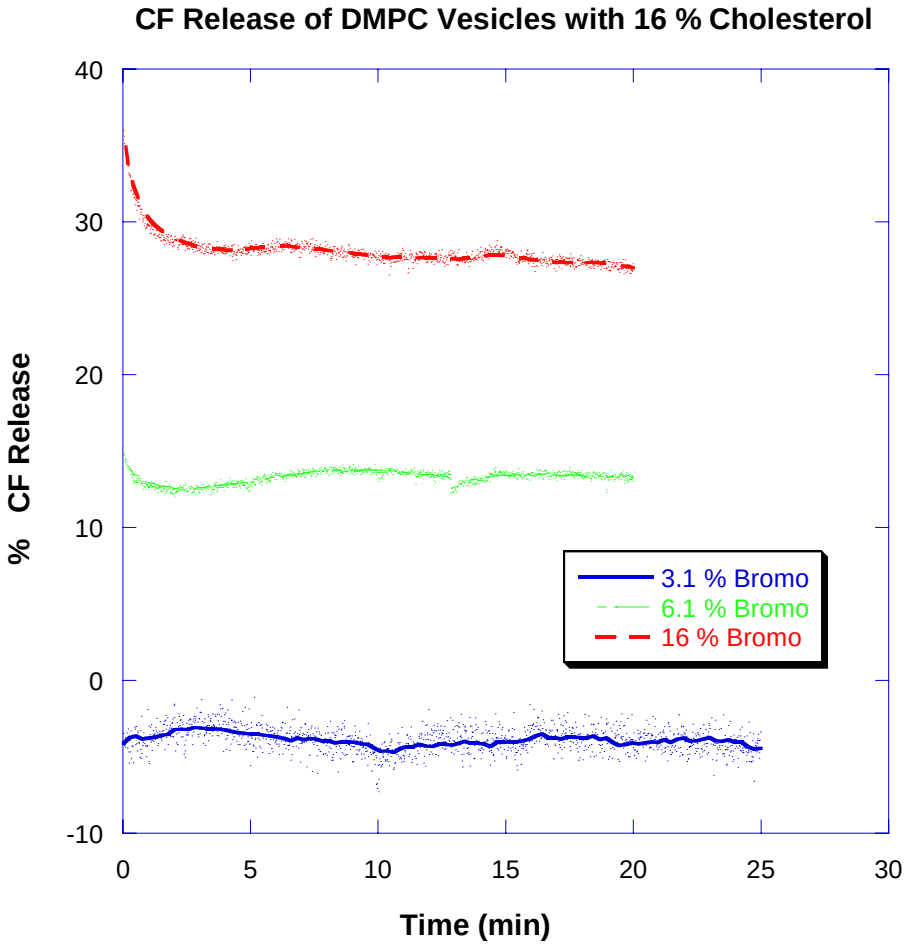

Figure 3-41 Percent changes in release of encapsulated carboxyfluorescein from DMPC -16 mole percent cholesterol in the presence of increasing concentrations of bromo derivative of iminosulfurane.

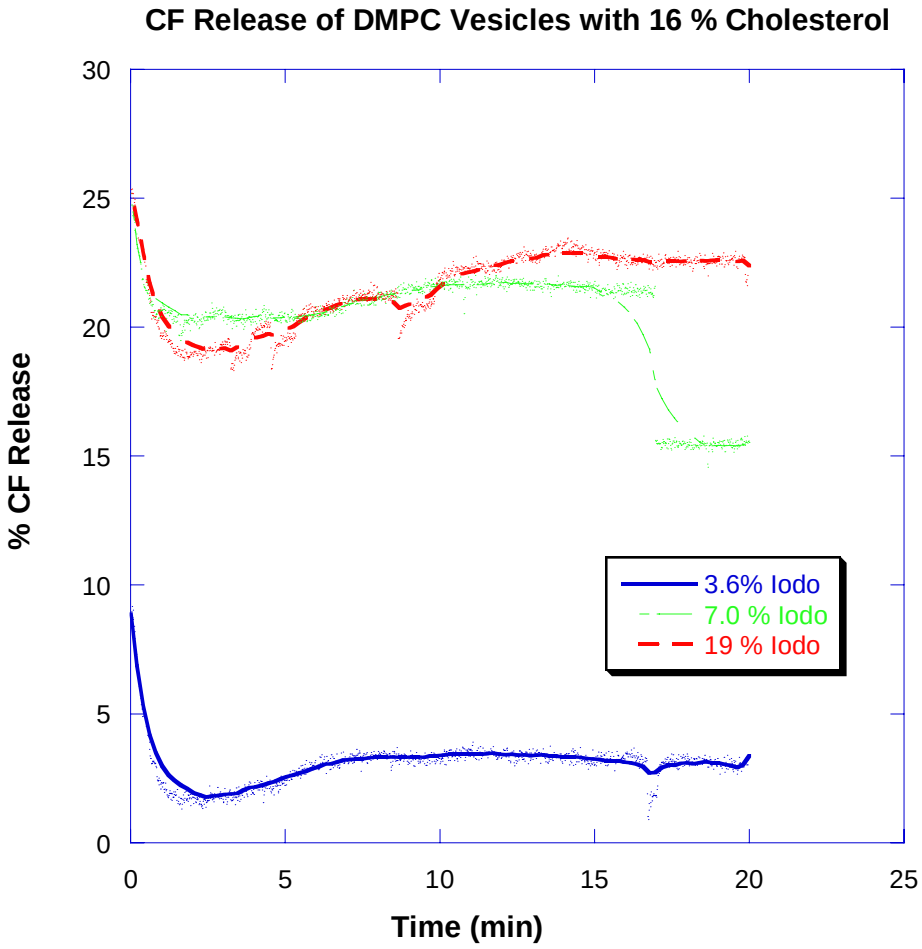

Figure 3-42 Percent changes in release of encapsulated carboxyfluorescein from DMPC -16 mole percent cholesterol vesicles in the presence of increasing concentrations of iodo iminosulfurane derivative.

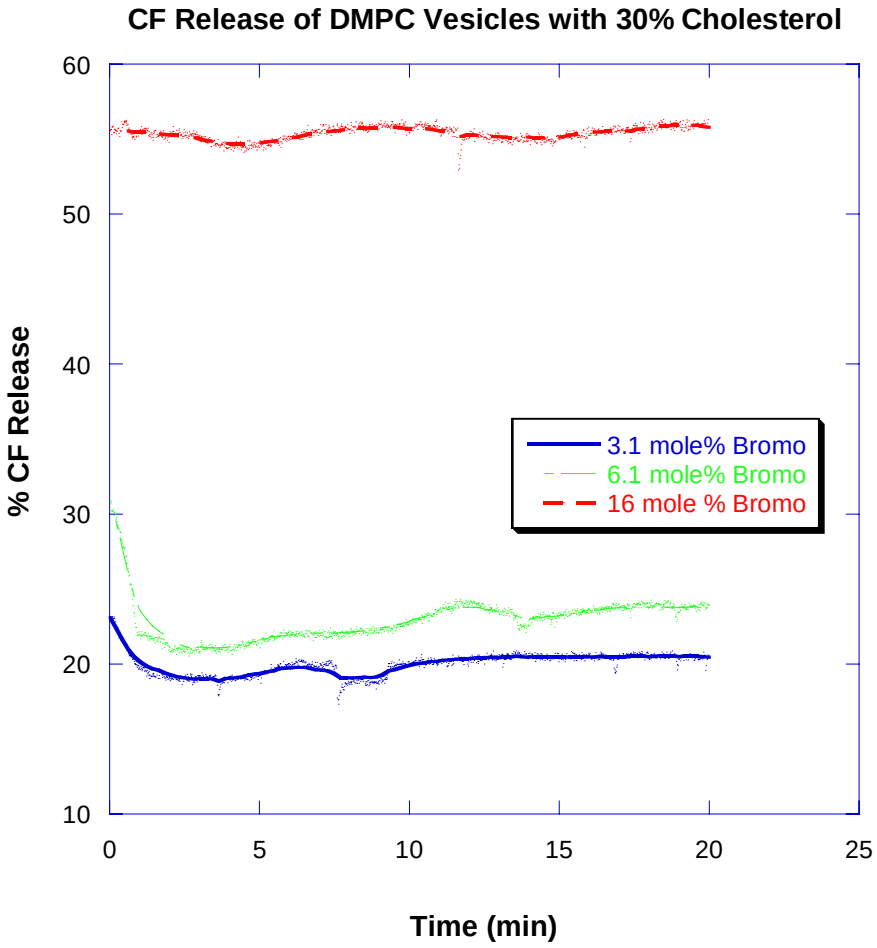

Figure 3-43 Percent changes in release of encapsulated carboxyfluorescein from DMPC -30 mole percent cholesterol vesicles in the presence of increasing concentrations of bromo iminosulfurane derivative.

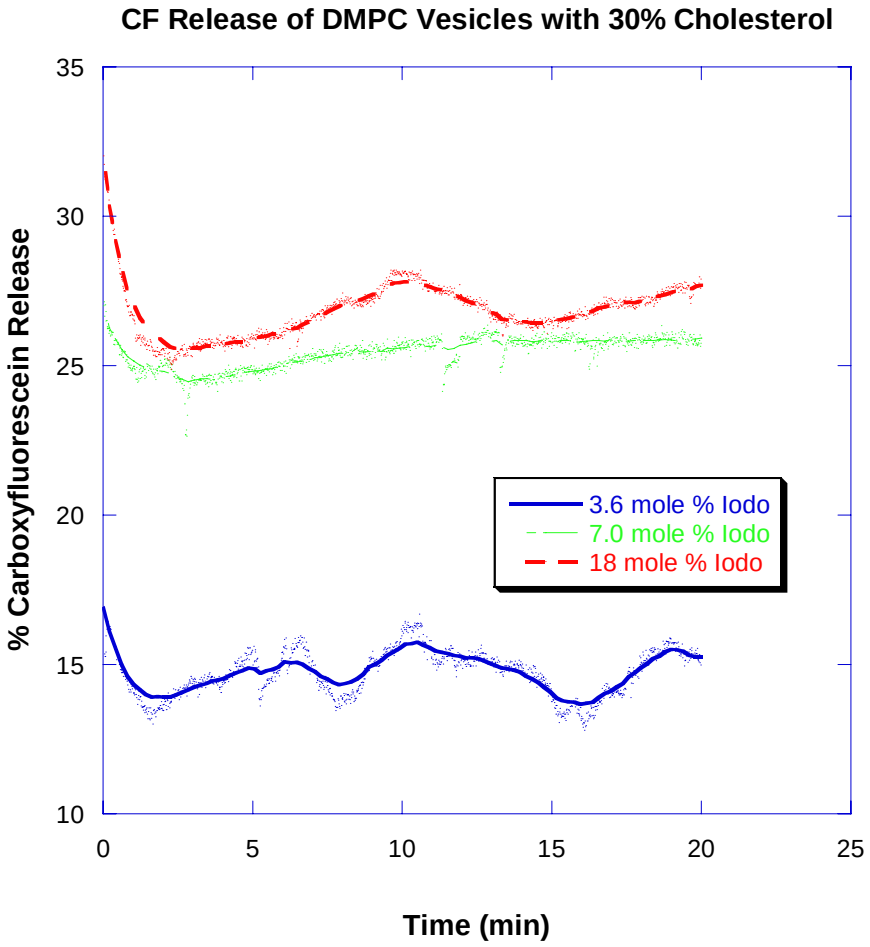

Figure 3-44 Percent changes in release of encapsulated carboxyfluorescein from DMPC -30 mole percent cholesterol in the presence of increasing concentrations of iodo derivative of iminosulfurane.

3.16. Summary of Carboxyfluorescein Release from Vesicles Containing Varying Concentrations of Cholesterol with Bromo and Iodo Iminosulfuranes Derivatives

Figure 3-45 illustrates the effect of the bromo and iodo derivatives on liposomes containing different concentrations of cholesterol. Percentage of CF released increases linearly with the concentration of bromo added in all of the observed DMPC preparations, DMPC, DMPC with 16 mole percent cholesterol, and DMPC with 30 mole percent cholesterol. The greatest amount of CF is released in the DMPC vesicles containing no cholesterol. The effect of increasing the amount of iodo in the cholesterol preparations has a small effect on the percentage of CF released.

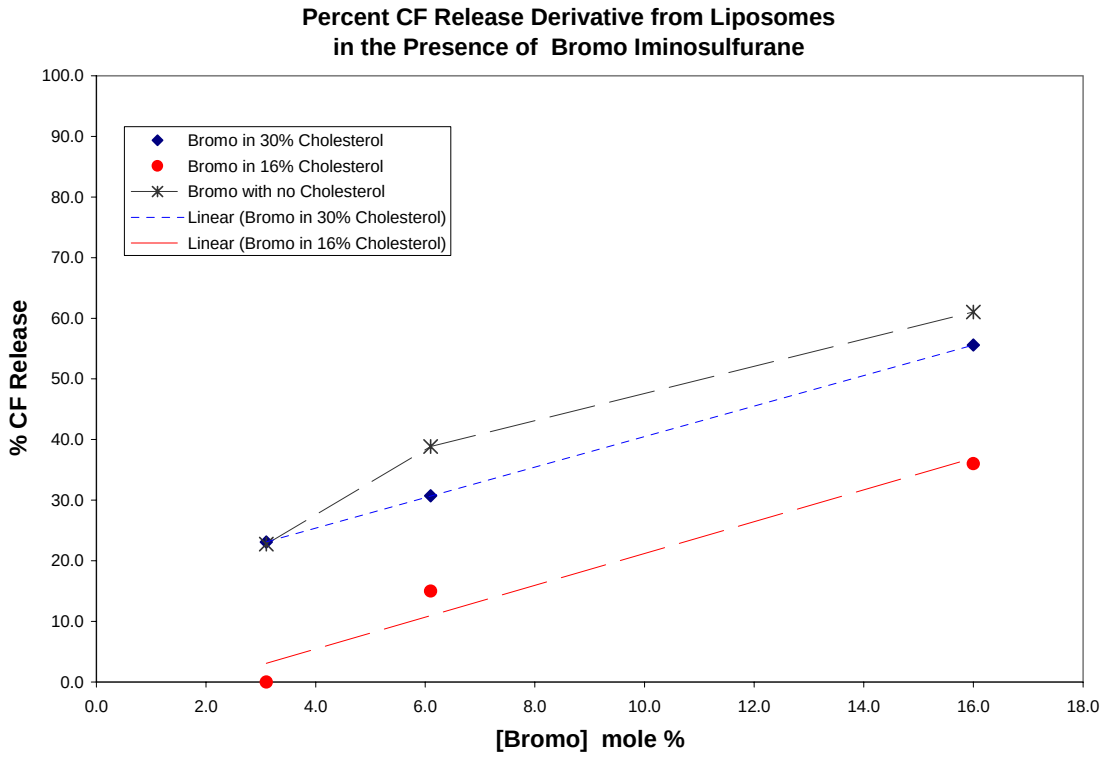

Figure 3-45 Percent changes in release of encapsulated carboxyfluorescein from liposomes in the presence of increasing concentrations of the bromo iminosulfurane derivative

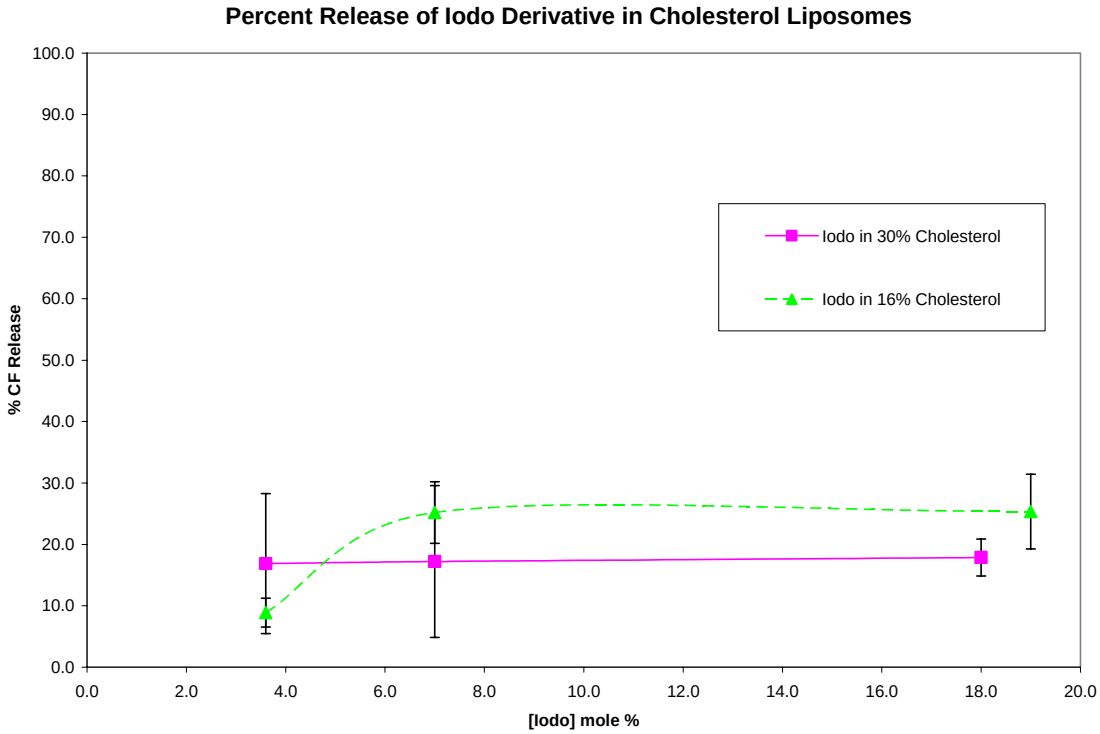

Figure 3-46 Percent changes in release of encapsulated carboxyfluorescein from DMPC - cholesterol liposomes in the presence of increasing concentrations of iodo iminosulfurane derivative.

4. Discussion of Results

4.1. DMPC Bilayers Interactions with Iminosulfurane Measured by Calorimetry

Barrow et al. examine the effects of chloro, bromo and iodo iminosulfurane derivatives on the two phase transitions of DMPC liposomes. During the first transition known as pretransition phase, the polar headgroups are believed to reorient and the lipid bilayer transitions from the gel to ripple layer organization. The main phase transition occurs when the lipid organization changes from ripple to fluid.[27] The pretransition peak broadens and becomes part of the baseline in the presence of 10 mole percent iminosulfurane derivatives. The disappearance of the pretransition peak could indicate that the mode of action of the iminosulfuranes is a surface interaction. The main phase transition occurs when the lipid organization changes from ripple to fluid. The bromo derivative of the iminosulfurane caused a shoulder to appear before the main phase transition of DMPC at a lower temperature. Since simulations of these data could not be reproduced using a single two state model, a multi-two state model was used. This multi-two state model could be indicative of the formation of multiple melting domains and consequently, the destabilization of the DMPC bilayer by the bromo derivative.[27] Additionally when the concentration of the chloro derivative was one mole percent, the profile was similar to the control. For the bromo and iodo derivatives, the profiles could be fit to a single two state model. Therefore, it is possible that the perturbation of the bilayer by iminosulfurane derivatives is concentration dependant.

4.2. Evaluation of Bilayer Penetration of Lipid Bilayer using NOESY

Using the Nuclear Overhauser Effect Spectroscopy (NOESY), strong cross peaks were found to exist between the phenyl protons of the iminosulfurane and the protons of the unresolved methylenes in the DMPC hydrophobic tail. [27] Table 4-1 shows the cross peak volumes as a function of the type of iminosulfurane derivatives at 10 mole percent. The cross peak volume is largest for the most biologically active compound, the bromo iminosulfurane. This observation suggests that there is a greater population of the bromo derivative in the bilayer. The cross peak volume of the iodo derivative is less that than that of the bromo derivative, which suggests that the iodo iminosulfurane does not interact with the fatty acid portion of the bilayer to the extent that the bromo derivative does.

Table 4-1 NOESY cross peak volumes of iminosulfurane derivatives.[27]

Substituent	Cross Peak Volume Methylene (mm^3)
H	0
Cl	2.10
I	5.79
Br	9.08

There are strong cross peaks between the N-methyl protons and the phenyl protons of the bromo and iodo derivatives at 10 mole percent. However, the same cross peaks are absent in the presence of 10 mole percent chloro derivative and one mole percent bromo and iodo derivatives.[27] These observations further support a concentration dependant effect on bilayer perturbation. The most notable result of this series of experiments is the appearance of a cross peak between the phenyl protons of the bromo derivative and the terminal methyl of the lipid tail, which suggests that the bromo derivative is able to

deeply penetrate into the bilayer.[27] All NOESY measurements are based on the assumption that the buildup rates are identical for all iminosulfuranes.[27]

4.3. Principles of ^{31}P NMR

Some atomic nuclei have magnetic moments that are sensitive to their environment and interact weakly with them. NMR exploits this propensity for dimagnetic nuclei such as ^{1}H, ^{2}H, ^{13}C, ^{14}N, ^{19}F and ^{31}P to interact with magnetic fields. Because most molecules contain at least one isotope with a magnetic moment, this interaction is useful for gaining molecular information and kinetic information about molecules with little disruption on the observed species.

When a magnetic nucleus, such as phosphorus is placed in a magnetic field, it adopts one of two possible orientations. The nucleus should either be in the same direction as the applied field (+½) or in the opposite direction of the applied field (-½). The nucleus has a lower energy level when it is parallel to the field and a higher energy level when it is antiparallel to the field. Sample magnetization from the NMR comes from the different distribution of nuclear dipoles in the two energy states. Because the energy difference the phosphorus nuclei is small, the population difference of energy levels is parts per million.

There are two ways in which NMR spectrum can be obtained, continuous wave and pulse. Modern NMR spectroscopy employs pulse techniques. The data collected is in the form of free induction decay (FID). Fourier transform converts the FID from time domain into a spectrum in the frequency domain.

Phosphorus-31 has 100 percent natural abundance and a high gyromagnetic ratio which makes it an ideal nucleus for probing the structure and interactions of lipids on a microscopic level. Phosphorus peaks are typically characterized by broad lineshapes

which are a result of the chemical shift anisotropy (CSA) due to limited phosphate group motion in vesicles. Since chemical bonds are generally magnetically anisotropic, they have different susceptibilities along the x, y, and z directions in space. Therefore, the magnetic moments induced by the external field B_o are not uniform. The effect of CSA can be minimized by the rotational diffusion of the molecule. Since the diffusional motion and conformation of the head group can affect the CSA experienced by the molecule, the lineshape of the phosphorus resonance is also a function of the motion and conformation and provides information about the phase of lipids.[42] The ^{31}P NMR lineshapes most commonly found in lipid bilayers are characteristic of three types of phases, isotropic, hexagonal and lamellar. The lineshape of lipids in the isotropic are characterized by narrow sharp resonances. In the case of the phosphorus found in the head group of small unilamellar vesicles (< 500 Å), the lineshape is narrow and sharp and the result of the fast tumbling and diffusion rates relative to the NMR scale.[43] The lineshape characteristic of a hexagonal phase is asymmetric and has a slight shoulder on the upfield from the peak. The characteristic lineshape of lamellar phases are also asymmetric with a shoulder on the downfield of the resonance. Lipids in the lamellar phase often transitioned to the hexagonal phase by increasing water content.[32]

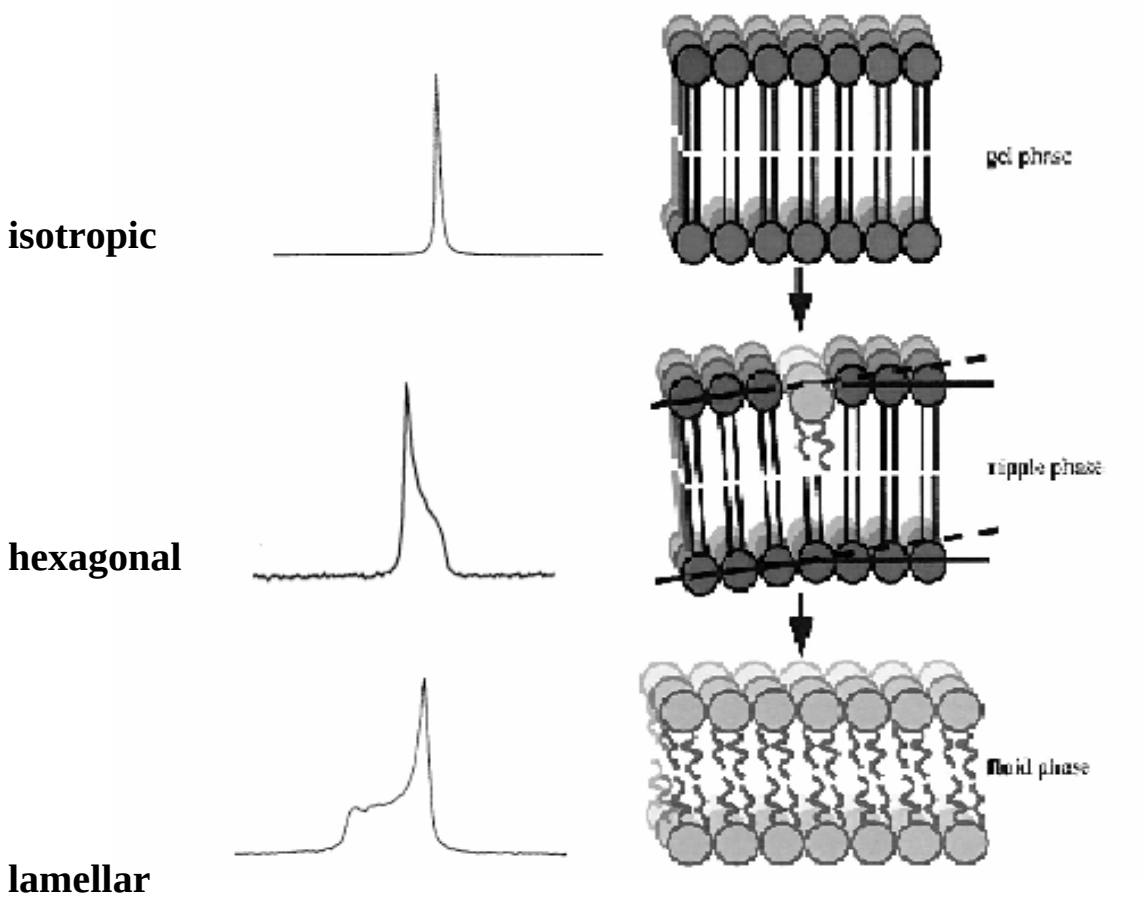

Figure 4-1 Characteristic ^{31}P lineshapes.[44-47]

At low magnetic field it is possible to observe the resonances from phosphorus in the inner and outer leaflet. Since CSA increases with the square of the magnetic field strength, at higher magnetic field, the peaks broaden so that the resonances of the inner and outer leaflet become indistinguishable. In order to use a higher magnetic field and be able to observe the resonances from the inner and outer leaflet, it becomes necessary to use a shift reagent to split the resonances. Since phosphorus nuclei, like all magnetic nuclei, are sensitive to their chemical environments, their sensitivity to chemical surroundings can be exploited with the use of a lanthanide metal shift reagent which does not significantly perturb the polar head group conformation.[37] Pr^{3+} is a paramagnetic species which interacts with the outer layer of the unilamellar vesicle via a pseudo contact process (Figure 4-1). [48] The pseudo contact process is an interaction that exists between the magnetic dipole of the paramagnetic species and the phosphorus nuclei (Equation 4-1). The resulting change in the resonance frequency is proportional to the geometry (ν), and the magnetic dipole moment of the paramagnetic species (K). Contact interaction varies inversely with the third power of distance (r). As a result, the shielding of the phosphorus moiety in the head group in the outer leaflet is reduced and the phosphorus group relaxes through an alternate pathway with a shortened relaxation time, relative to that of a Pr^{3+} free control, which causes the peak of the outer leaflet to broaden and shift downfield.

Hence, the ^{31}P resonances of DMPC and DMPC-cholesterol unilamellar vesicles are split into two signals by the slowly penetrating paramagnetic metal ion Pr^{3+}. The extent to which this splitting is attenuated by transdermal penetration enhancers is indicative of the extent to which such deep penetration has occurred and has been investigated as a

function of the time over which the DMPC and DMPC-cholesterol preparations are exposed to Pr^{3+} utilizing the iminosulfuranes described in Figure 1-4.

The extent of the iminosulfurane-induced perturbation of the bilayer preparations can be observed over time as a reduction in the Pr^{3+} - mediated ^{31}P resonance separation. As the iminosulfurane-induced perturbation of the bilayer develops, the collapse of the ^{31}P resonances suggests that Pr^{3+} is gaining access to the phosphate groups on the inner leaflet on a short distance scale since the contact interaction varies inversely with the third power of the distance between the phosphorus moiety and the paramagnetic species (Equation 4-1). This observation confirms that the perturbation induced by these iminosulfuranes extends to an appreciable extent across the bilayer, i.e. it is a transmembrane effect and implies deep penetration of these compounds into the bilayer.

$$\Delta_{Dip} = K\frac{3\cos^2\upsilon - 1}{r^3}$$

Equation 4-1 Pseudocontact term.[48]
Δ_{Dip} is shift in resonance frequency.
K is constant that depends on the magnetic dipole moment of the paramagnetic ion.
υ is the angle between the paramagnetic ligand and the observed nuclei.

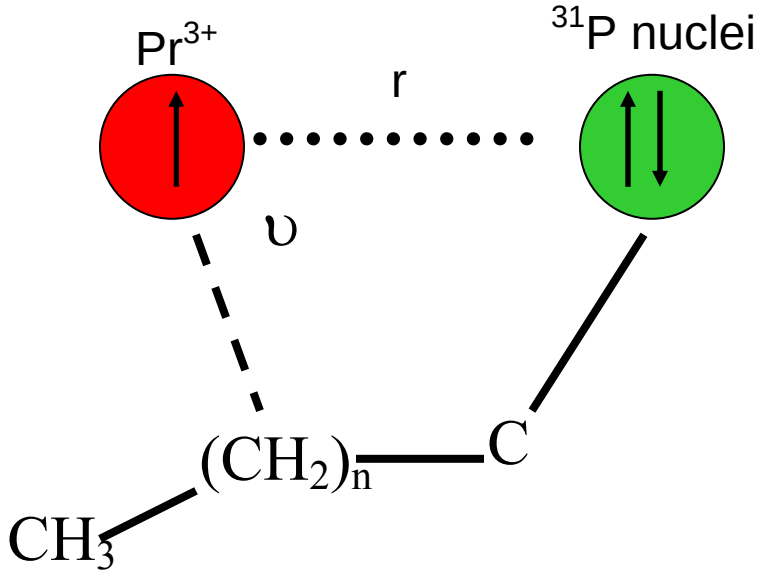

Figure 4-2 Interaction of phosphorus nuclei with praseodymium shift reagent.[48]

4.4. Evaluation of Iminosulfurane Activity Using ^{31}P NMR

In the DMPC vesicle system prepared in HEPES buffer with EDTA, concentrations of bromo and iodo iminosulfuranes below 1 mole percent actually impede the collapse of peak separation relative to the control suggesting that perhaps there is a threshold concentration at which the bromo derivative becomes active similar to DMSO which is most effective at 60 percent. Five mole percent bromo compound provides a marginal increase in decay. However, it is within the limits of error for the control. Ten mole percent bromo provides a significant increase in the decay of resonance peak separation relative to the control. The peak collapses completely to zero which indicates that in the presence of 10 mole percent bromo, the Pr^{3+} is able to gain access to the inner leaflet of the bilayer.

4.5. Effect of Concentration Dependence on Iminosulfurane Activity Using ^{31}P NMR

In the DMPC vesicles suspended with HEPES buffer containing EDTA, iminosulfurane concentrations below 1 mole percent may actually impede the collapse of peak separation relative to the control suggesting that perhaps there is a threshold concentration at which the bromo derivative is able to perturb the bilayer. This observation is also supported by the DSC heat profiles and NOESY cross peak reported by Barrow et al.[27] The concentration dependence of efficacy is also a characteristic of DMSO which has a threshold concentration at which it is most effective.[25] Five mole percent bromo compound provides a marginal increase in decay. However, it is within the limits of error for the control. Ten mole percent bromo provides a significant increase

in the decay of resonance peak separation relative to the control. The peak collapses completely to zero, which suggests that in the presence of 10 mole percent bromo, the Pr^{3+} is able to gain access to the inner leaflet of the bilayer.

One tenth of a percent of iodo derivative seems to have a stabilizing effect on the collapse of peak separation, whereas one percent has no effect on the decrease in peak separation. Ten mole percent iodo collapses the peak separation to 6 ppm with in 30 hours. At this concentration, the iodo peak separation does not reach zero. Therefore the iodo compound causes less of a bilayer disruption.

Comparison of the bromo, iodo, and chloro derivatives at 10 mole percent, 10 mole percent, and 20 mole percent, respectively, support the biological data that the bromo compound is the most active. Additionally, 10 mole percent of bromo caused the collapse of peaks within 50 hours.

These results correlate with the NOESY cross peak data and permeation studies (Figures 4-3 and 4-4). Based on the biological activities of the halogenated iminosulfuranes, the bromo derivative is the most active, followed by the iodo derivative and finally by the chloro derivative, the least active of the series (Figures 4-3).

Slowly penetrating paramagnetic metal ions differentially shorten the relaxation time of the phosphate moieties in the inner and outer leaflets of the lipid bilayers.[39] This observation further suggests that a perturbation of sufficient extent to accommodate the passage of the hydrated form of the Pr^{3+} is probably developed (i.e., a water channel is induced by the iminosulfuranes in order for the highly charged ion to gain access to the phosphorus moiety in the inner leaflet of the membrane bilayer).

4.6. Effect of Praseodymium Ion on DMPC Liposomes

Since phosphate groups are binding sites for positive metal ions, each vesicle has a fixed number of binding sites. [39] Assuming that all phosphate groups in the outer leaflet of the bilayer are equally accessible, an increasing metal concentration will eventually saturate the available binding sites and cause the peak separation between the inner and outer leaflets to reach a maximum. It is possible that as the Pr^{3+} concentration approaches 4.5 mM, the peak separation approaches a maximum because the sites approach maximum capacity.

Increasing the concentration of Pr^{3+} results in an increase of peak separation between the inner and outer leaflet of the lipid bilayer, because the amount of shielding experienced by the phosphate groups in the outer leaflet of the bilayer is greater than that of the inner leaflet. As result of the shielding, resonances due to the phosphate groups on the outer leaflet shift downfield and broaden. Since the increased concentration of shift reagent does not alter the time that it takes for the two resonances to collapse into one peak, the peak separation decay rate increases with increasing concentrations.

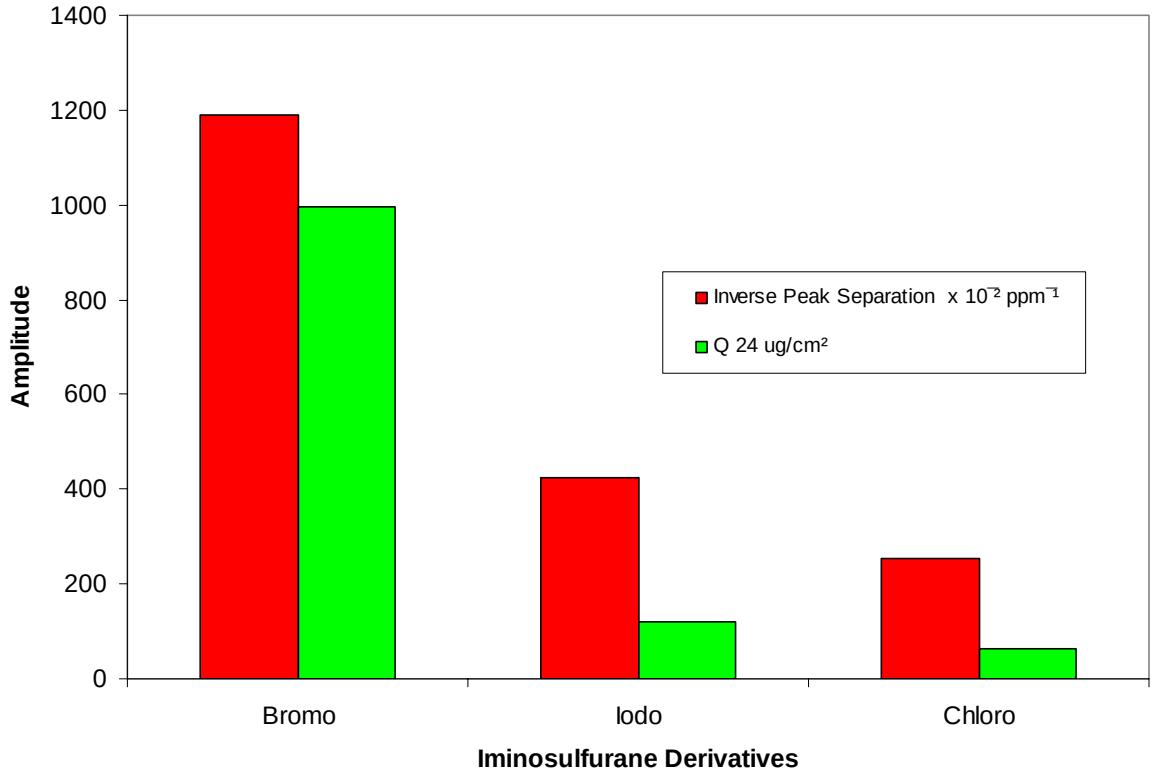

Figure 4-3 Comparison of inverse peak separation and Q_{24}, a measure of biological activity of the iminosulfuranes.

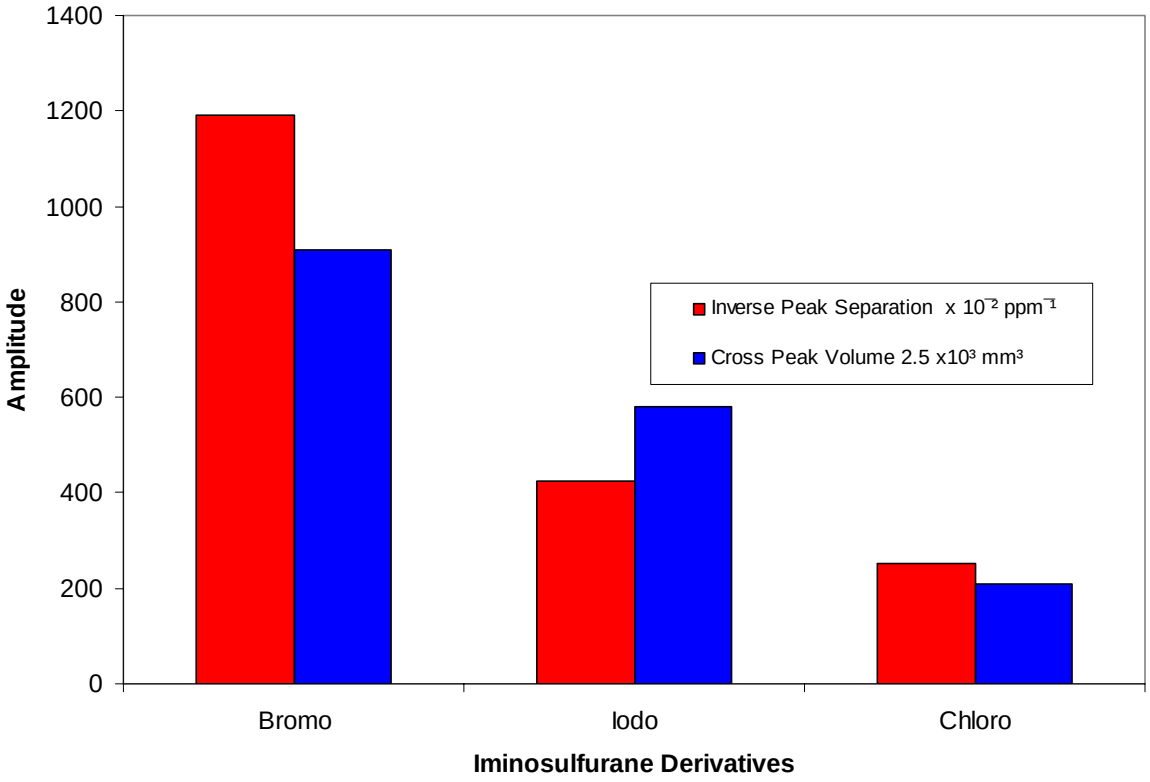

Figure 4-4 Comparison of inverse peak separation and cross peak volumes measured with the NOESY DMPC vesicles and iminosulfurane derivatives.

4.7. Interaction of Bromo and Iodo Iminosulfuranes with DMPC Liposomes

In DMPC liposome suspended in HEPES with no EDTA, there is an appearance of third peak 16 hours after the addition of shift reagent. Since phosphate lineshapes are indicative of a polymorphism of the lipid bilayers, the appearance of an additional spectral component indicates that the phosphate group is in a different orientation therefore experiencing a different magnetic moment from what is normally found in lipids. [49] This spectral components supports the notion that there is a transition of the lipid from a bilayer to hexagonal phase, a change that most probably the results from movement of the Pr^{3+} ion across the bilayer.[49] Within the 6 hours, the additional spectral component disappears and the spectra once again become typical for lipid bilayer phases. The shift reagent therefore induces a transient change in phosphate head group conformation.[50] The effect of 10 mole % of iminosulfuranes, bromo and iodo derivatives, on DMPC liposome further supports the biological data and NOESY cross peak volumes discussed in sections 1-3 and 4-2, respectively. The peak separation of the inner and outer leaflet of the bilayer collapse to zero within 52 hours. This complete collapse supports the theory that the bromo derivative induces the formation of a pore or channel that allows the praseodymium ion to move through the bilayer and shield the phosphate groups in the inner leaflet. Conversely, the effect of the iodo has a smaller effect on the collapse of peak separation. During the time of the experiment, the peak separation decreased from 15 ppm to 8 ppm within 64 hours. While the iodo derivative is active, it is not as active as the bromo compound.

4.8. Decay of ^{31}P Resonance Separation as a Function of Cholesterol Concentration

It has been suggested that cholesterol induces a new state that is different from the gel state or the liquid-crystalline state. The new state is referred to as the liquid ordered state.[33] The presence of the rigid steroid nucleus of cholesterol inserts itself into bilayer reducing the number of kinks in the hydrophobic tail of the lipids.[33] The reduction of kinks in lipids containing less than 18 carbons causes the membrane to thicken. In addition to these morphological changes, cholesterol decreases the permeability of small molecules across the membrane bilayer. Normally small molecules are able to permeate the membrane via transient channels in the bilayer that result from lipids packing defects.[33] The ordering of the bilayer by cholesterol minimizes these packing defects. Consequently, the permeability of small molecules decreases with increasing cholesterol content. Finally, the cholesterol interferes with the electrostatic interactions and hydrogen bonds that form between phosphate head groups.[33]

The decays of ^{31}P resonances were monitored as a function of cholesterol concentration. The most obvious change that occurred was the increased stability of the system as a result of the increased cholesterol concentration. The time needed for the Pr^{3+} ion to gain access to the inner leaflet increased with greater cholesterol concentration. This observation is supported by the fact that cholesterol reduces the permeability of small molecules. The time required for the liposomes to achieve maximum peak separation at constant shift reagent concentration was directly proportional to the cholesterol concentration. It may be that the interference of cholesterol with head group interaction alters the time needed for the Pr^{3+} ion to bind to phosphate groups.

4.9. Effect of Iminosulfurane on Liposomes Containing 16 Mole Percent Cholesterol

The effect of bromo, iodo, chloro, and hydrogen derivatives on splitting was monitored as a function of time over a period of 90 hours in DMPC vesicles containing 16 mole percent cholesterol. The addition of the bromo derivative caused a collapse of the splitting to zero within 30 h and broadened the lineshape of the resonance of the outer leaflet. The collapse of peak separation within 30 hours suggests that the 10 mole percent bromo induces a change in the bilayer such that the permeability of the praseodymium ion is increased relative to that experienced by the control. The characteristic line broadening has been suggested to be a consequence of the action of membrane active agents.[49] The line broadening in this region is explained by idea that part of the lipid bilayer is immobilized and disorganized by the presence of a membrane active compound such as the bromo derivative of the iminosulfurane. Yet it remains in equilibrium with the bilayer.[49] Both observations of the bromo derivative support the findings discussed earlier. Biological data as well as NOESY cross peak volumes and DSC heat profiles indicate that activity of the bromo compound is a function of deep penetration into the bilayer and the formation of pores or channels that allow small molecules to move across the membrane.

Ten mole percent of the iodo compound is less active than the bromo, an observation that confirms biological data. However based on the decay of peak separations, the iodo compound perturbs the bilayer more than the chloro and hydrogen derivatives. Examination of the peak shapes after the addition of iodo derivative and comparison to the chloro and hydrogen derivatives clearly shows that there is a greater perturbation

caused by the iodo compound. The activity of the chloro and hydrogen derivatives is minimal in contrast to that of the bromo and iodo derivatives.

4.10. Effect of Iminosulfurane on Liposomes Containing 30 Mole Percent Cholesterol

The effect of iminosulfurane derivatives on the peak separation was monitored as a function of time over a period of 90 hours in DMPC vesicles containing 30 mole percent cholesterol. The addition of iminosulfurane derivatives at 10 and 20 mole percent caused a collapse of the splitting that was not significantly different from the control. This observation is a consequence of the ordering and reduced permeability of the membrane bilayer caused by the incorporation of cholesterol into the membrane. However upon close examination of the spectra of the bromo and iodo derivatives at 10 and 20 mole percents (Figures 3-24, 3-25, 3-27 and 3-28), there is a difference in the linewidths of the resonance due to the inner leaflet when compared to that from the control. The bromo and iodo derivatives perturb the bilayer to a greater extent than that of the either the chloro or hydrogen derivatives as shown by examination of the spectra.

4.11. Principles of Fluorescence

Fluorescence is one of the types of molecular luminescence spectroscopy that occurs when a photon of light is absorbed. The absorbed photons are then emitted in one of two ways. The first type of emission is known as resonance fluorescence where the absorbed and emitted photon has the same energy or wavelength. The second type is observed more often and results from a Stokes' shift which occurs when the emitted photon has a longer wavelength or is less energetic than the absorbed photon.

In fluorescence, an electron is excited at a particular wavelength. The excited electron moves from the ground state (S_o) to a vibrational level in the singlet state through a nonradiative process. A photon is emitted as the electron falls from the singlet state to the ground state (Figure 4-5). The amount of time required for the emission is greater than the time required for absorption. However, when compared to phosphorescence, which involves a forbidden transition, spin flip inversion, the lifetime for fluorescence is relatively short, picoseconds to nanoseconds.

There are many processes that compete with fluorescence, for example: internal conversion, predissociation, external conversion, and intersystem crossing. Internal conversion occurs when the absorbed photon goes to a lower electronic energy state nonradiatively. Predissociation and dissociation occur with the rupture of a molecular bond and chromophore, respectively. External conversion is a function of the environment, because energy transfer between the species, solvent and other surrounding molecules can deactivate the excited state. Intersystem crossing is a forbidden process, but it does occur when the electron relaxes from an excited singlet to a triplet and undergoes spin flip inversion. Despite these competing processes, a molecule that fluoresces has several advantages over a molecule that can only be detected by absorption spectroscopy. Fluorescence is particularly useful because the linear concentration range is greater and more sensitive than absorption spectroscopy.

4.12. Selection of Fluorophore

Lipids are devoid of intrinsic fluorescence. Therefore, in order to examine the effect of iminosulfuranes on membrane integrity using fluorescence, it becomes necessary to use an extrinsic fluorophore. An ideal fluorophore for this system must not

bind to the membrane, must undergo self quenching, have a small Stokes shift, and absorb in the far red region. Several classes of fluorophores were considered: e.g., fluorescein analogs, cyanines, rhodamines, xanathamide fluorescent dyes, fluorescent sterols, and styryls. Cyanines, rhodamines, xanathamide, fluorescent dyes, fluorescent sterols, and styryls tend to bind or anchor to the lipid bilayers, whereas carboxyfluorescein has very little association with membranes. [51-56]

The ideal fluorophore should exhibit a small Stokes Shift, the difference in the wavelength between absorbed and emitted quanta (Figure 4-6). The emitted wavelength is equal to or longer than the excitation wavelength. Small overlap of excitation and emission spectra will permit the fluorescence of the dye to be self-quenched at high concentrations such as could exist in the interior of a vesicle. Self- quenching occurs when there is a large number of species in solution, resulting in collisions between molecules. These collisions cause a radiationless energy transfer. The efficiency of which varies inversely with sixth power of the distance between two molecules of the fluorophore. This radiationless transfer competes with the fluorescence and hence lowers the quantum yield of fluorescing species at high concentrations. The structure of carboxyfluorescein is shown in Figure 4-7. It is an ideal fluorophore for this assay in that it exhibits minimal association with lipid bilayers, undergoes self-quenching at concentrations greater than 100 mM via the formation of dimers (Figure 4-8) and absorbs in the far red region of the visible spectrum

4.13. Structural Characterization of Vesicles Encapsulated with CF

The increase in the diameter of the vesicles encapsulated with CF raises the question as to why the presence of the dye shifts the diameter to a larger size (Figure 3-37). There were two possible considerations that could account for the shift. The possibilities are the osmotic swelling of the vesicles or fusion of two or more vesicles.[37] Bammel et al. used electron micrographs and T_2 relaxation time NMR experiments to determine the phenomena responsible for these observations. Electron micrographs showed that vesicle fusion continues until all of the vesicles aggregated while there was no minimal concentration necessary for the decrease in T_2 relaxation times.[37] Based on these results, it was inferred that vesicle fusion is principally responsible for the increase in diameter.[37]

4.14. Stern-Volmer Plots of Bromo and Iodo Derivatives

The heavy atom effect of halogenated compounds is an important consideration for the use of halogenated iminosulfuranes in an assay measuring fluorescence. The Stern-Volmer plots of the bromo and iodo derivatives had a slope of zero when the concentrations of the compounds were in the micromolar range, indicating that the diffusional quenching constant is zero. Consequently, there is no heavy atom effect exhibited by these compounds in the micromolar range.

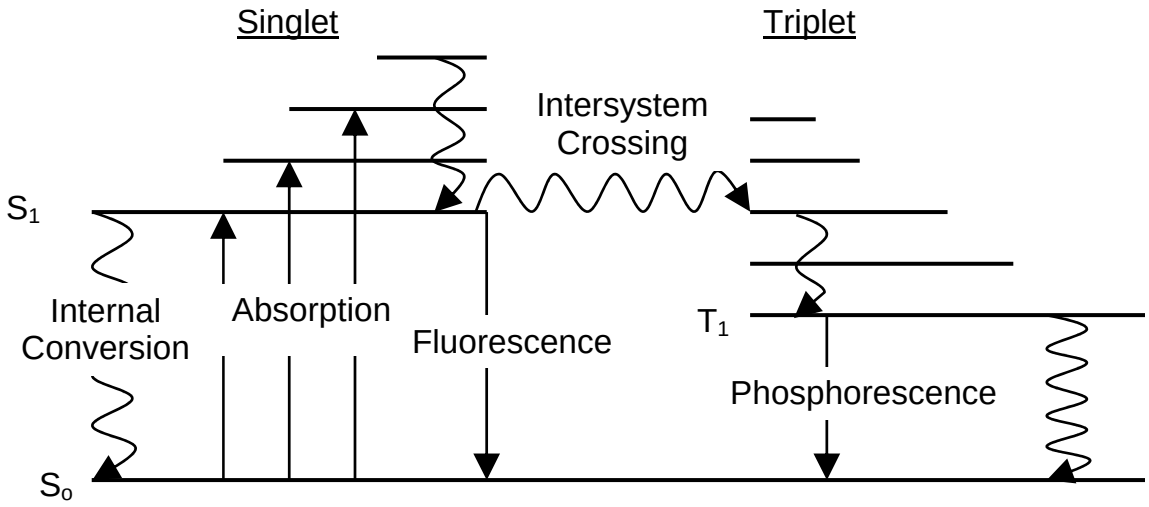

Figure 4-5 Jablonski diagram.

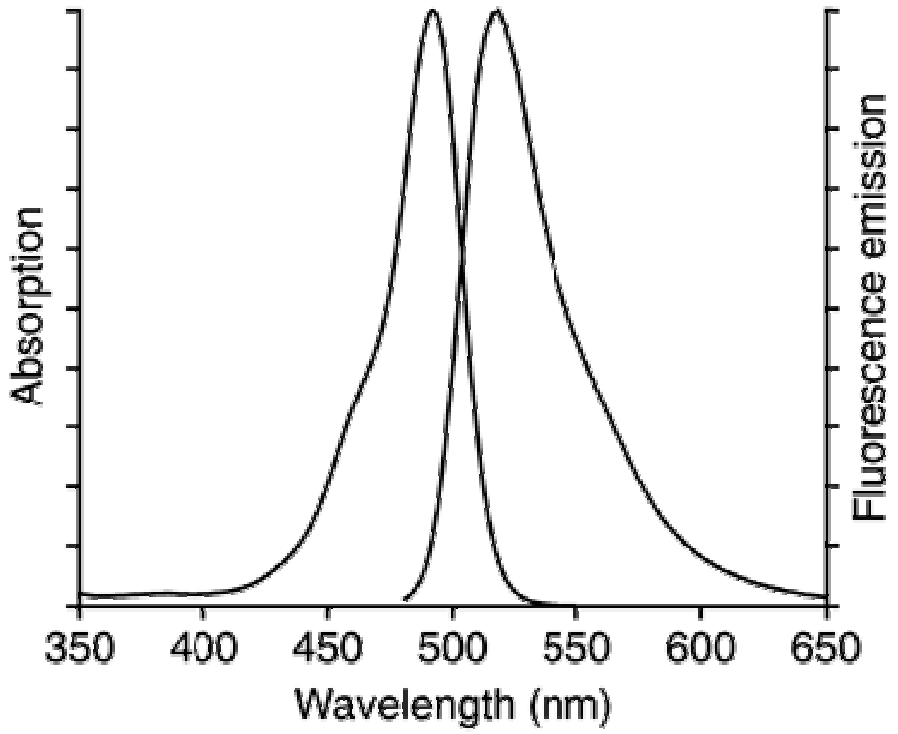

Figure 4-6 Excitation and emission spectra of carboxyfluorescein.[57]

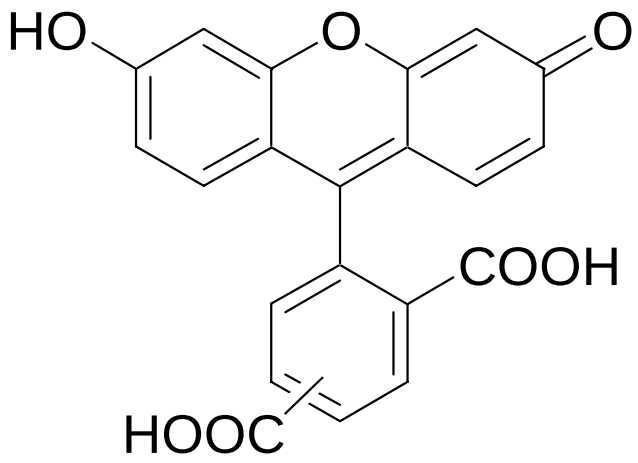

Figure 4-7 Structure of carboxyfluorescein.

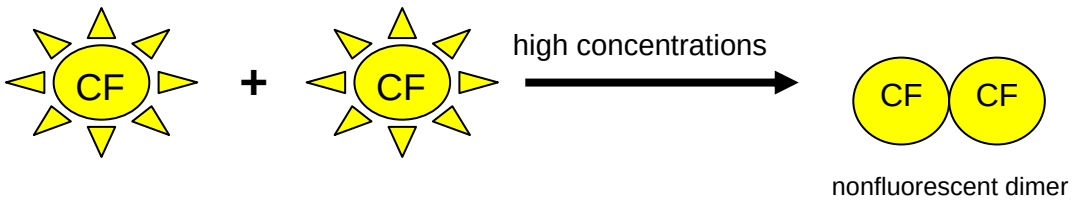

Figure 4-8 Quenching of carboxyfluorescein at concentrations greater than 100 mM.

4.15. Interaction of Triton X-100 on Bilayer Integrity

The CF release curve exhibited an increase in CF release until a plateau was reached, when 100 percent of the CF had been released. It has been suggested that nonionic surfactant monomers incorporate into the bilayer to induce pore formation or stabilize transient pores.[58-60] The plateau is achieved when all of the CF has been released. Nonionic surfactants are effective TPEs. Understanding the behavior of Triton X-100 is important 20 percent (v/v) Triton X-100 is added the ended of the CF quenching assay in order to determine the maximum fluorescence intensity (Equation 4-1).

4.16. Bilayer Integrity Measured by Carboxyfluorescein Release from DMPC Vesicles and DMPC Vesicles with Cholesterol

The objective of this assay was to determine the effect of iminosulfurane derivatives on the bilayer integrity of vesicles. All CF release curves decrease exponentially where the maximum amount of CF is released within the time of mixing the sample. The amount of CF released increases linearly with increased concentrations of bromo derivative. It is likely that the bromo derivative induces the formation of channels in the membrane bilayer by interacting with the polar head groups of the lipid matrix and displacing surrounding water molecules similar to DMSO. The iodo derivative causes a CF release that is much smaller than that induced by the bromo derivative. These results are supported by the reported biological activity, where the bromo derivative is the most active in the series of compound.[26] These results are further supported by the observation of the effect of these transdermal penetration enhancers on the decay of peak separation in the ^{31}P NMR experiments. In the presence of bromo

derivative, the Pr^{3+} was able to gain access to the inner leaflet more quickly than the time required to gain access in the presence of the iodo derivative.

4.17. Summary of Interactions of Iminosulfurane Derivatives

The bromo derivative is the most active iminosulfurane in this series of compounds followed by the iodo and chloro derivatives.[26] The time course of the collapse of the ^{31}P NMR resonance correlates with this activity in that the splitting is collapsed most rapidly by the bromo derivative as shown in DMPC and DMPC/ 16 mole percent cholesterol models. The collapse of the two phosphorus peaks indicates that the Pr^{3+} is able to gain access to the both the outer and inner leaflets on a time scale of hours. The collapse of the Pr^{3+} -split ^{31}P resonances in the presence of iminosulfuranes occurs significantly faster than in their absence. This critical observation is highly supportive of a mode of action dependent on the deep penetration of these iminosulfuranes into the bilayer, but surface interaction with the lipids also remains a complementary mechanism for the activity of these transdermal penetration enhancers.

Furthermore, the effect of these molecules on bilayer integrity can be seen with a carboxyfluorescein release assay. Results based on the TPE-induced release of carboxyfluorescein trapped in the internal volume of DMPC vesicles further indicate that these iminosulfuranes disrupt the bilayer sufficiently to allow for the release of the fluorophore. The addition of the bromo derivative, the most active compound, causes a greater release in CF than that caused by the iodo derivative.

4.18. Mechanism of Action of Halogenated Iminosulfuranes

The mechanism of action supported by the results summarized suggest the active iminosulfuranes may act by penetrating the bilayer and inducing channels or pores in the membrane that allow for the movement of small molecules across the bilayer in the presence and absence of cholesterol. The incorporation of cholesterol at 16 mole percent stabilized the lipid bilayer and made it easier to see the effect of the iminosulfurane derivatives, whereas 30 mole percent cholesterol almost completely sealed the bilayer so that was the difference between the types and concentrations of iminosulfuranes were almost indistinguishable. The differential in the TPE activity of the bromo in contrast to that of the other three derivatives may be a result of enhanced residence time of the bromo derivative in the bilayer.

4.19. Further Studies on Halogenated Iminosulfuranes

The overarching question that needs to be answered is why the bromo derivative is the most active in this series of halogenated iminosulfuranes. Based solely on electronegativity, the expectation would be that the fluoro derivative would be the most biologically active. However, the fluoro derivative is biologically inactive. In contrast, comparison of relative size would support the iodo derivative being the most biologically active in this series. Since the neither the fluoro derivative or the iodo derivative are the most active, there must be other physico-chemical considerations that make the bromo derivative the most effective transdermal penetration enhancer. Perhaps, the bromo derivative has more available binding sites on the bilayer than the other derivatives which would cause an appreciable increase in the amount of channels induced in the DMPC

membrane. As a result, the number of channels induced in the membrane would be directly proportional to the amount of drug able to permeate the lipid matrix of the skin. Binding studies and scatchard analysis of iminosulfurane derivatives present in different concentrations may provide further insight into the increased efficacy of the bromo derivative relative to the other halogenated iminosulfuranes. The great extent to which the bromo derivative perturbs the bilayer may also be a function of the nature of the halogen oxygen bonds that may form with the iminosulfurane derivative. Characterization and comparison of these bonds may further support the biological activity of this series of iminosulfuranes.

References

1. Wood, E. J.; Bladon, P. T., *Studies in biology -the human skin*. Edward Arnold Ltd: London, Great Britain, 1985; Vol. 164, p 6-12.

2. Forslind, B.; Lindberg, M., *Structure and function of the skin barrier*. Marcel Dekker: New York, New York, 2004; Vol. 26, p 11-20.

3. Bouwstra, J. A., The skin barrier, a well-organized membrane. *Colloids and Surfaces A: Physicochemical and Engineering Aspects* **1997,** 123-124, 403-413.

4. *Percutaneous Penetration Enhancers*. 2nd ed.; CRC Press Taylor & Francis Group: Boca Raton, 2006.

5. Barry, B. W., *Penetration enhancer classification*. 2nd ed.; Taylor & Francis Group: Boca Raton, FL, 2006; p 3-15.

6. Hadgraft, J. J., Passive enhancement strategies in topical and transdermal drug delivery. *International Journal of Pharmaceutics* **1999,** 184, (1), 1-6.

7. Preat, V.; Vanbever, R., *Skin electroporation for transdermal and topical drug delivery*. 2nd ed.; Marcel Dekker, Inc.: New York, N.Y., 2003; Vol. 123, p 383.

8. Barry, B. W., Breaching the skin's barrier to drugs. *Nature Biotechnology* **2004,** 22, (2), 165.

9. Dempsey, D., Skin, thick trichrome. In *http://www.nku.edu/~dempseyd/SKIN.htm*, Highland, Kentucky.

10. Ltd., B. U., Schematic diagram of the brick and mortar model. In *http://www.eucerin.co.uk/skin/skincell_3.html*, Beiersdorf: Birmingham United Kingdom.

11. Smith, E. W.; Maibach, H. I., Percutaneous penetration enhancers. **2006**, 3-13.

12. Delgado-Charro, M. B.; Guy, R., *Iontophoresis: applications in drug delivery and noninvasive monitoring*. 2nd ed.; Marcel Dekker, Inc.: New York, N.Y., 2003; Vol. 123, p 383.

13. Meidan, V., *Sonophoresis: ultrasound-enhanced transdermal drug delivery*. 2nd ed.; Marcel Dekker, Inc.: New York, N.Y., 2003; Vol. 123, p 383.

14. Wester, R. C.; Maibach, H. I., *Penetration enhancement by hydration*. 1st ed.; CRC Press Taylor and Francis Group: Boca Raton, Fl, 1995; p 500.

15. Sasaki, H.; Nishida, K.; Nakamura, J., *Pyrrolidones as penetration enhancers*. 1st ed.; CRC Press: Boca Raton, Fl, 1995; p 500.

16. Kanikkannan, N.; Babu, R. J.; Singh, M., *Structure-Activity Relationship of Chemical Penetration Enhancers*. 2nd ed.; CRC Press Taylor and Francis Group: Boca Raton, Fl, 2006; p 432.

17. Aungst, B., *Fatty acid as skin penetration enhancer*. 1st ed.; CRC Press: Boca Raton, Fl, 1995; p 500.

18. Babu, R. J.; Singh, M.; Kanikkannan, N., *Fatty alcohols and fatty acids*. 2nd ed.; CRC Press Taylor & Francis Group: Boca Raton, Fl, 2006; p 432.

19. Ruddy, S. E., *Surfactants*. 1st ed.; CRC Press: Boca Raton,Fl, 1995; p 500.

20. Williams, A. C., *Urea and its derivatives as penetration enhancers*. 1st ed.; CRC Press: Boca Raton, Fl, 1995; p 500.

21. Thakur, R. A.; Wang, Y.; Michniak, B. B., *Essential oils and terpenes*. 2nd ed.; CRC Press Taylor & Francis Group: Boca Raton, Fl, 2006; p 432.

22. Harrison, J. E. J., Azone induced fluidity in human stratum corneum. A fourier transform infrared spectroscopy investigation using the perdeuterated analog. *Journal of Controlled Release* **1996,** 41, (3), 283.

23. Song, Y.; Xiao, C.; Mendelsohn, R.; Zheng, T.; Strekowski, L.; Michniak, B., Investigation of iminosulfuranes as novel transdermal penetration enhancers: enhancement activity and cytoxicity. *Pharmaceutical Research* **2005,** 22, (11), 1918-1925.

24. Aoyagi, T.; Nagase, Y., *Silicone based polymers*. 1st ed.; CRC Press: Boca Raton, Fl, 1995; p 500.

25. Franz, T. J.; Lehman, P. A.; Kegy, M. K., *Dimethylsulfoxide*. 1st ed.; CRC Press: Boca Raton, Fl, 1995; p 500.

26. Kim, N.; El-Khalili, M.; Henary, M. M.; Strekowski, L.; Michniak, B. B., Percutaneous penetration enhancement activity of aromatic S,S-dimethyliminosulfuranes. *International Journal of Pharmaceutics* **1999,** 187, (2), 219-222.

27. Barrow, D. J., Jr.; Chandrasekaran, S.; Heerklotz, H. H.; Henary, M. M.; Michniak, B. B.; Nguyen, P. M.; Song, Y.; Smith, J. C.; Strekowski, L., Mechanistic

studies on percutaneous penetration enhancement by N-(4-halobenzoyl)-S,S-dimethyliminosulfuranes. *Journal of Lipid Research* **2005,** 46, (10), 2192-2201.

28. Strekowski, L. H., M.M.; Kim, N.; Michniak, B.B., N-(4-Bromobenzoyl)-S,S-dimethyliminosulfurane, a potent dermal penetration enhancer. *Bioorganic & medicinal chemistry letters* **1999,** 9, (7), 1033.

29. de Jager, M. W.; Gooris, G. S.; Dolbnya, I. P.; Bras, W.; Ponec, M.; Bouwstra, J. A., Novel lipid mixtures based on synthetic ceramides reproduce the unique stratum corneum lipid organization. *Journal of Lipid Research* **2004,** 45, 923-932.

30. Wertz, P. W.; Abraham, W.; Landmann, L.; Downing, D. T., Preparation of liposomes from stratum corneum lipids. *Journal of Investigative Dermatology* **1986,** 87, 582-584.

31. Bouwstra, J. A.; Honeywell-Nguyen, P. L., Skin structure and mode of action of vesicles. *Advanced Drug Delivery Reviews* **2002,** 54, (Suppl. 1), S41-S55.

32. Mouritsen, O. G., *Life-as a matter of fat: the emerging science of lipidomics*. Springer: New York, 2005; p 276.

33. Yeagle, P. L., *The roles of cholesterol in the biology of cells*. 2nd ed.; CRC Press: Boca Raton, Fl, 2005; p 540.

34. Johnson, M. E.; Berk, D. A.; Blankschtein, D.; Golan, D. E.; Jain, R. K.; Langer, R. S., Lateral diffusion of small compounds in human stratum corneum and model lipid bilayer systems. *Biophysical Journal* **1996,** 71, (5), 2656.

35. Lewis, R. N. A. H.; McElhaney, R. H., *The mesomorphic phase behavior of lipid bilayers*. 2nd ed.; CRC Press LLC: Boca Raton, Fl, 2005; p 540.

36. Cafiso, Z.-C. X. a. D. S., Phospholipid packing and conformation in small vesicles revealed by two- dimensional 1H nuclear magnetic resonance cross-relaxation spectroscopy. *Biophysical Journal* **1986,** 49, 779-783.

37. Bammel, B. P.; Brand, J. A.; Simmons, R. B.; Evans, D.; Smith, J. C., The interaction of potential-sensitive molecular probes with dimyristoylphosphatidylcholine vesicles investigated by 31P-NMR and electron microscopy. *Biochimica et Biophysica Acta* **1987,** 896, 136-152.

38. Jan Zuidam, N.; de Vrueh, R.; Crommelin, D. J. A., *Liposomes a practical approach*. 2nd ed.; Oxford University Press: New York, 2003; Vol. 264, p 396.

39. Hutton, W. C. W., The interaction of lanthanide and calcium salts with phospholipid bilayer vesicles: the validity of the nuclear magnetic resonance method for determination of vesicle bilayer phospholipid surface ratios. *Chemistry and Physics of Lipids* **1977,** 19, (3), 255.

40. Chen, R. F.; Knutson, J. R., *Analytical Biochemistry* **1988,** 172, 61-77.

41. Lakowicz, J. R., *Principles of fluorescence spectroscopy*. 2nd ed.; Kluwer Academic / Plenum Publishers: New York, New York, 1999; p 698.

42. Gruner, S. A., *Nonlamellar lipid phases*. 2nd ed.; CRC Press: Boca Raton, Fl, 2005; p 540.

43. De Kruijff, B.; Morris, G. A.; Cullis, P. R., Application of 31P-NMR saturation transfer techniques to investigaate phospholipid motion and organization in model and biological membranes. *Biochimica et Biophysica Acta* **1980,** 598, 206-211.

44. Hallock, K. J.; Lee, D.-K.; Omnaas, J.; Mosberg, H. I.; Ramamoorthy, A., Membrane composition determines pardaxin's mechanism of lipid bilayer disruption. *Biophysical Journal* **2002,** 83, 1004–1013.

45. Dave, P. C.; Tiburu, E. K.; Damodaran, K.; Lorigan, G. A., Investigating structural changes in the lipid bilayer upon insertion of the transmembrane domain of the membrane-bound protein phospholamban utilizing 31P and 2H solid-state NMR spectroscopy. *Biophysical Journal* **2004,** 86, 1564–1573.

46. Auger, M., Biological membrane structure by solid-state NMR. *Current Issues in Molecular Biology* **2000,** 2, (4), 119-124.

47. Wenk, M. R.; Seelig, J., Proton induced vesicle fusion and the isothermal L_α -H_{II} phase transition of lipid bilayers: a 31P-NMR and titration calorimetry study. *Biochimica et Biophysica Acta* **1998,** 1372, 227-236.

48. Friebolin, H., *Basic one- and two- dimensional NMR spectroscopy*. 1st ed.; VCH Publishers: New York, New york, 1991; p 344.

49. Smith, I. C. P.; Ekiel, I. H., *Phosphorus-31 NMR of Phospholipids in Membranes*. Academic Press: Orlando, Florida, 1984; p 604.

50. Heimburg, T., A model for the lipid pretransition: coupling of ripple formation with the chain-melting transition. *Biophysical Journal* **2000,** 78, (3), 1154-1165.

51. Brown; Brennan; Krull, Self-quenching of nitrobenzoxadiazole lableled phospholipids in lipid membranes. *Journal of Chemical Physics* **1994,** 100, (8), 6019-6027.

52. Domecq, A.; al., e., A stability test of liposomes preparations using steady-state fluorescent measurements. *Drug Delivery* **2001,** 8, 155-160.

53. Klausner; Wolf, Selectivity of fluorescent lipid analogues for lipid domains. *Biochemistry* **1980,** 19, 6199-6203.

54. Bashford, C. L.; Chance, B.; Smith, J. C.; Yoshida, T., The behavior of oxonol dyes in phospholipid dispersions. *Biophysical Journal* **1979,** 25, 63-85.

55. Ohvo-Rekila, H.; Akerlund, B.; Slotte, J. P., Cyclodextrin-catalyzed extraction of fluorescent sterols from monolayer membranes and small unilamellar vesicles. *Chemistry and Physics of Lipids* **2000,** 105, 167-178.

56. Gallegos, A.; Atshaves, B. P.; Storey, S.; Schoer, J.; Kier, A. B.; Schroeder, F., Molecular and fluorescent sterol approaches to probing lysosomal membrane lipid dynamics. *Chemistry and Physics of Lipids* **2002,** 116, 19-38.

57. Invitrogen™, 5-FAM/pH 9.0. In *http://probes.invitrogen.com/servlets/spectra?fileid=1359ph9*, Molecular Probes: Carlsbad, California.

58. de la Maza, A.; Lopez, O.; Cocera, M.; Coderch, L.; Parra, J. L., Influence of the level of ceramides in the permeability of stratum corneum lipid liposomes caused by sodium dodecyl sulfate. *Chemistry and Physics of Lipids* **1998,** 94, 181-191.

59. Cocera, M.; Lopez, O.; Coderch, L.; Parra, J. L.; de la Maza, A., Alterations in Stratum Corneum Lipid Liposomes due to the Action of Triton X-100 Influence of Ceramides on this Process. *Journal of Controlled Release* **2000,** 68, 387-396.

60. Lopez, O.; Cocera, M.; de la Maza, A.; Coderch, L.; Parra, J. L., Different stratum corneum lipid liposomes as models to evaluate the effect of sodium dodecyl sulfate. *Biochimica et Biophysica Acta* **2000,** 1508, 196-209.